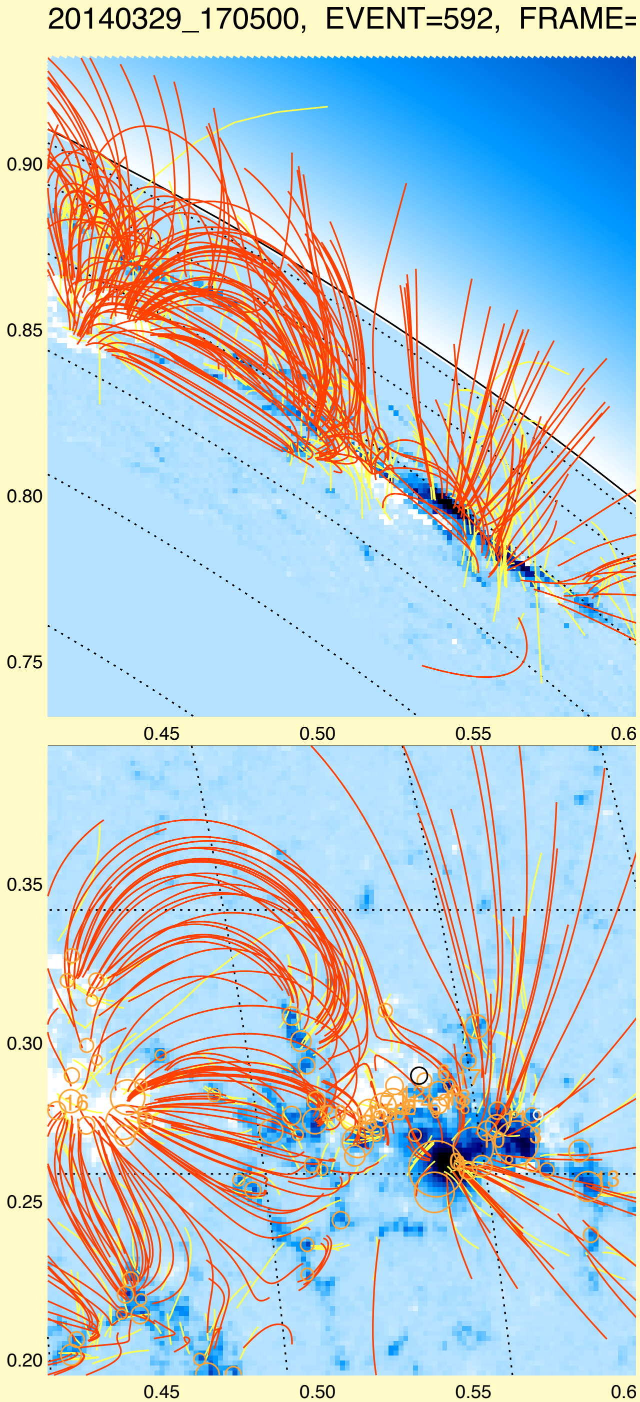

Tracing the Chromospheric & Coronal Magnetic Field with AIA, IRIS, IBIS & ROSA

Markus J. Aschwanden (LMSAL)
Bart De Pontieu (LMSAL)
Kevin Reardon (NSO)
Dave Jess (QUB)

ALMA-IRIS-DKIST Workshop, March 15, 2016
NSO, Boulder, Colorado

http://www.lmsal.com/~aschwand/ 2016_chromo_aschwanden.ppt

Outline of Talk:

1) Previous work on chromospheric magnetic fields

2) The VCA-NLFFF method to compute magnetic fields:
   - 2.1 Potential field from buried magnetic sources
   - 2.2 Automated tracing of curvi-linear features
   - 2.3 Forward-fitting of nonpotential magnetic field

3) Data Analysis:
   - AIA/SDO, HMI/SDO
   - IRIS
   - IBIS
   - ROSA

4) Discussion and conclusions:
   - Suitability of chromospheric field tracing
   - Altitudes of chromospheric magnetic field tracers
   - Coronal vs. chromospheric free energy

Static and Dynamic Chromospheric Models

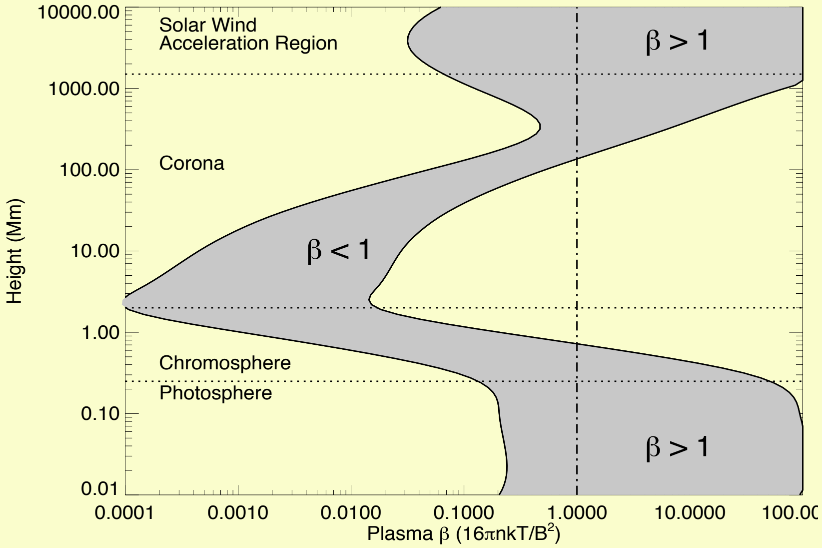

The plasma β-parameter is <1 in most coronal and upper chromospheric regions. Gary 2001

Chromospheric density models:

-VAL-C (Vernazza, Avrett, & Loeser 1981
-FAL-C (Fontentla, Avrett & Loeser 1990
-Gu et al. 1997, Maltby et al. 1986,
-Ding & Fang 1989; Obridko & Staude 1988
-Gabriel 1976 (canopy model),
-CICM Caltech Irreference Chromospheric model
-radio sub-millimeter limb observations
 (Ewell et al. 1993);
-RHESSI thick-target model, energy-dependent
 height centroids → chromospheric density model
 (Aschwanden, Brown & Kontar 2002)
→ Dynamic chromosphere extends up to ~5000 km

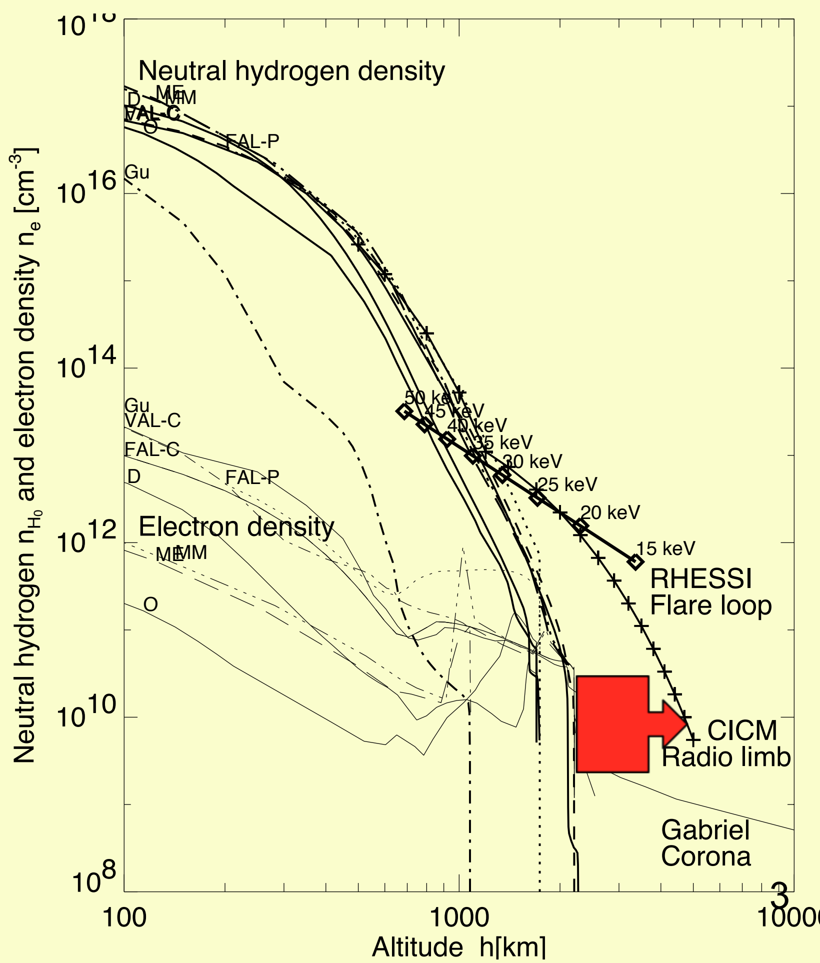

Nomenclature of chromospheric structures

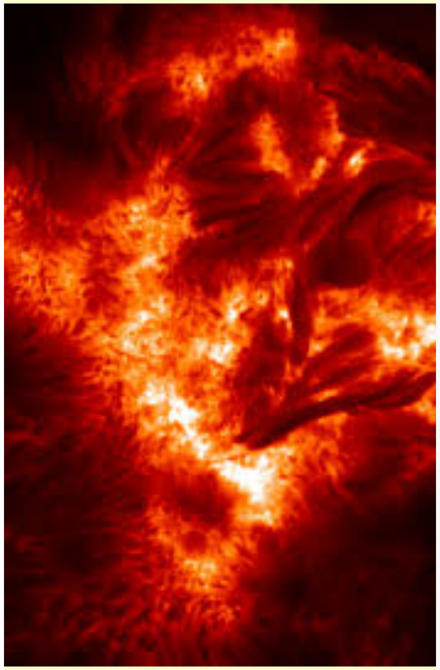

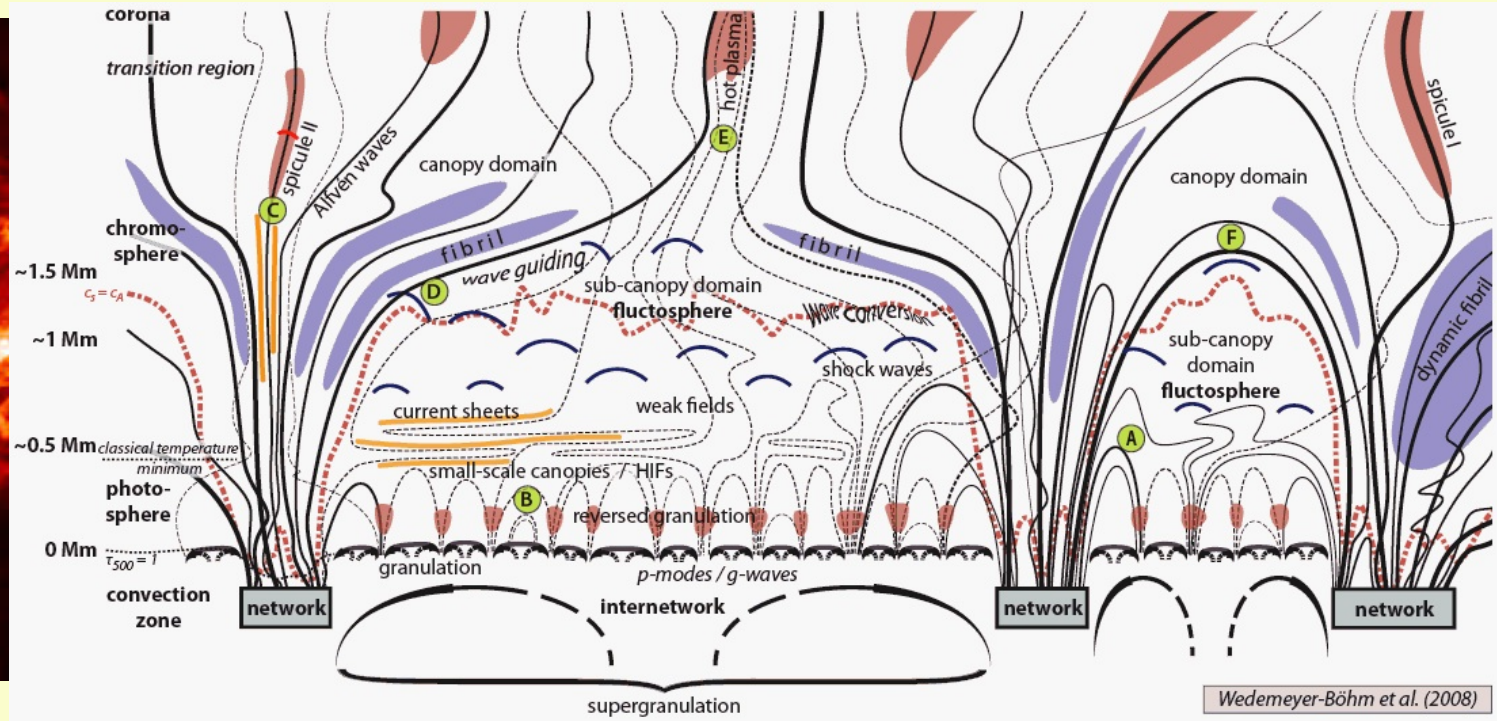

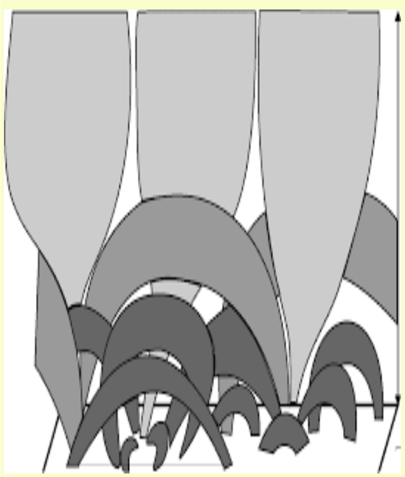

Chromospheric structures:

- Footpoints of field-aligned coronal loops
- Fibrils in active regions and sunspot penumbra
- Spicules (when observed near and above limb)
- Mottles (when observed in Quiet Sun)

(DePontieu et al. 2007; Pietrarila et al. 2009)

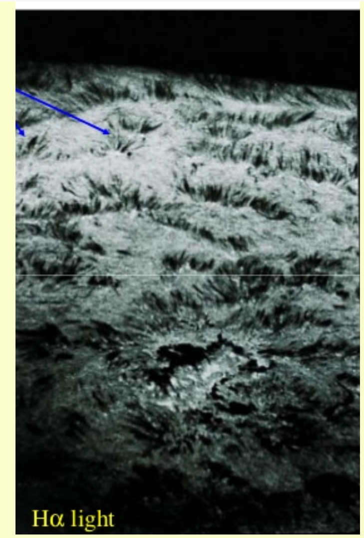

The lower chromosphere is not force-free

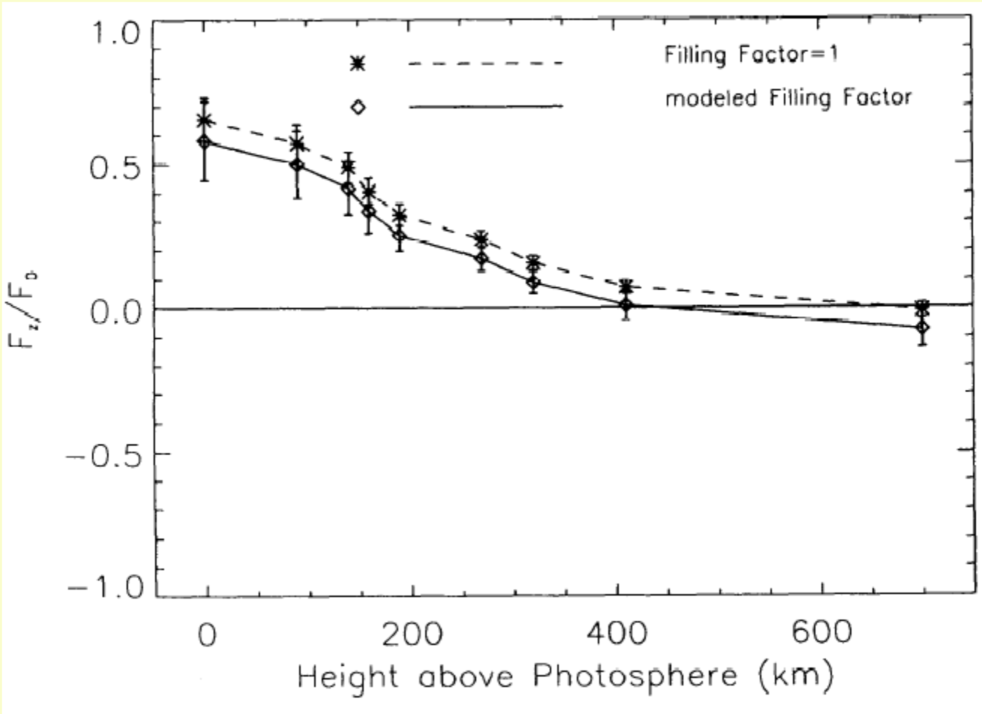

Metcalf et al. 1995

At what height is the transition between plasma β-parameter >1 to < 1 ?
Setting the total Lorentz force equal to the magnetic pressure force,
Metcalf et al. (1995) found that chromosphere is not force-free for h<400 km.
The implication is that magnetic field extrapolation from photospheric
data violates the force-free assumption
→ Tracers in the upper chromosphere and corona are needed

Link between chromospheric network and corona

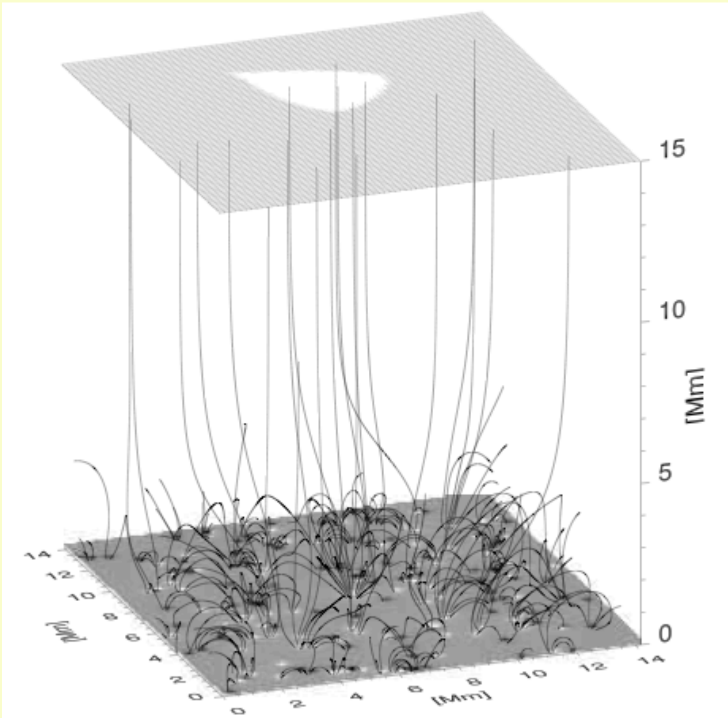

Fig. 1. Composite plot of the magnetic field at the bottom (lower BC), field lines of the extrapolated magnetic field, and a mask of the area at 15 Mm height that is magnetically connected to the central strong network magnetic patch (white).

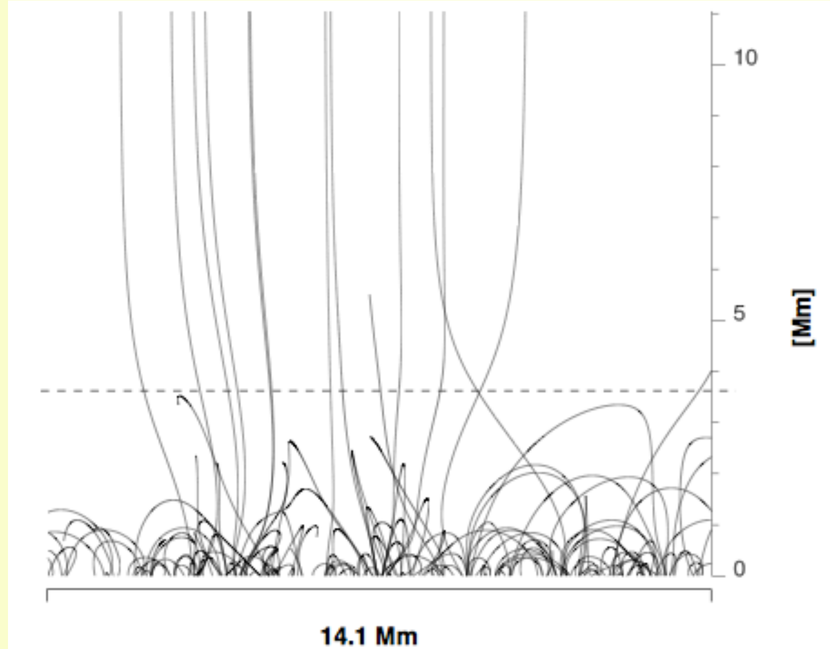

Fig. 3. A selection of field lines starting from the inter-network are drawn for an unsigned mean internetwork flux density of 60 Mx/cm^2. Here the computational domain is viewed from the side. The dashed line indicates the maximum height of the highest-reaching closed field line from this selection. See Sect. 3.2.

Schrijver & Title 2002; Jendersie & Peter 2006

Many magnetic field lines rooted in small-scale network (salt & pepper) field concentrations close inside the lower chromosphere and do not extend up into the corona, which hampers magnetic field extrapolation methods

→ tracing of upper chromospheric and coronal structures is needed.

Chromospheric magnetic field

- 137 solar active regions observed with NSO/KP in Ca II 8542 A (most sensitive at h=800 km) reveal non-potentiality of magnetic field when comparing extrapolated with measured field.

  (Harvey et al. 1999; Choudhary et al. 2001)

- The Ca II 8542 A line is particularly suited to observe the fine structure of fibril-like features, to measure their geometry and orientation, and to determine their magnetic field alignment and non-potentiality.

  (Pietarila et al. 2009; Jing et al. 2011, de la Cruz Rodriguez & Socas-Navarro 2001; Schad et al. 2013)

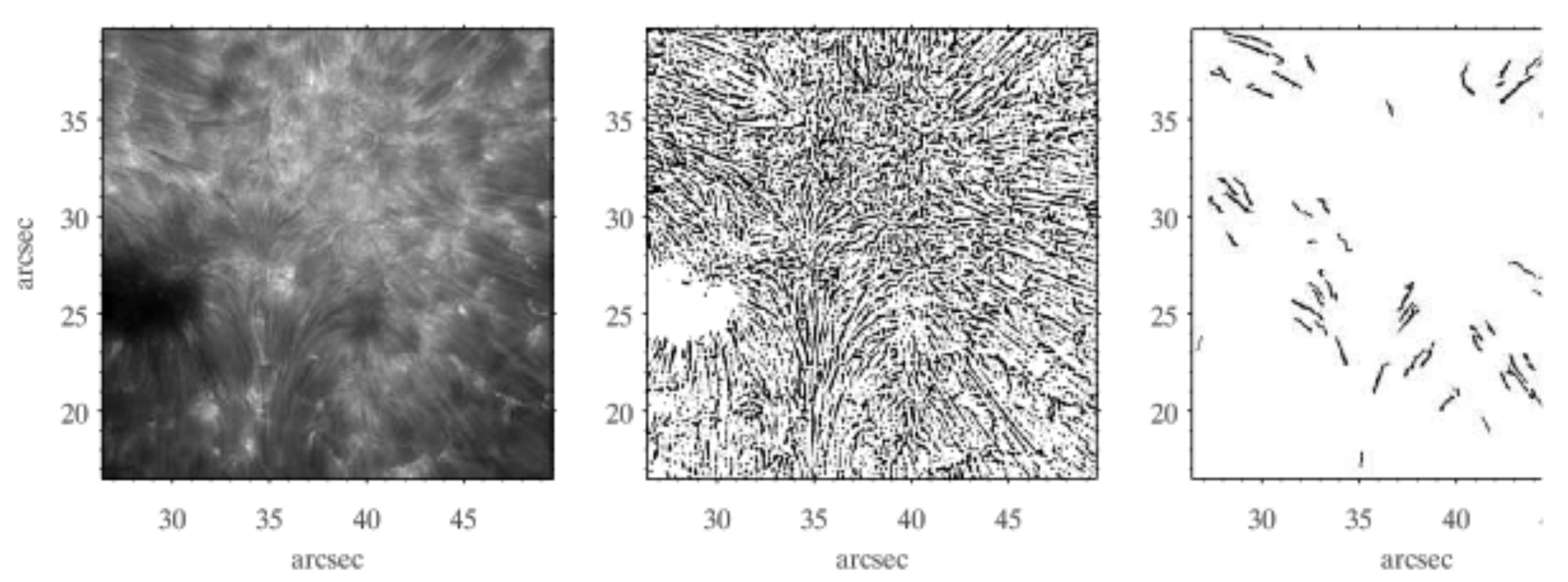

Pietarila et al. 2009

Do chromospheric fibrils trace the magnetic field ?

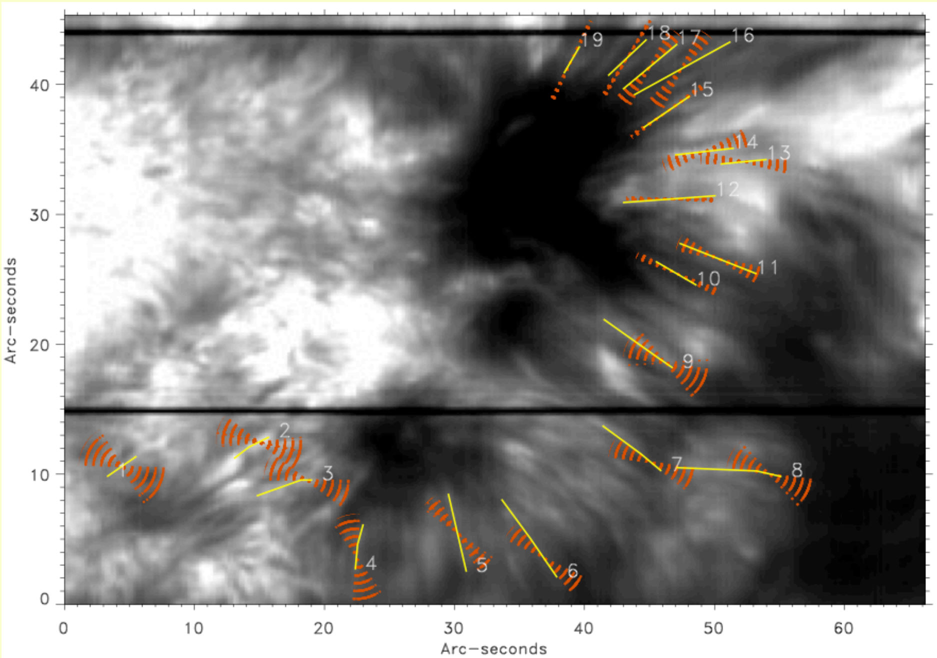

Ca II 8542 A, SPINOR, Stokes Q and U profile
De la Cruz Rodriguez & Socas-Navarro (2011)

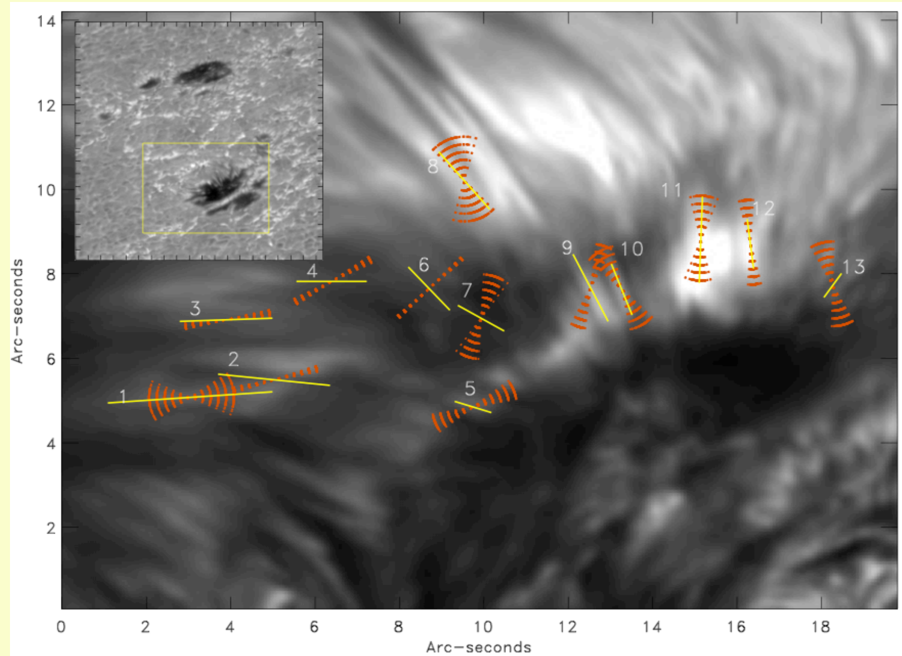

wing of Ca II 8542, CRISP
De la Cruz Rodriguez & Socas-Navarro (2011)

Spectropolarimetric observations of Ca II lines
Indicate the chromospheric fibrils trace the field mostly, but not always

Do chromospheric fibrils trace the magnetic field ?

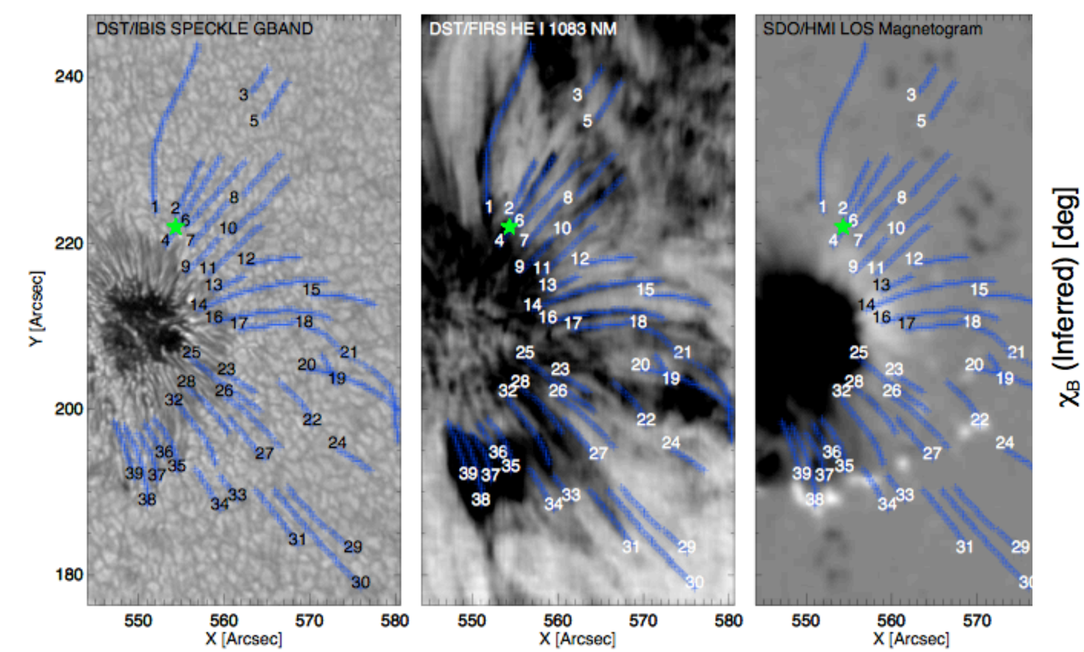

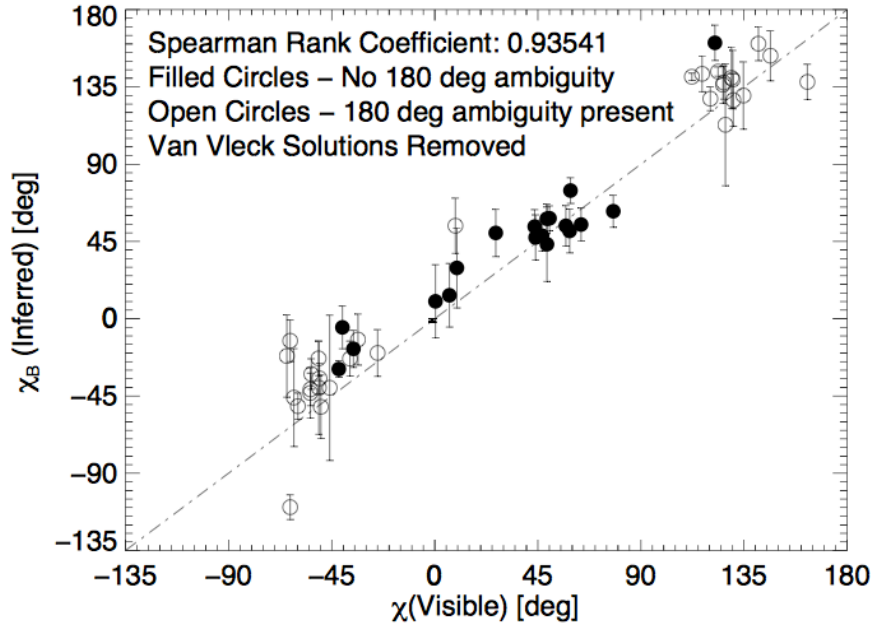

39 manually traced fibrils, He I, CRISPEX,
Schad, Penn, & Lin (2013)

Magnetic field direction vs. projected angle of fibrils
Schad, Penn, & Lin (2013)

Full vector magnetometry of super-penumbral fibrils observed in He I 10830 A, H-alpha 6563 A, and Ca II 8542 A (at DST) show that the Projected angle of the fibrils is aligned with the magnetic field within ±10 deg.

Outline of Talk:

1) Previous work on chromospheric magnetic fields

2) The VCA-NLFFF method to compute magnetic fields:
- **2.1 Potential field from buried magnetic sources**
- **2.2 Automated tracing of curvi-linear features**
- **2.3 Forward-fitting of nonpotential magnetic field**

3) Data Analysis:
- AIA/SDO, HMI/SDO
- IRIS
- IBIS
- ROSA

4) Discussion and conclusions:
- Suitability of chromospheric field tracing
- Altitudes of chromospheric magnetic field tracers
- Coronal vs. chromospheric free energy

Vertical Current Approximation Non-Linear Force-Free Field (VCA-NLFFF) Code

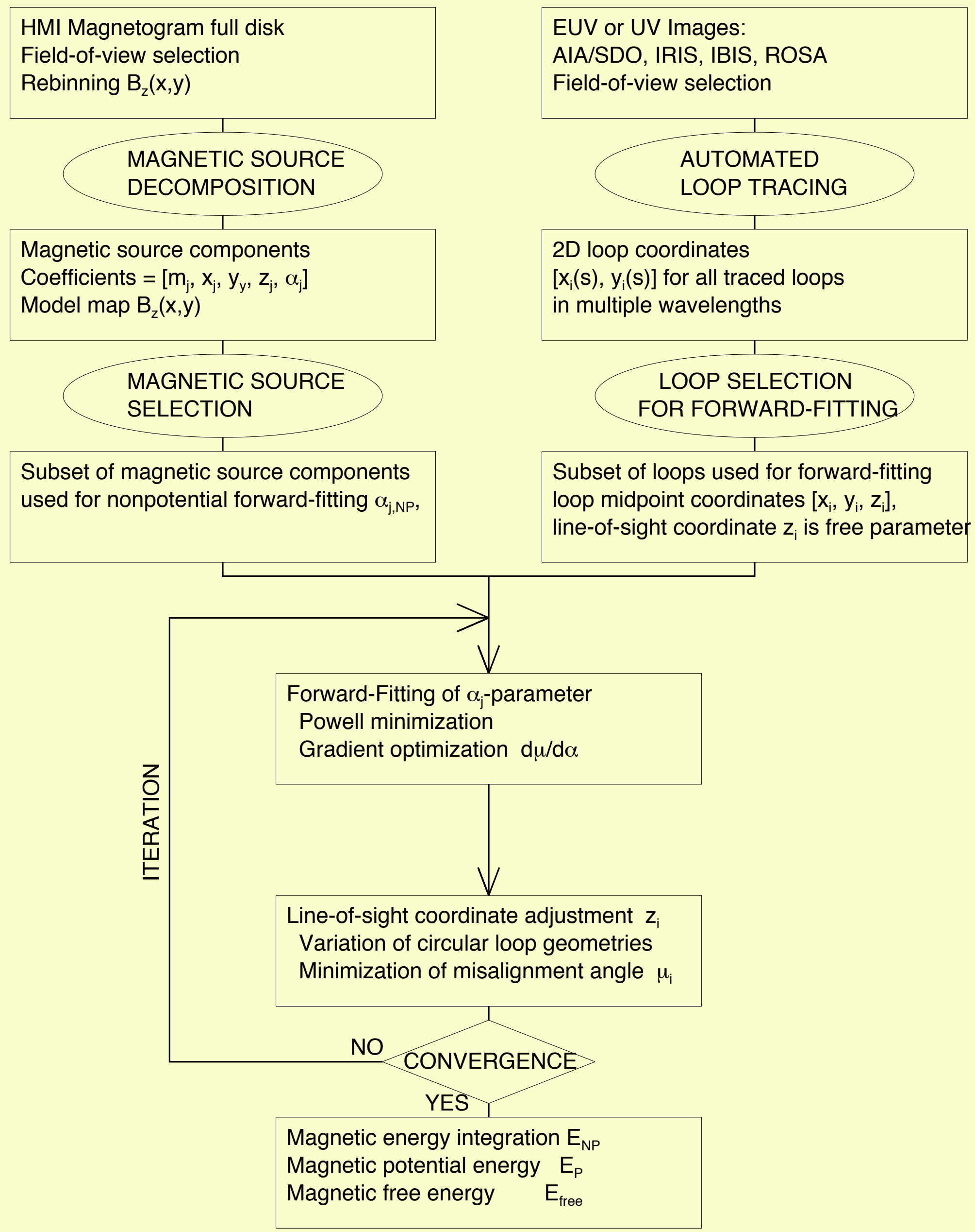

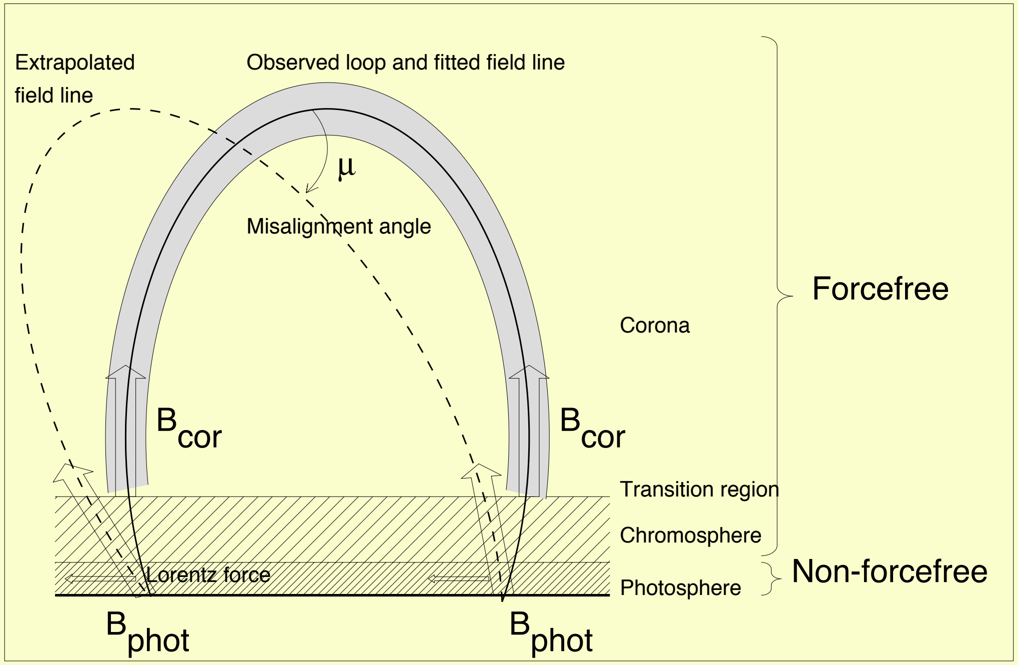

Potential field: PFSS code (no free energy available for flares or coronal heating)

Non-Potential field codes:

(1) Standard-NLFFF codes (extrapolation ignores non-forcefree zones, use vector-magnetograph LOS + transverse field, but are misaligned to geometry of coronal loops)

(e.g. Wheatland et al. 2000; Wiegelmann 2004; Grad & Rubin 1958)

(2) VCA-NLFFF code: Forward-fitting of analytical NLFFF approximation to coronal loops, transverse field is free parameter and can minimize misalignment with coronal loops)

(Aschwanden 2013, Aschwanden, Sun, & Liu 2014)

Photospheric vs. Coronal Magnetic Field Measurement Methods

	Standard NLFFF (Wiegelmann et al. 2008)	VCA-NLFFF (Aschwanden 2013)
Input:	Photospheric 3D vectors (B_x, B_y, B_z)	Photospheric B_z magnetogram Coronal loop coordinates [x(s),y(s)] or [x(s),y(s),z(s)]
Method:	Force-free α-parameter optimization	Forward-fitting of analytical NLFFF solution based on the **V**ertical **C**urrent **A**pproximation
Problems:	Non-forcefree photophere (→ preprocessing) Misalignment of coronal loops	Sparse loops near sunspots, false loop detection in moss areas, neglects horizontal currents
Computation time:	2-12 hrs/run	1-3 min/run

VCA-NLFFF with stereoscopy (3D) or without (2D loop coordinates)

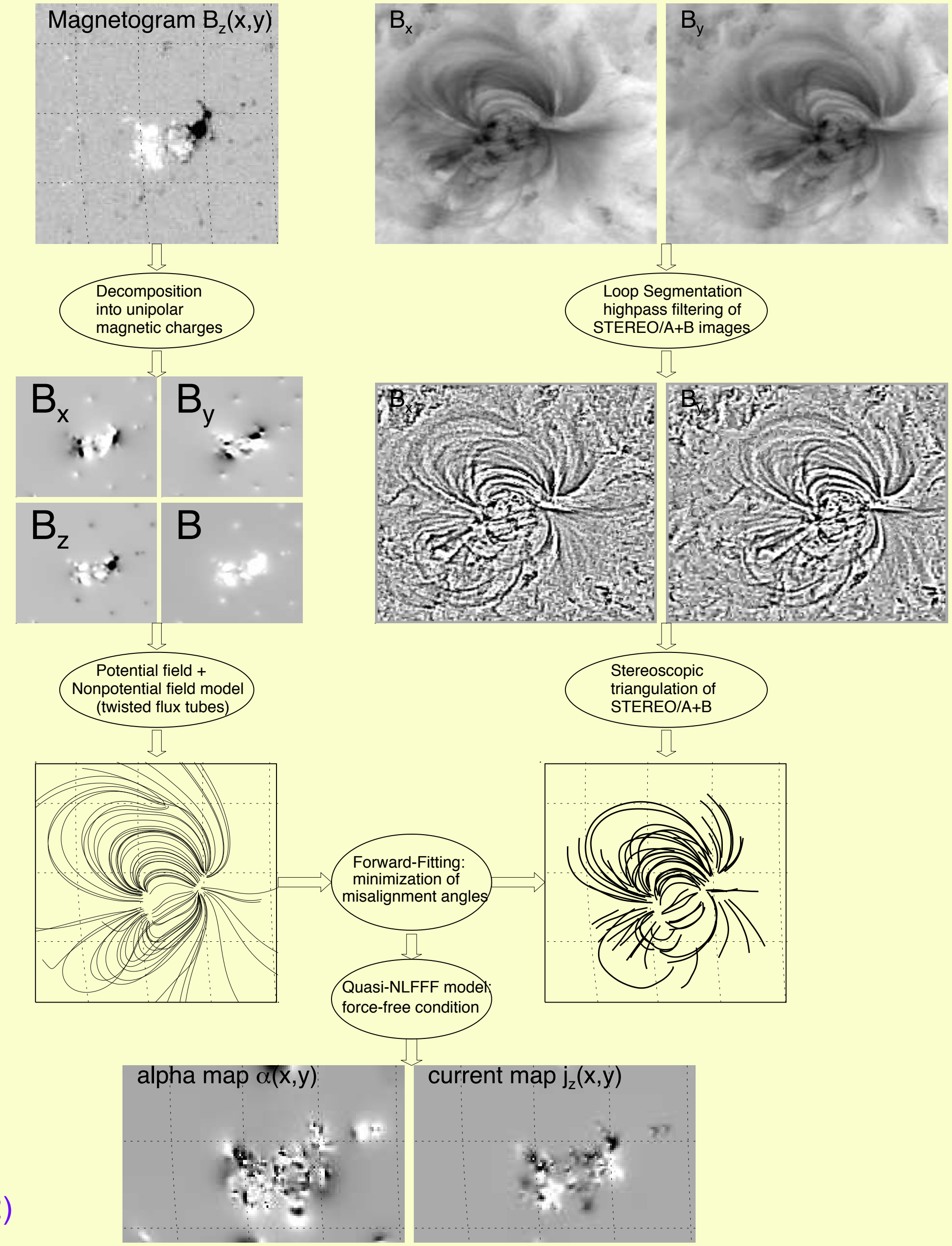

Aschwanden et al. (2012)

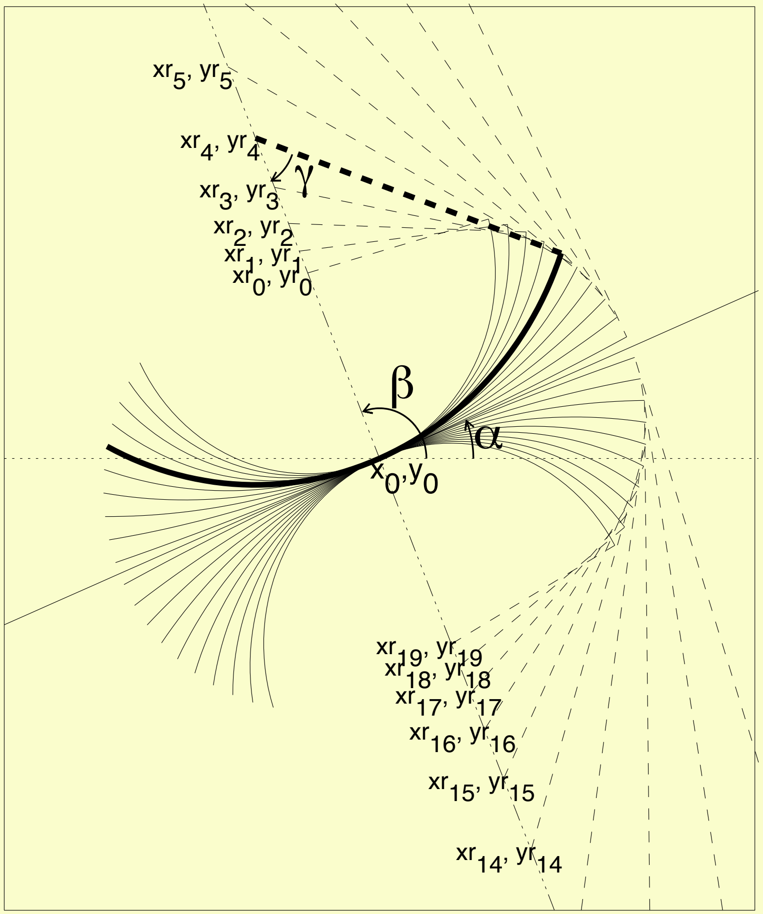

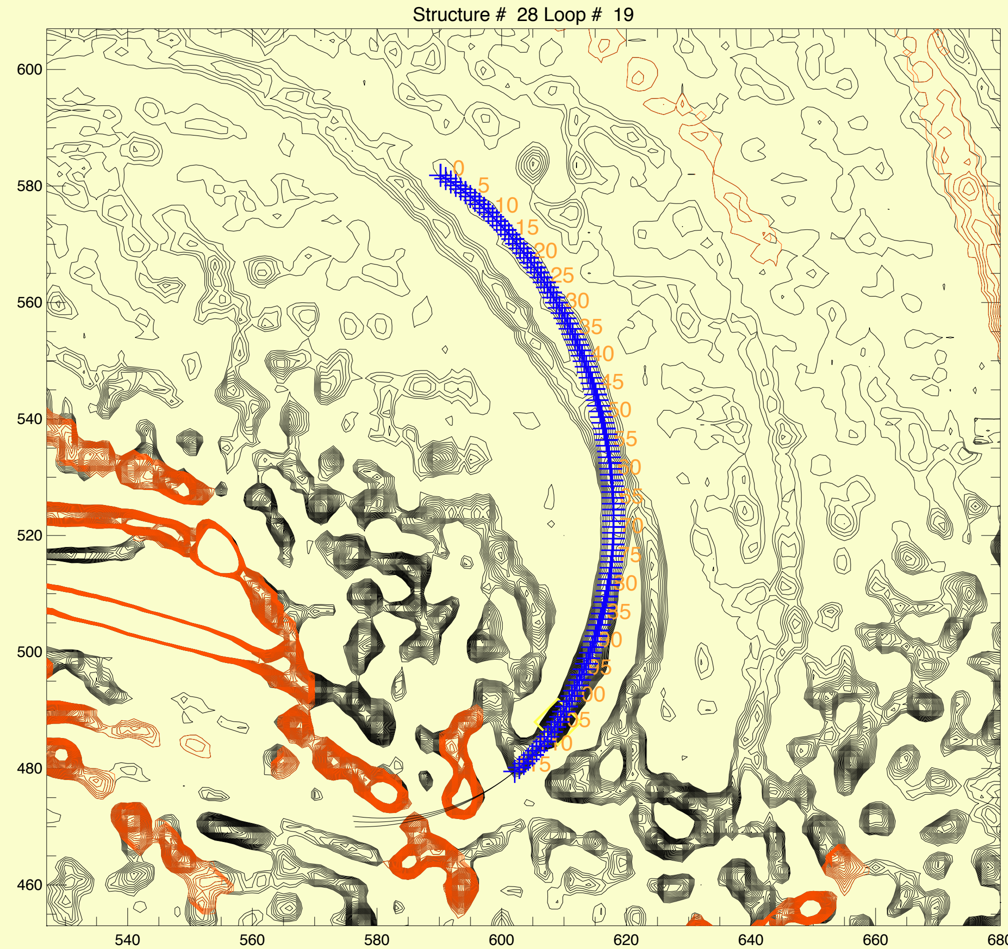

OCCULT-2 Code:
Local curvature radius
provides guiding of
directional
changes in tracing a
curvi-linear structure

Challenges:
-crossing loops
-data noise
-background confusion moss)
-saturation, pixel bleeding
-entrance filter diffraction pattern

The Vertical-Current Approximation Non-Linear Force-Free Field Method

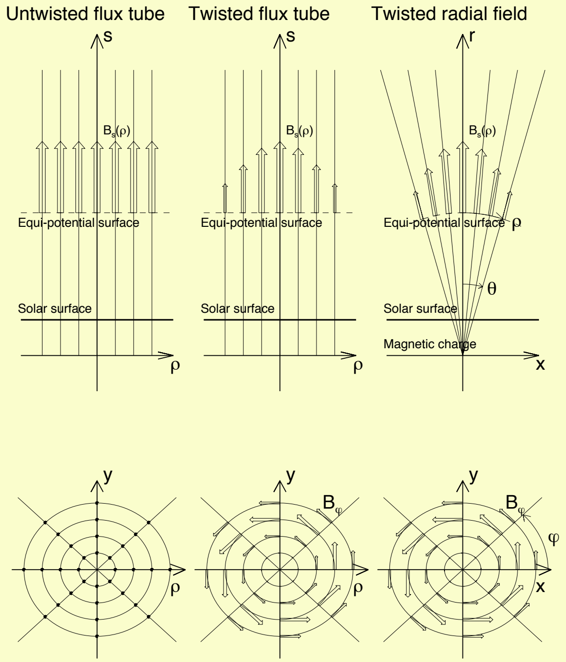

Aschwanden 2013

Approximative nonlinear force-free solution (neglecting second-order terms)

$$\frac{1}{r^2}\frac{\partial}{\partial r}(r^2 B_r) \approx 0 \ , \tag{26}$$

$$\frac{1}{r\sin\theta}\frac{\partial}{\partial\theta}(B_\varphi \sin\theta) = \alpha B_r \ , \tag{27}$$

$$-\frac{1}{r}\frac{\partial}{\partial r}(r B_\varphi) \approx 0 \ , \tag{28}$$

$$-\frac{1}{r}\frac{\partial B_r}{\partial\theta} \approx \alpha B_\varphi \ . \tag{29}$$

Ansatz for azimuthal component

$$B_\varphi = B_r b r \sin\theta \ , \tag{30}$$

differential equation

$$\frac{\partial}{\partial\theta}\left[B_r(1+b^2 r^2 \sin^2\theta)\right] = 0 \ . \tag{31}$$

Solution of differential equation (neglecting second-order terms)

$$B_r(r,\theta) = B_0 \left(\frac{d^2}{r^2}\right) \frac{1}{(1+b^2 r^2 \sin^2\theta)} \ , \tag{32}$$

$$B_\varphi(r,\theta) = B_0 \left(\frac{d^2}{r^2}\right) \frac{b r \sin\theta}{(1+b^2 r^2 \sin^2\theta)} \ , \tag{33}$$

$$B_\theta(r,\theta) \approx 0 \ , \tag{34}$$

$$\alpha(r,\theta) = \frac{2b\cos\theta}{(1+b^2 r^2 \sin^2\theta)} \ . \tag{35}$$

Untwisted (potential) fields

Twisted (non-potential) fields

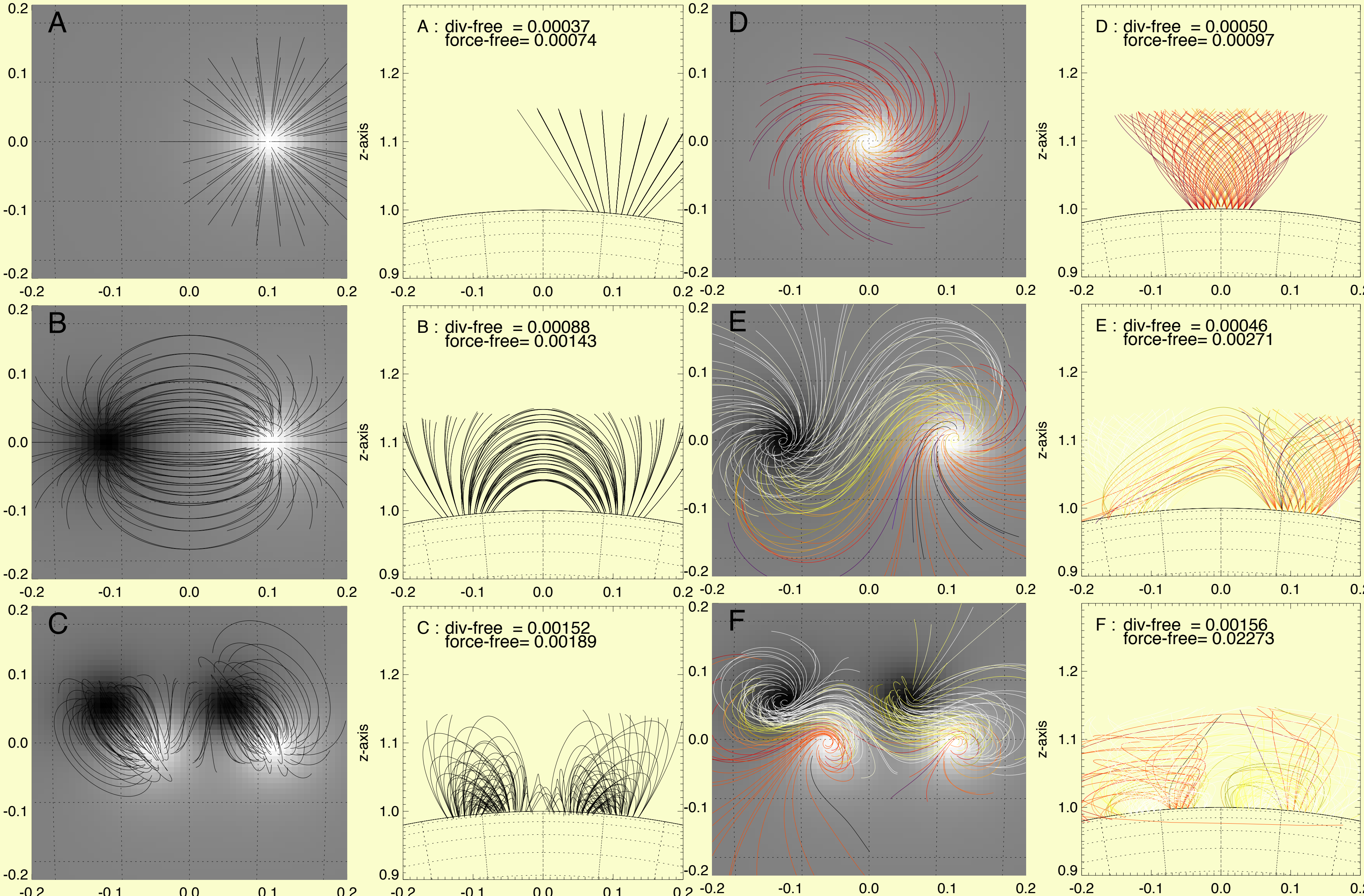

Outline of Talk:

1) Previous work on chromospheric magnetic fields

2) The VCA-NLFFF method to compute magnetic fields:
   - 2.1 Potential field from buried magnetic sources
   - 2.2 Automated tracing of curvi-linear features
   - 2.3 Forward-fitting of nonpotential magnetic field

3) Data Analysis:
   - **AIA/SDO, HMI/SDO**
   - **IRIS**
   - **IBIS**
   - **ROSA**

4) Discussion and conclusions:
   - Suitability of chromospheric field tracing
   - Altitudes of chromospheric magnetic field tracers
   - Coronal vs. chromospheric free energy

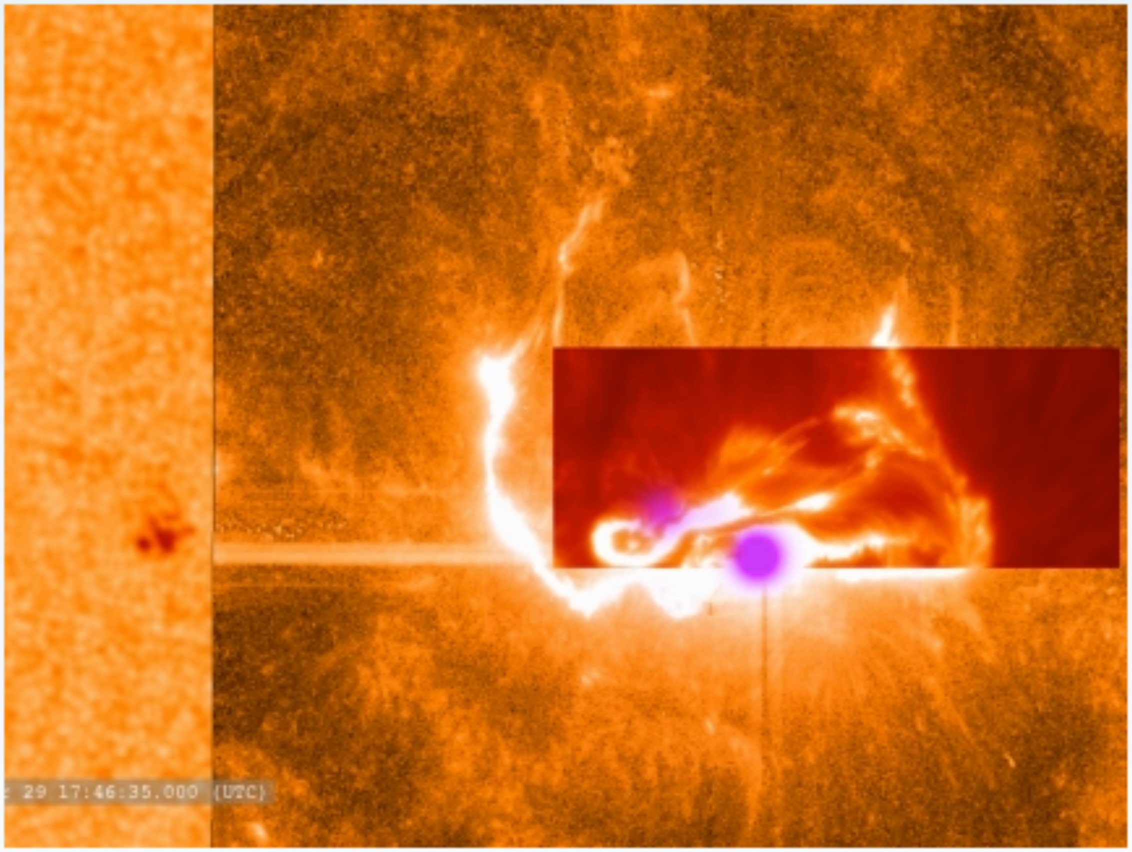

March 29 X-class Flare - 1

This combined image shows the March 29, 2014, X-class flare as seen through the eyes of different observatories. SDO is on the bottom/left, which helps show the position of the flare on the sun. The darker orange square is IRIS data. The red rectangular inset is from Sacramento Peak. The violet spots show the flare's footpoints from RHESSI.

› **Link to associated news item**

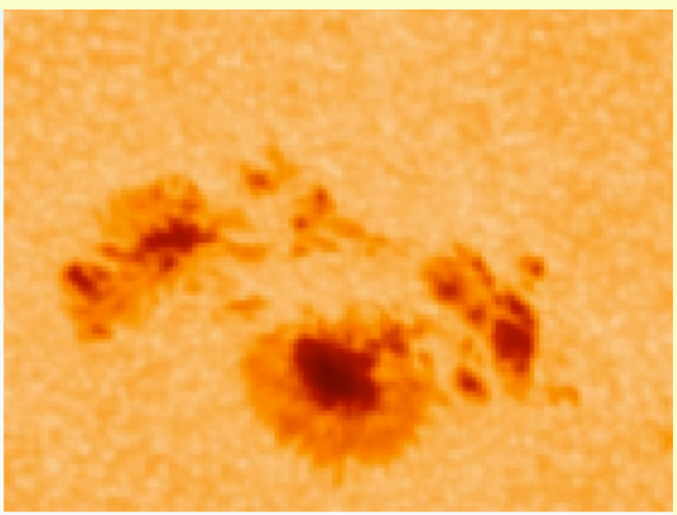

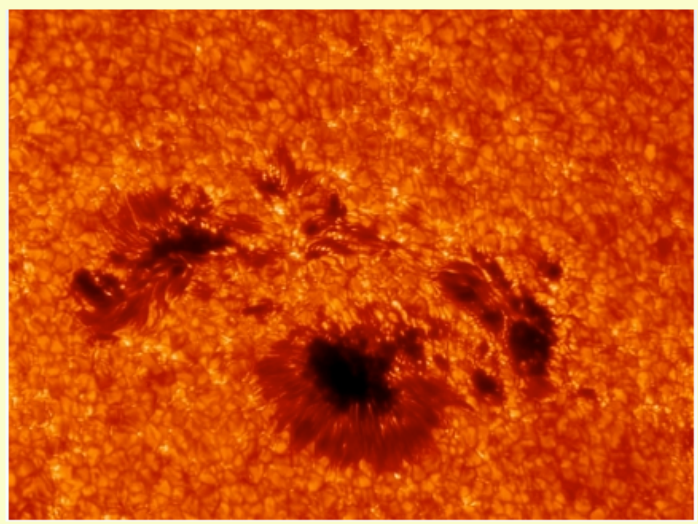

NSO IBIS G-band

Automated Tracing of Coronal Loop Structures

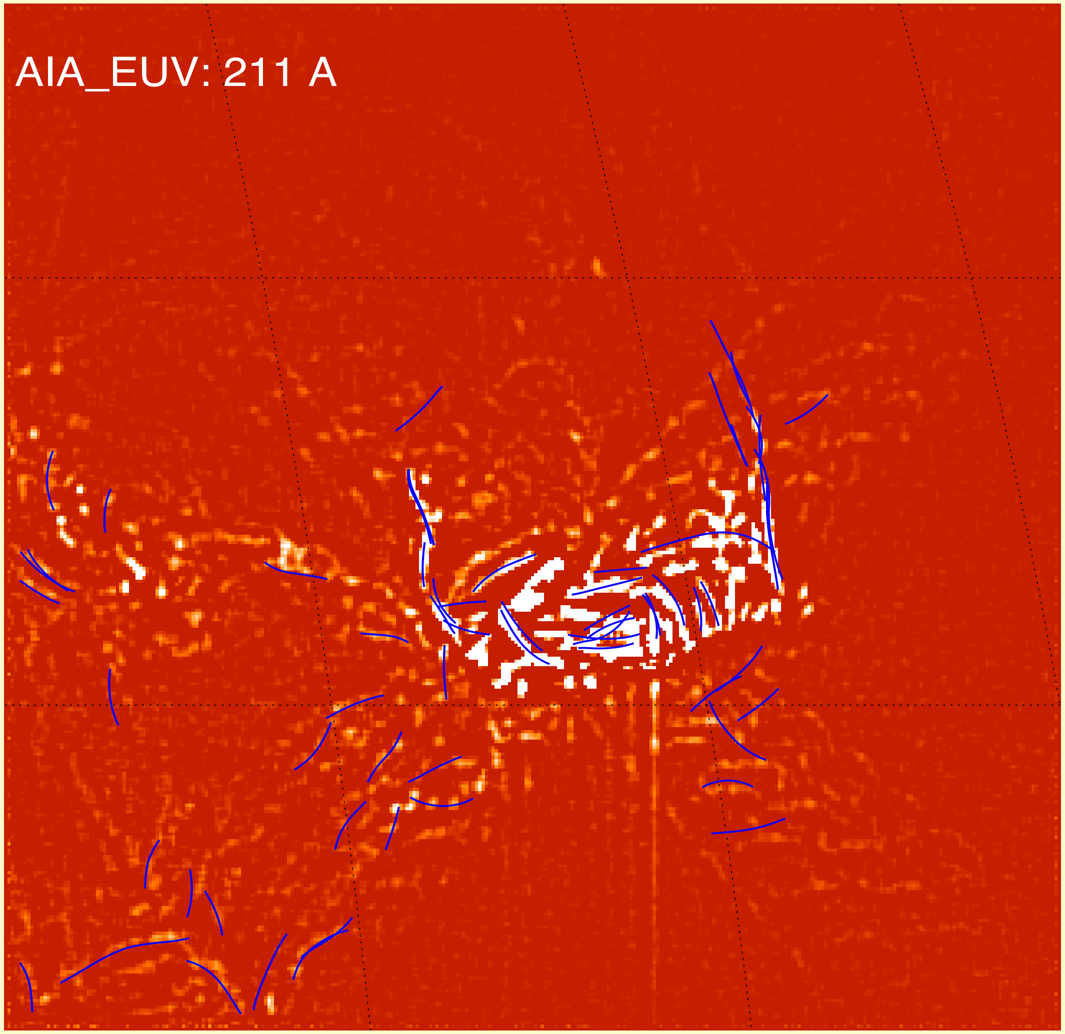

Automated Tracing of Chromospheric Structures

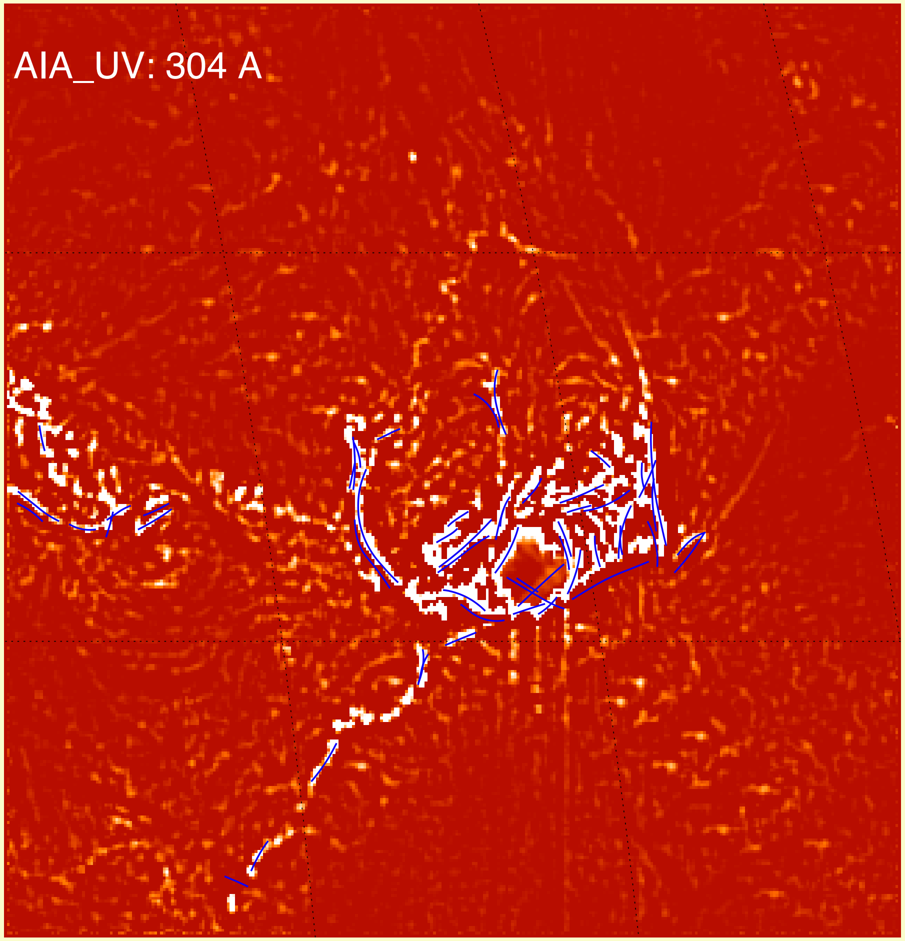

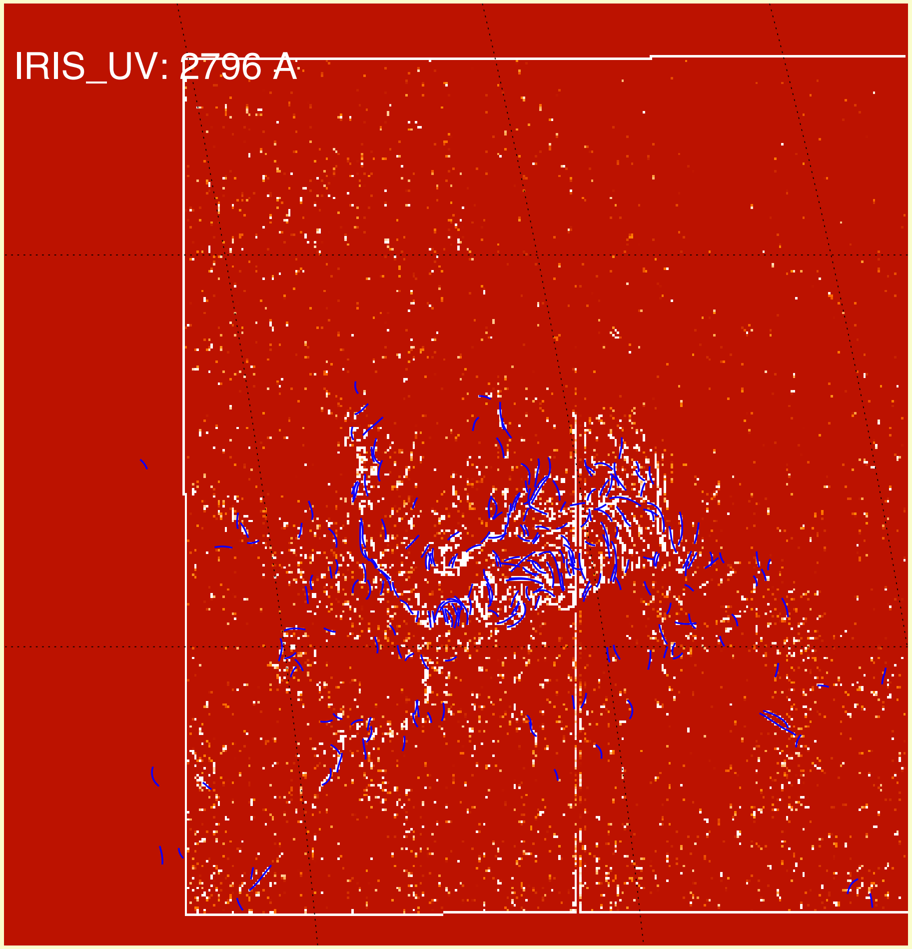

Non-linear Force Free Field (VCA-NLFFF) before and after flare

20140329_170500, EVENT=592, FRAME= 0 / 26, RUN=AIA_EUV_01

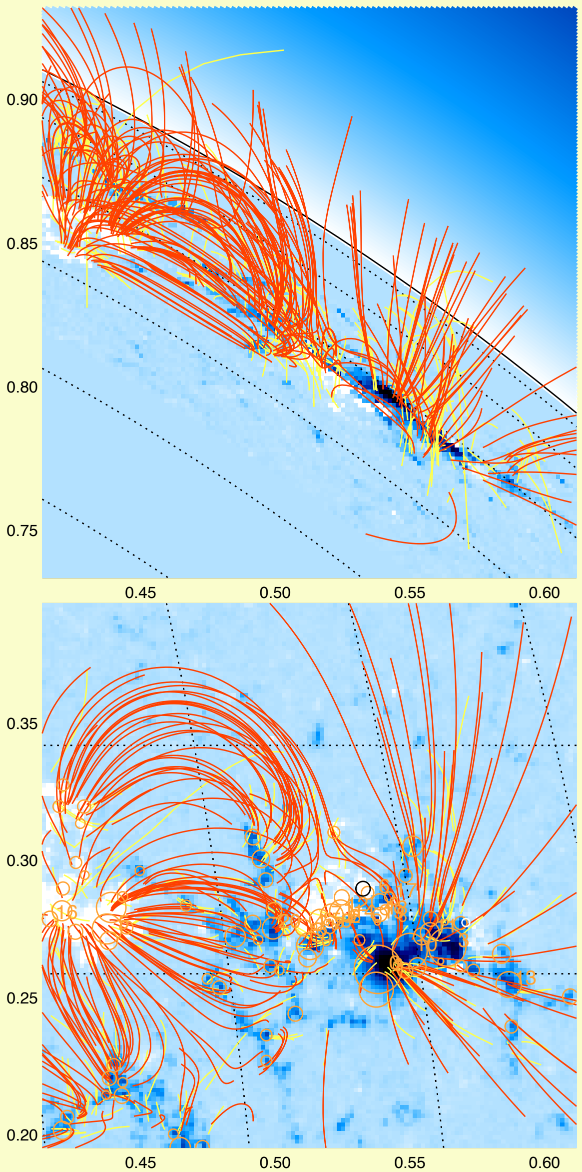

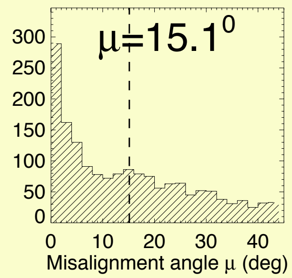

NOAA	=12017
Hel.pos.	=N11W32
FOV	=0.20
[x1,x2]	= 0.4134, 0.6134
[y1,y2]	= 0.1954, 0.3954
wave,nsm1,	= 6, 3
thresh0,2,nsig	= 0.00, 0.01, 3.00
rmin,lmin,ngap	= 15, 15, 0
ds,nh	=0.0020, 10
dx_euv	= 0.000625 R_{sun}
dx_mag	= 0.001500 R_{sun}
nmag	= 100 / 100
n_nlfff	= 97
dprox,magwid	= 5.000, 2.0
nloopw,qripple	= 200, 0.50
nall,ngood,nf	= 406/275/275
n1,n2,n3,n4,n5	=116/1/1/13/0
niter	= 10 / 20/ 20
hmin,hmax	=0.001, 0.050
nseg,mdim	= 7, 2
nsmax	= 200
da0	= 1.0
misalign	= 15.1 deg
div-free	= 9.2e-07
force-free	= 4.8e-07
weight curr	= 1.5e-01
qB_rebin	= 1.035
qB_model	= 1.233
qiso_corr	= 2.467
E_P	= 211.2 x 10^{30} erg
E_free	= 1.5 x 10^{30} erg
E_NP/E_P	= 1.007
CPU	= 324.0 s

20140329_182300, EVENT=592, FRAME=26 / 26, RUN=AIA_UV_05

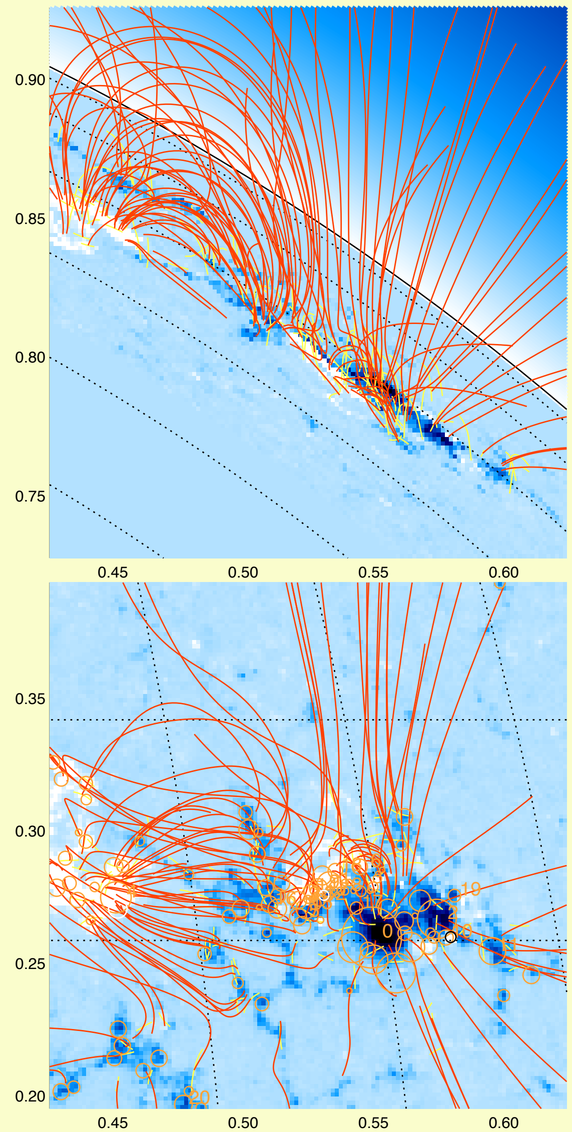

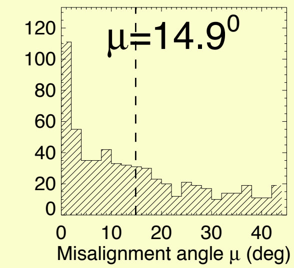

NOAA	=12017
Hel.pos.	=N11W32
FOV	=0.20
[x1,x2]	= 0.4257, 0.6257
[y1,y2]	= 0.1954, 0.3954
wave,nsm1,	= 2, 3
thresh0,2,nsig	= 0.00, 0.05, 3.00
rmin,lmin,ngap	= 15, 10, 0
ds,nh	=0.0020, 10
dx_euv	= 0.000634 R_{sun}
dx_mag	= 0.001500 R_{sun}
nmag	= 100 / 100
n_nlfff	= 97
dprox,magwid	= 5.000, 2.0
nloopw,qripple	= 200, 0.50
nall,ngood,nf	= 204/102/102
n1,n2,n3,n4,n5	=78/0/0/24/0
niter	= 10 / 20/ 20
hmin,hmax	=0.001, 0.200
nseg,mdim	= 7, 2
nsmax	= 200
da0	= 1.0
misalign	= 14.9 deg
div-free	= 7.2e-07
force-free	= 6.4e-05
weight curr	= 7.7e-01
qB_rebin	= 1.034
qB_model	= 1.180
qiso_corr	= 2.467
E_P	= 197.2 x 10^{30} erg
E_free	= 7.6 x 10^{30} erg
E_NP/E_P	= 1.038
CPU	= 134.7 s

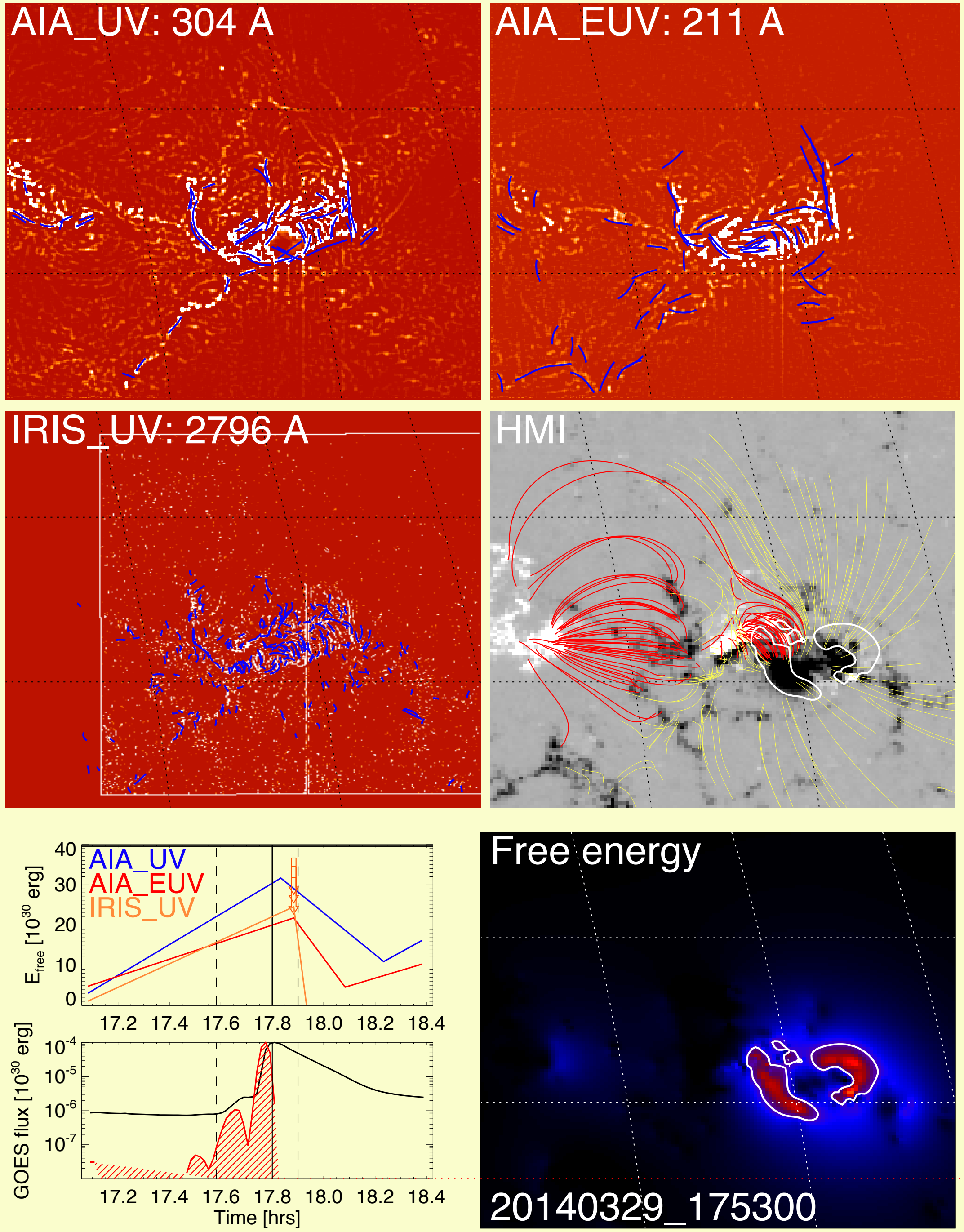
AIA_UV: 304 A
AIA_EUV: 211 A
IRIS_UV: 2796 A
HMI
AIA_UV
AIA_EUV
IRIS_UV
E_free [10^30 erg]
GOES flux [10^30 erg]
Time [hrs]
Free energy
20140329_175300

Slide 23

Time evolution of free energy:

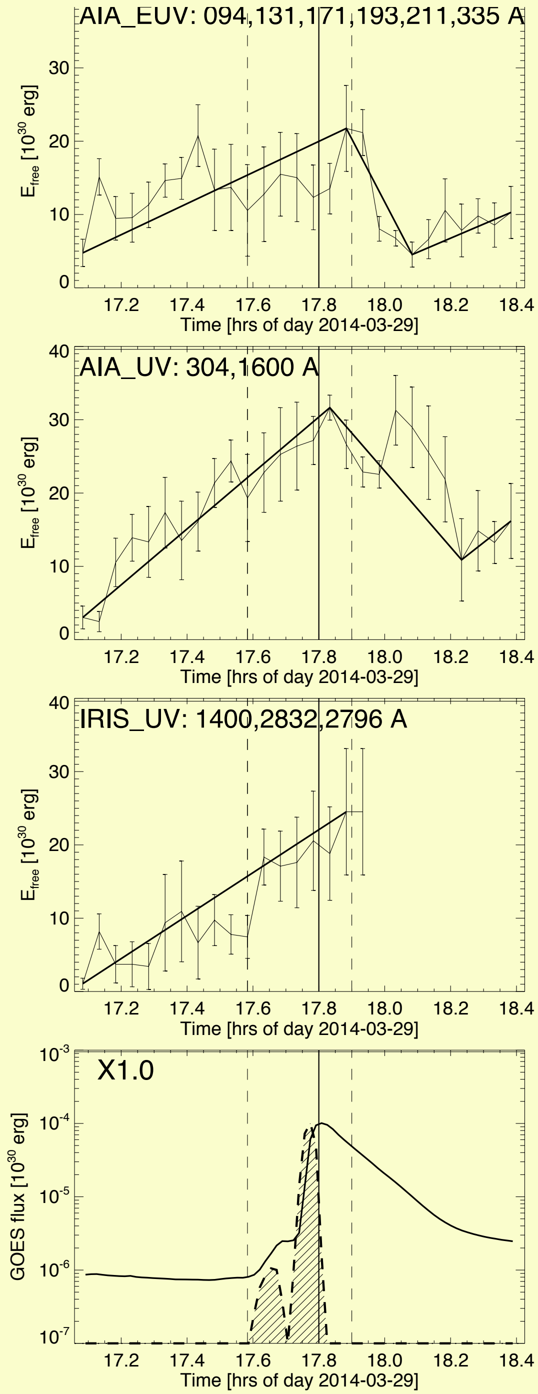

Coronal (AIA-EUV)

Chromospheric (AIA-UV)

Chromospheric (IRIS)

GOES 1-8 A flux & time derivative

Observations with AIA, IRIS, IBIS, & ROSA

Observation date and time [UT]	Active Region NOAA	Heliographic Position [deg]	Instrument	Wavelength Å	Temperature range log(T[K])
2010-08-03 15:23:00	11092	N12W02	AIA	171, 193, 211	5.8-7.3
2010-08-03 15:23:00	11092	N12W02	AIA	304	4.7
2010-08-03 15:23:00	11092	N12W02	IBIS	8542	3.8
2010-08-03 15:23:00	11092	N12W02	IBIS	6563	3.8
2014-08-24 14:06:38	12146	N09W25	AIA	171, 193, 211	5.8-7.3
2014-08-24 14:06:38	12146	N09W25	AIA	304	4.7
2014-08-24 14:06:38	12146	N09W25	ROSA	6563	3.8
2014-08-30 14:40:22	12149	N12W44	AIA	171, 193, 211	5.8-7.3
2014-08-30 14:40:22	12149	N12W44	AIA	304	4.7
2014-08-30 14:40:22	12149	N12W44	IRIS	2796	3.7-4.2
2014-08-30 14:40:22	12149	N12W44	ROSA	6563	3.8

Aschwanden, Reardon, and Jess (2016; ApJ subm).

IBIS Ca II 8542 A image of active region NOAA 11092, observed on 2010 Aug 3, 15:03-15:43 UT, FOV=0.1 R_{sun}, pixel=0.1”

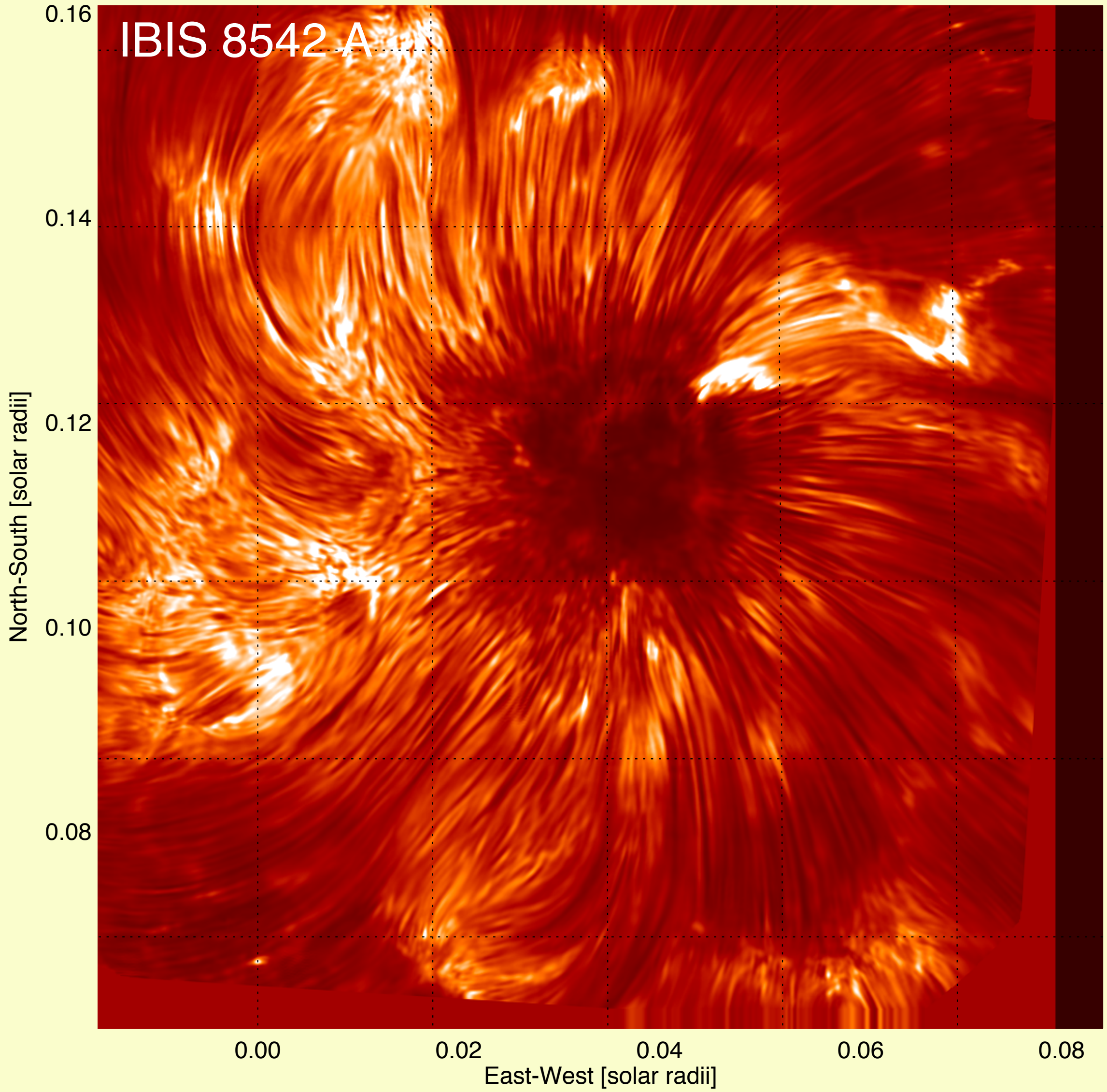

Aschwanden, Reardon & Jess (2016)

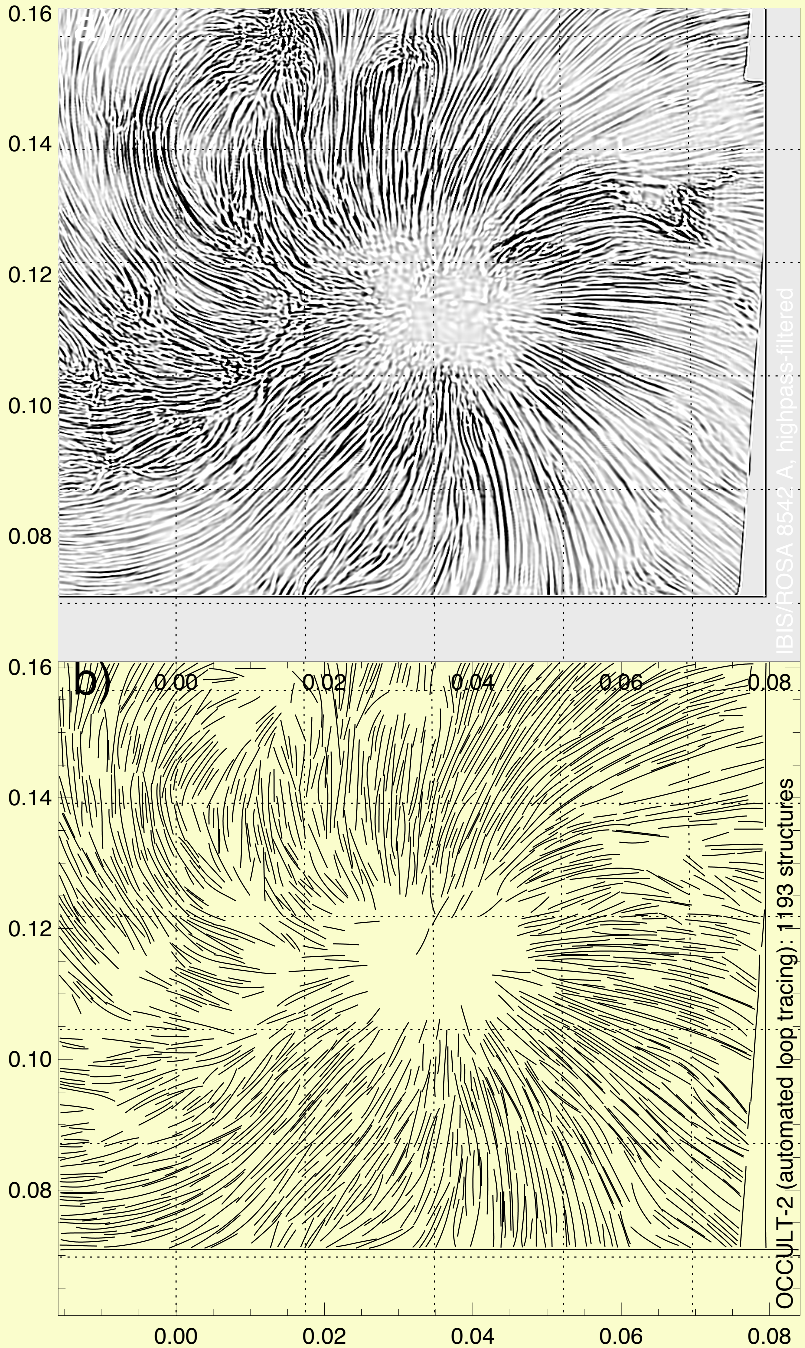

Highpass-filtered image of IBIS 8542 A

Automated tracing of curvi-linear Features with OCCULT-2 code
→ 1193 features

Union-finding algorithm

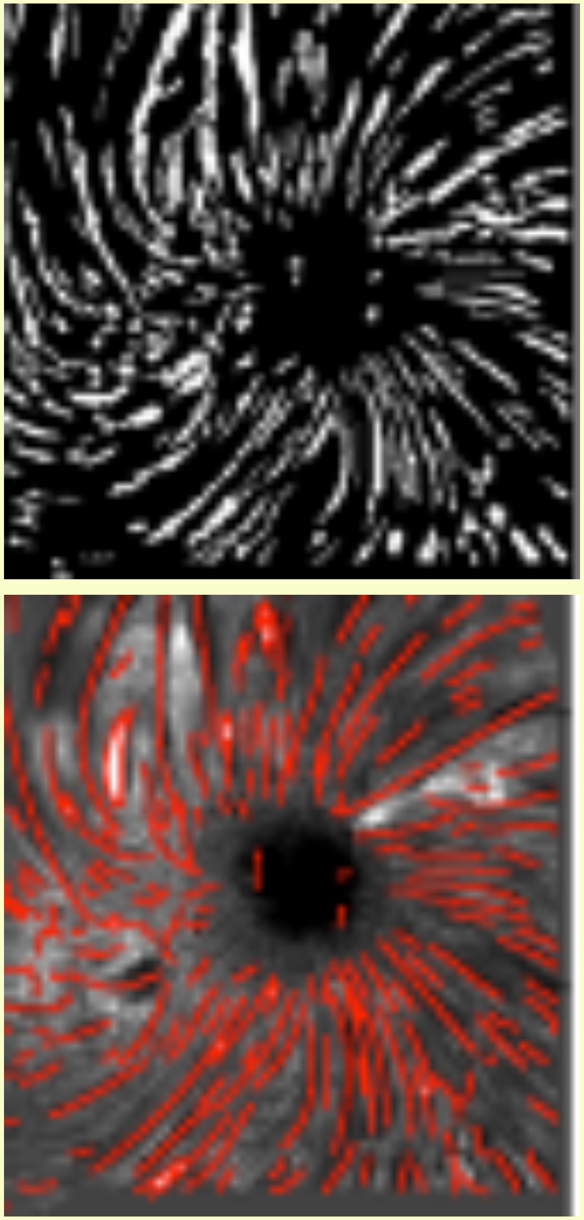

Sedgewick (2002); Jing et al. (2011)

Oriented Coronal CUrvature Loop Tracing algorithm (OCCULT-2)

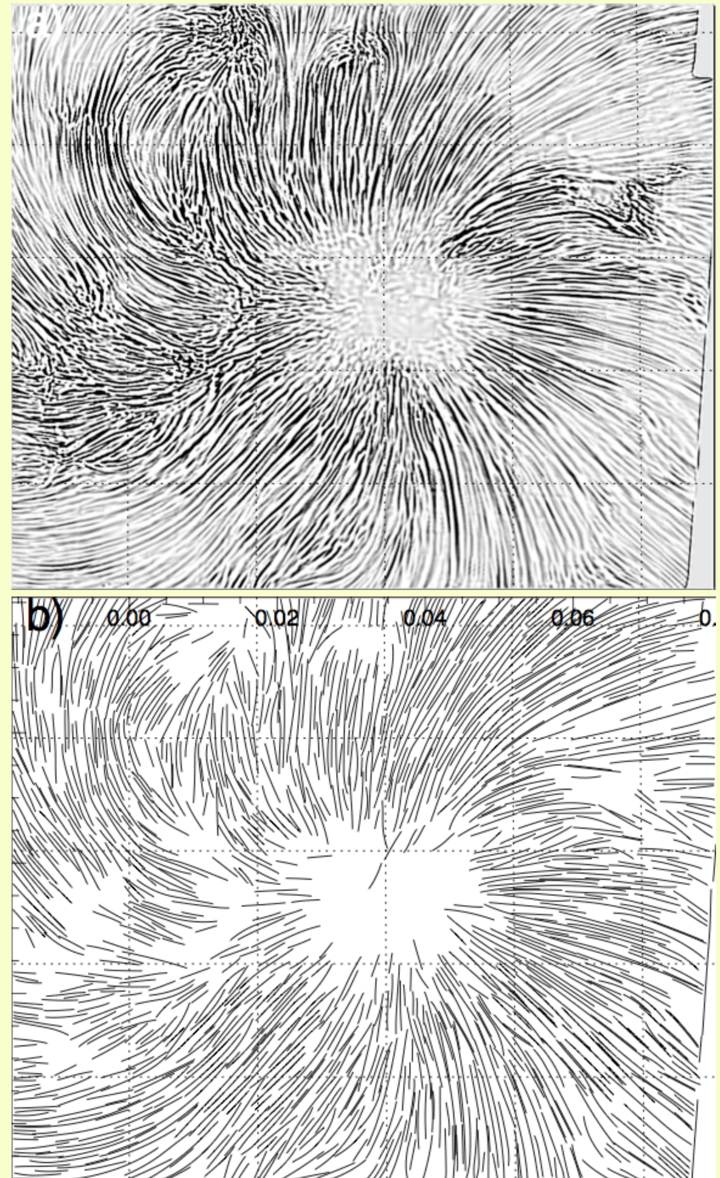

Aschwanden et al. (2013; 2016)

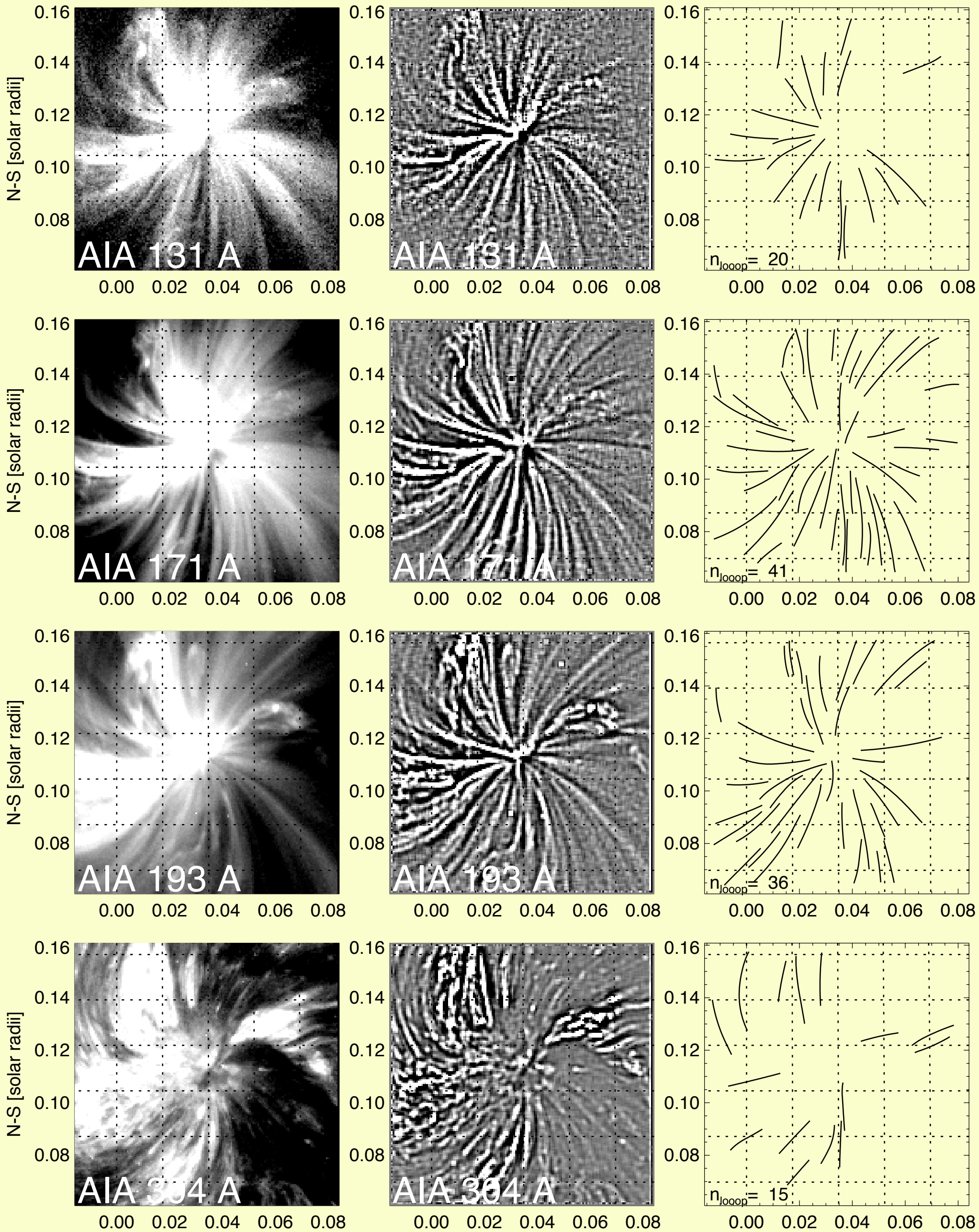

Tracing of coronal loop structures in 131, 171, 193, 304 A

AIA/SDO (0.6” pixel) has a 6 times lower resolution than IBIS (0.1” pixels)

The number of pixels is 36 times smaller, explaining the smaller number of detected structures: N=15-41 in AIA, vs. N=1193 fibrils in IBIS

20100803_152300, time step=1, AIA/SDO 94, 131, 171, 193, 211, 335 A

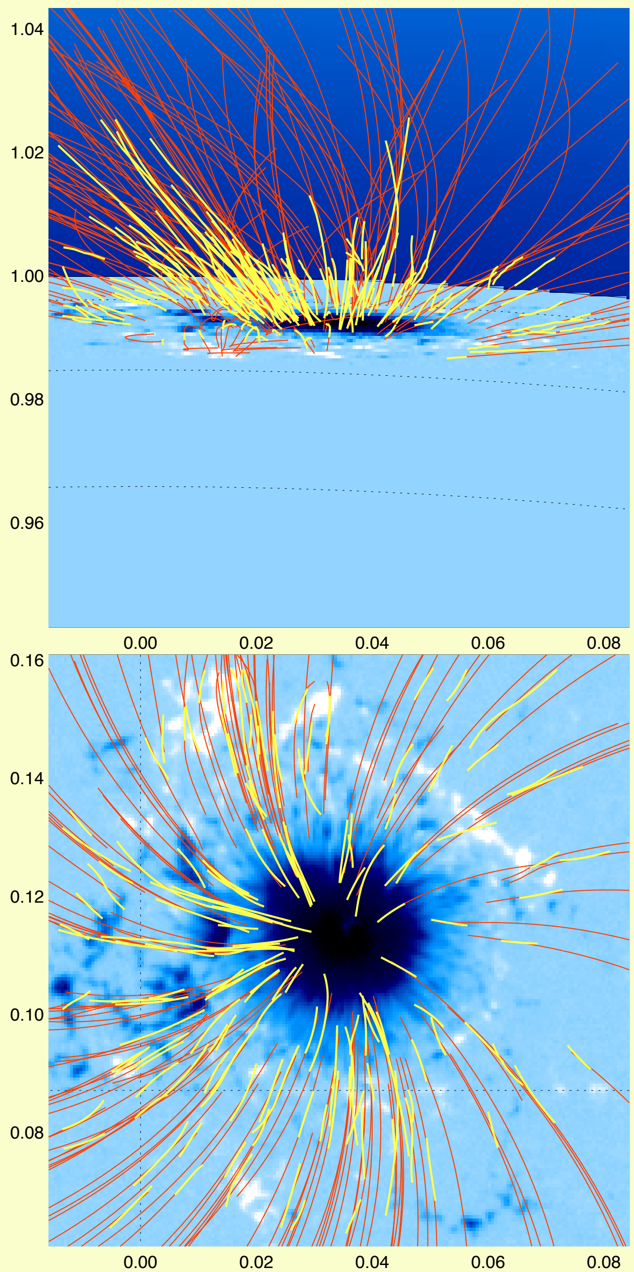

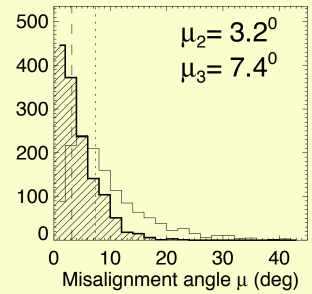

INPUT:

Instrument	=AIA
NOAA	=11092, N12W02
Wavelengths	=94,131,171,193,211,3
fov	=0.100
amis	= 20.0
nsm1	= 1
nmag_p,np	= 30, 30
nstruc	=1000
nitmin,nitmax	= 40, 100
prox_min	=10.0
lmin,rmin	= 5, 8
qthresh1,2	= 0.00, 0.00

OUTPUT:

[x1,x2]	=-0.0159, 0.0841
[y1,y2]	= 0.0608, 0.1608
dpix HMI	=0.0005, 0.51 arcsec
dpix AIA	=0.0006, 0.61 arcsec
nloop,ndet	= 155 / 209
nloop/ndet	= 0.742
misalign	= 3.2, 7.4 deg
div-free	= 1.2e-02
force-free	= 1.9e-02
weight curr	= 9.9e-01
qe_rebin	= 0.985
qe_model	= 1.014
qiso_corr	= 2.467
E_P	= 581.3 x 10^{30} erg
E_free	= 16.4 x 10^{30} erg
E_NP/E_P	= 1.028
Iterations	= 42
CPU	= 98.0 s

Forward-fitting of VCA-NLFFF code to 209 structures detected with AIA and traced with OCCULT-2 (yellow)

The NLFFF field (red) has a potential energy of E_P=581x10^{30} erg, and a free energy of E_{np}=16x10^{30} erg, With E_{np}/E_p=1.028

Misalignment angles:
3.2 deg (2D)
7.4 deg (3D)

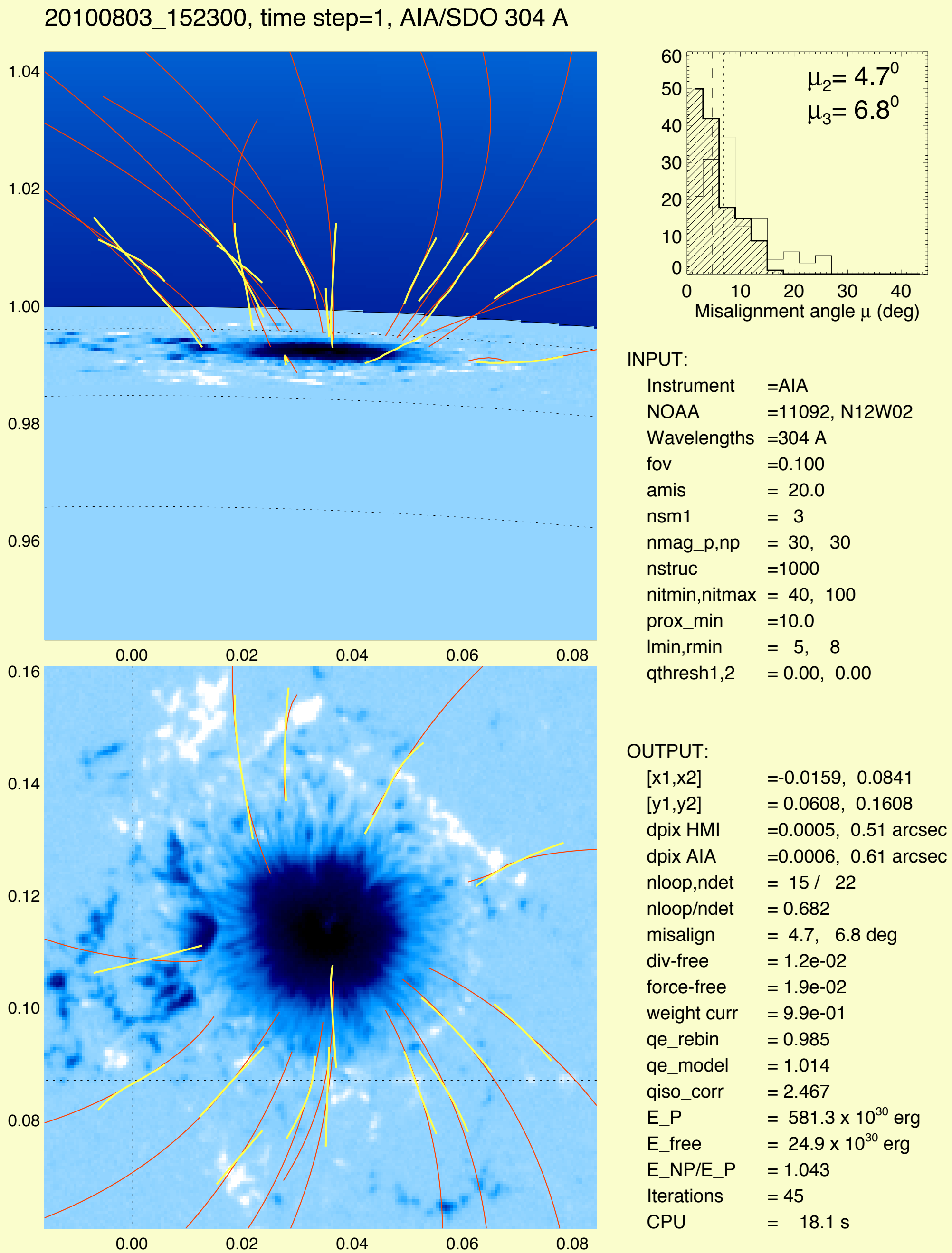

Forward-fitting of VCA-NLFFF code to 22 structures detected with AIA 304 and traced with OCCULT-2 (yellow)

The NLFFF field (red) has a potential energy of E_P=581x10^{30} erg, and a free energy of E_{np}=24x10^{30} erg, With E_{np}/E_p=1.043

Misalignment angles:
4.7 deg (2D)
6.8 deg (3D)

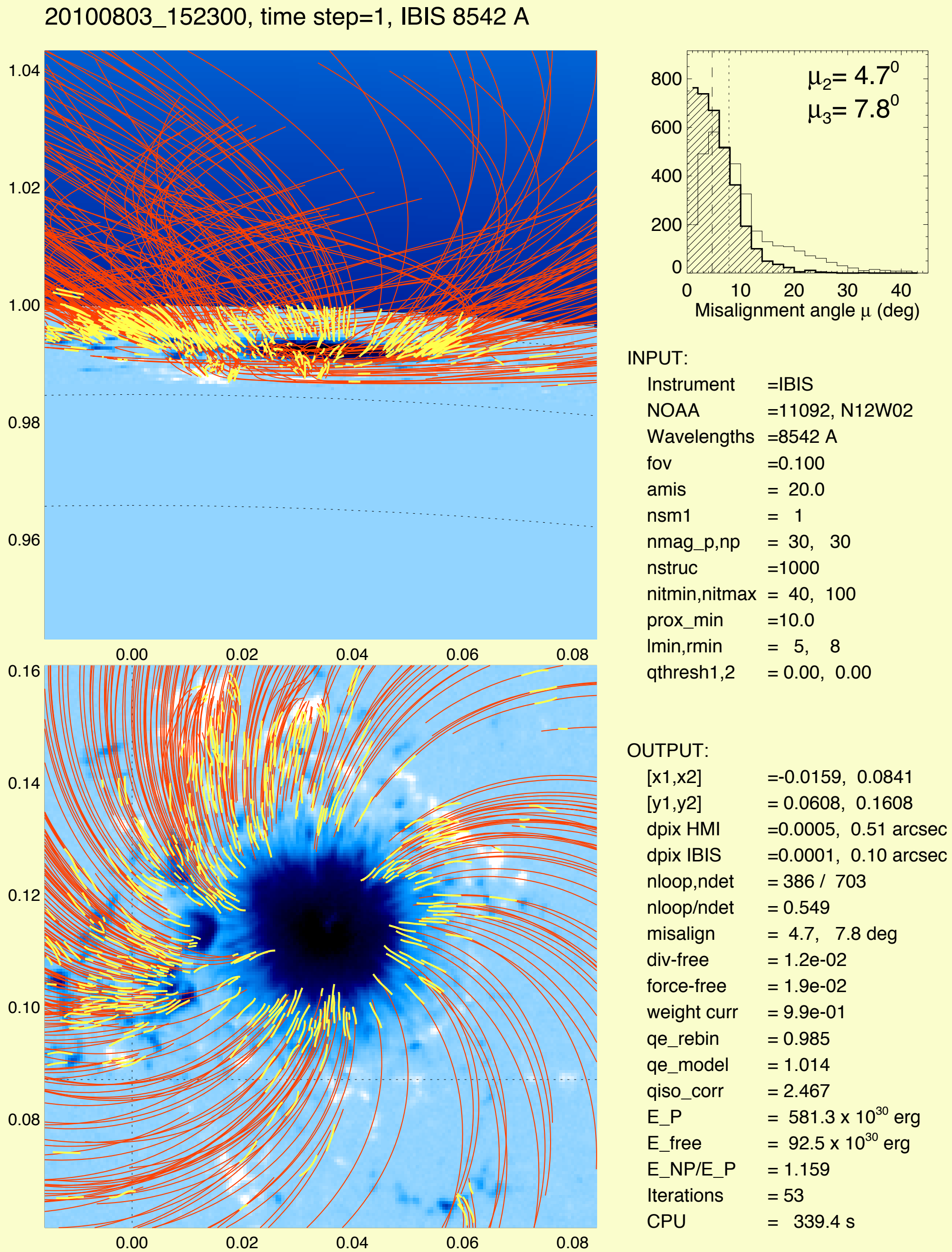

Forward-fitting of VCA-NLFFF code To 703 structures detected with IBIS 8542 A and traced with OCCULT-2 (yellow)

The NLFFF field (red) has a potential energy of E_P=581x10^{30} erg, and a free energy of E_{np}=92x10^{30} erg, With E_{np}/E_p=1.159

Misalignment angles:
4.7 deg (2D)
7.8 deg (3D)

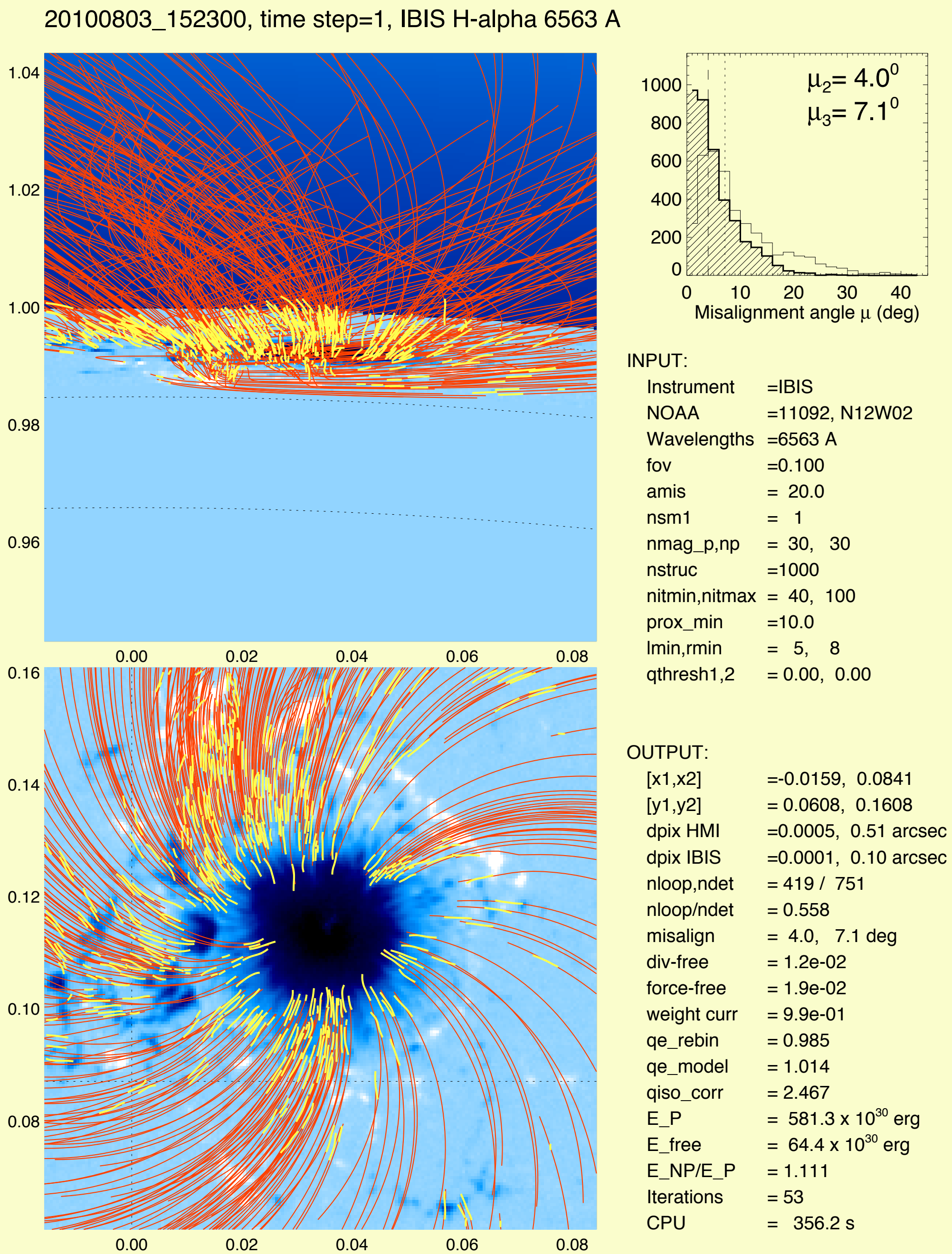

Forward-fitting of VCA-NLFFF code To 703 structures detected with IBIS Ha 6563 A and traced with OCCULT-2 (yellow)

The NLFFF field (red) has a potential energy of E_P=581x10^{30} erg, and a free energy of E_{np}=64x10^{30} erg, With E_{np}/E_p=1.111

Misalignment angles:
4.7 deg (2D)
7.8 deg (3D)

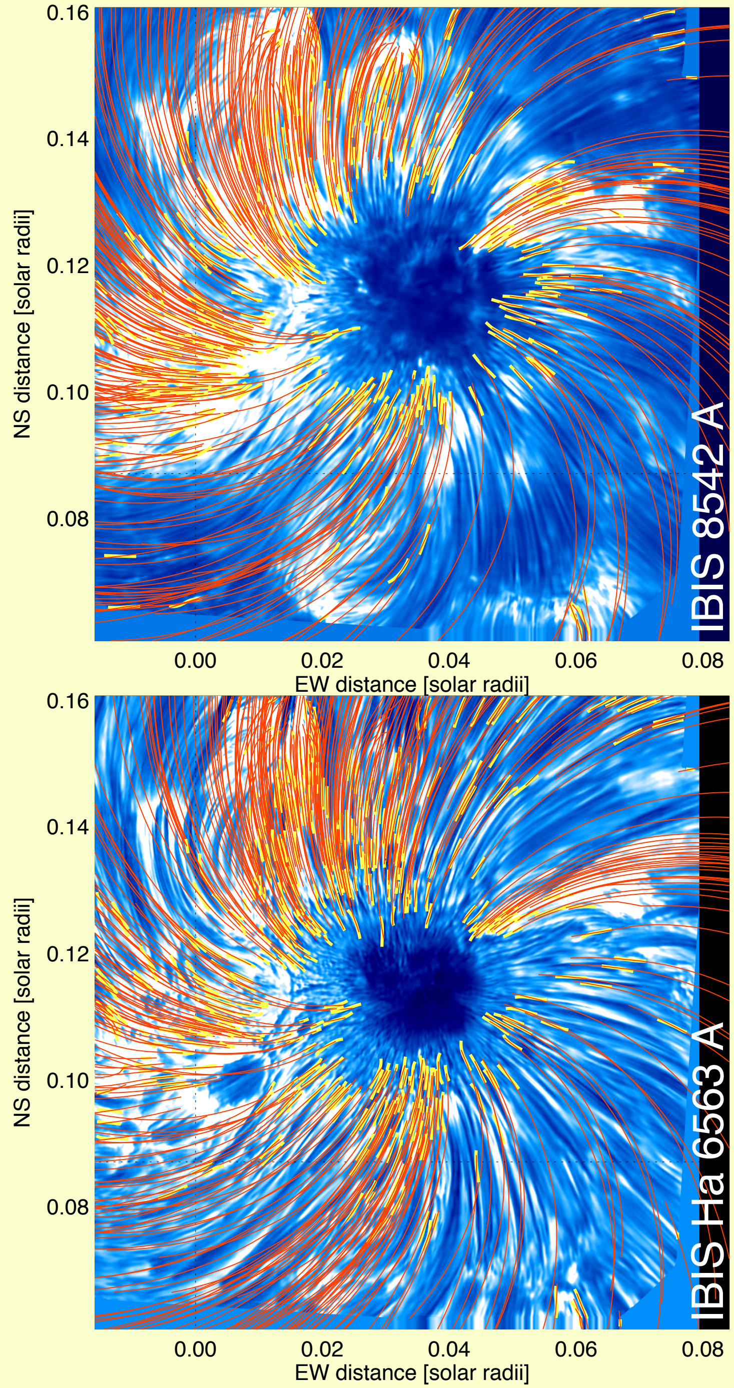

Overlay of forward-fitted
VCA-NLFFF solution
on fibril structures
detected with lthe
OCCULT-2 code,
Oberlayed on
IBIS Ha 6563 A (bottom)
and Ca II 8542 A (top)
Images.

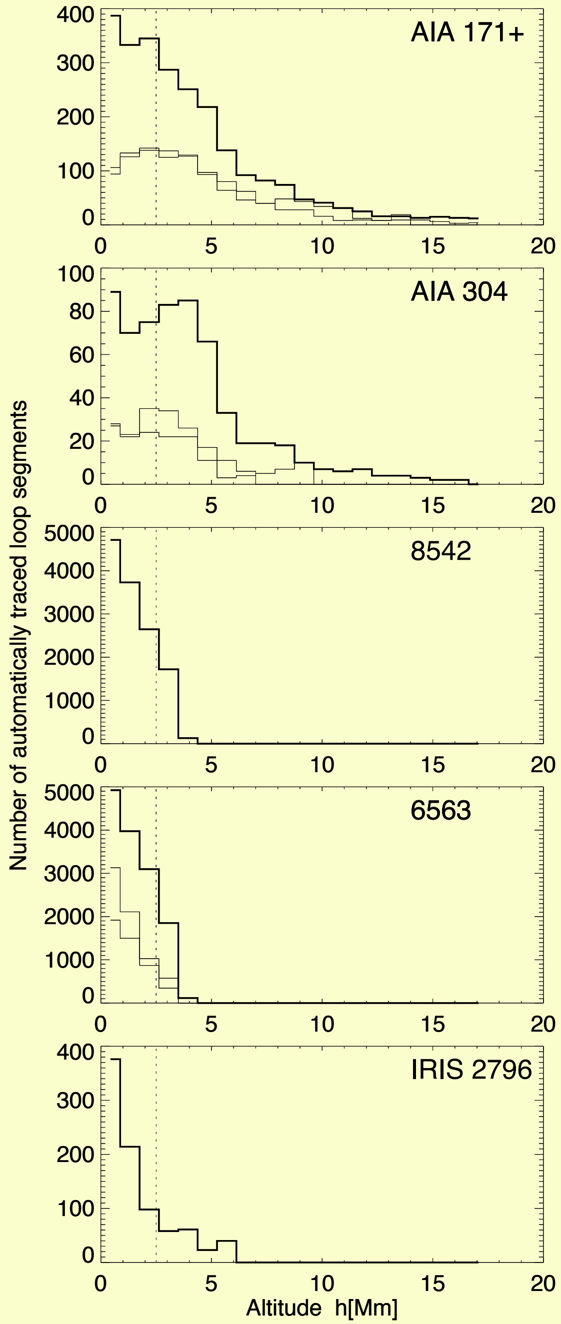

Altitude contribution function

The altitude distribution of the automatically traced curvi-linear elements is obtained from the 3D-model of the magnetic non-potential field solution (VLA-NLFFF).

Chromospheric fibrils observed in Ca II 8542 A, Ha 6563 A, and IRIS Mg II 2796 appear to be confined to altitudes of h < 4000 km.

Coronal loops observed with AIA 121, 171, 193 A as well as 304 A extend to altitudes up to h< 15,000 km.

Free energy in active regions

Observation date	Instrument	Detected loops n_{det}	Fitted loops n_{loop}	Misalignment angle 2-D μ_2 [deg]	Misalignment angle 3-D μ_3 [deg]	Potential energy E_P [10^{30} erg]	Free energy ratio q_{free}
2010-08-03	AIA 171+	222 ± 76	167 ± 36	$5.0° \pm 3.2°$	$7.8° \pm 0.5°$	571	0.03 ± 0.01
2010-08-03	AIA 304	63 ± 27	38 ± 14	$4.2° \pm 0.4°$	$7.2° \pm 0.9°$	571	0.06 ± 0.03
2010-08-03	IBIS 8542	656 ± 121	338 ± 62	$4.0° \pm 0.6°$	$7.1° \pm 0.7°$	571	0.13 ± 0.04
2010-08-03	IBIS 6563	712 ± 114	421 ± 75	$4.0° \pm 0.4°$	$7.2° \pm 0.8°$	571	0.11 ± 0.01
2014-08-24	AIA 171+	186 ± 88	82 ± 30	$5.5° \pm 1.3°$	$8.9° \pm 1.5°$	551	0.18 ± 0.06
2014-08-24	AIA 304	45 ± 21	17 ± 6	$7.4° \pm 2.2°$	$7.5° \pm 1.5°$	551	0.11 ± 0.05
2014-08-24	ROSA 6563	654 ± 98	232 ± 75	$6.5° \pm 1.3°$	$8.5° \pm 1.8°$	551	0.26 ± 0.01
2014-08-30	AIA 171+	190 ± 87	83 ± 34	$5.4° \pm 1.2°$	$10.9° \pm 2.4°$	559	0.10 ± 0.05
2014-08-30	AIA 304	43 ± 22	16 ± 7	$7.0° \pm 1.0°$	$10.7° \pm 2.4°$	559	0.10 ± 0.09
2014-08-30	IRIS 2796	206 ± 52	65 ± 19	$6.1° \pm 1.4°$	$11.3° \pm 2.5°$	559	0.26 ± 0.01
2014-08-30	ROSA 6563	556 ± 89	299 ± 79	$6.6° \pm 0.5°$	$14.2° \pm 2.3°$	559	0.17 ± 0.04

The free energy is underestimated by a factor of 2-4 from coronal loops compared with chromospheric fibrils observed with IBIS and/or ROSA
→Is larger amount of nonpotential or free energy due to higher spatial resolution? Are chromospheric fibrils more non-potential than coronal loops?

Plasma β-parameter of chromospheric tracers

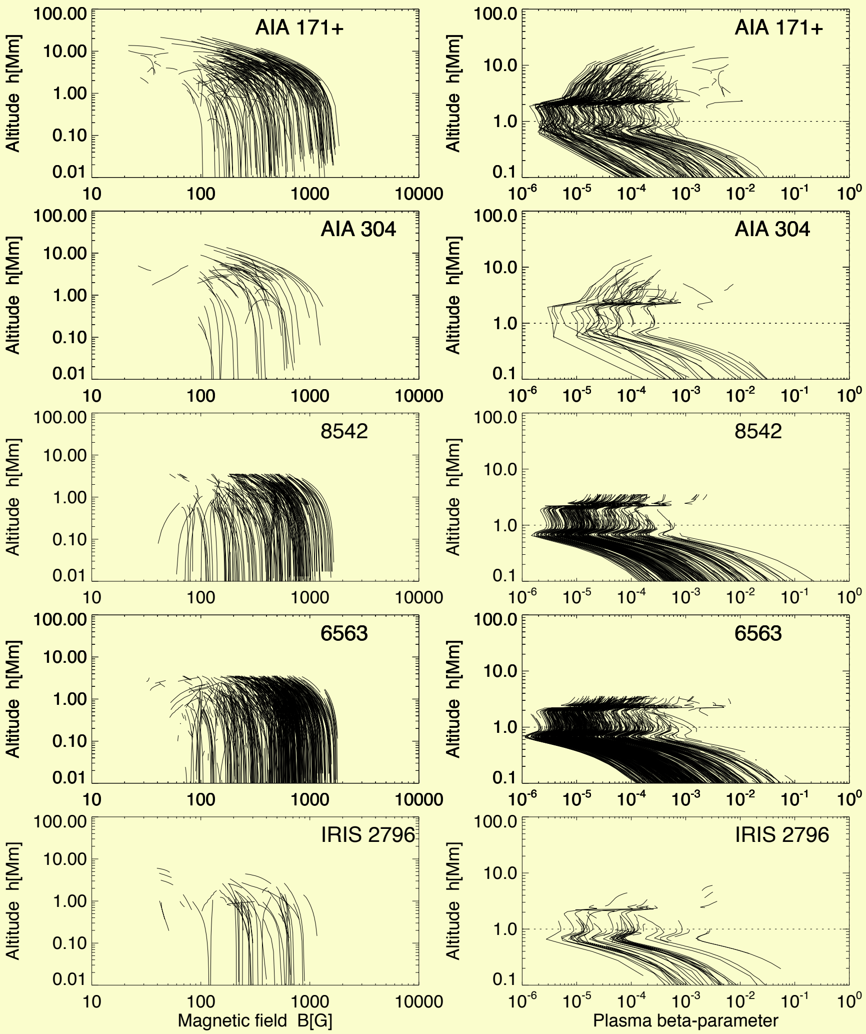

$$\beta(h) = \frac{p_{th}(h)}{p_{mag}(h)} = 6.94 \times 10^{-15} n_e(h) T_e(h) B(h)^{-2} \, .$$

The magnetic field of traced coronal loops and chromospheric fibrils varies in the range of B=100-1000 G.

The plasma β-parameter of fibrils and loops varies in a range of B=10^{-5}-10^{-1},
→ Confirms magnetic confinment in corona and upper chromosphere.

Outline of Talk:

1) Previous work on chromospheric magnetic fields

2) The VCA-NLFFF method to compute magnetic fields:
   - 2.1 Potential field from buried magnetic sources
   - 2.2 Automated tracing of curvi-linear features
   - 2.3 Forward-fitting of nonpotential magnetic field

3) Data Analysis:
   - AIA/SDO, HMI/SDO
   - IRIS
   - IBIS
   - ROSA

4) Conclusions:
   - Suitability of chromospheric field tracing
   - Altitudes of chromospheric magnetic field tracers
   - Coronal vs. chromospheric free energy

Conclusions:

(1) Chromospheric images reveal crisp curvi-linear structures (loop segments, fibrils, spicules) that are extremely well-suited for constraining magnetic models.

(2) The chromospheric fibrils are field-aligned with the best-fit VCA-NLFFF solution within a misalignment angle of 4^0-7^0.

(3) The free (non-potential excess) energy obtained from coronal loops under-estimates that of chromospheric features by a factor of 2-4.

(4) Chromospheric features are confined to altitudes of $h<4000$ km, while coronal structures are detected up to $h<15,000$ km

(5) The plasma β-parameter is β=10-5-10-1 for fibrils and loops, and the magnetic field is B=100-1000 G.

(6) Chromospheric data are important for magnetic modeling and free energy estimates for flares, CMEs, and coronal heating.

http://www.lmsal.com/~aschwand/2016_chromo_aschwanden.ppt

SSW

VCA-NLFFF code: http://www.lmsal.com/~aschwand/software/
OCCULT-2 code: http://www.lmsal.com/~aschwand/software/

Appendix :

The Vertical-Current Approximation Nonlinear Force-Free Field Code – Description, Performance Tests, and Measurements of Magnetic Energies Dissipated in Solar Flares

(Aschwanden 2016, subm.)

Vertical Current Approximation Non-Linear Force-Free Field (VCA-NLFFF) Code

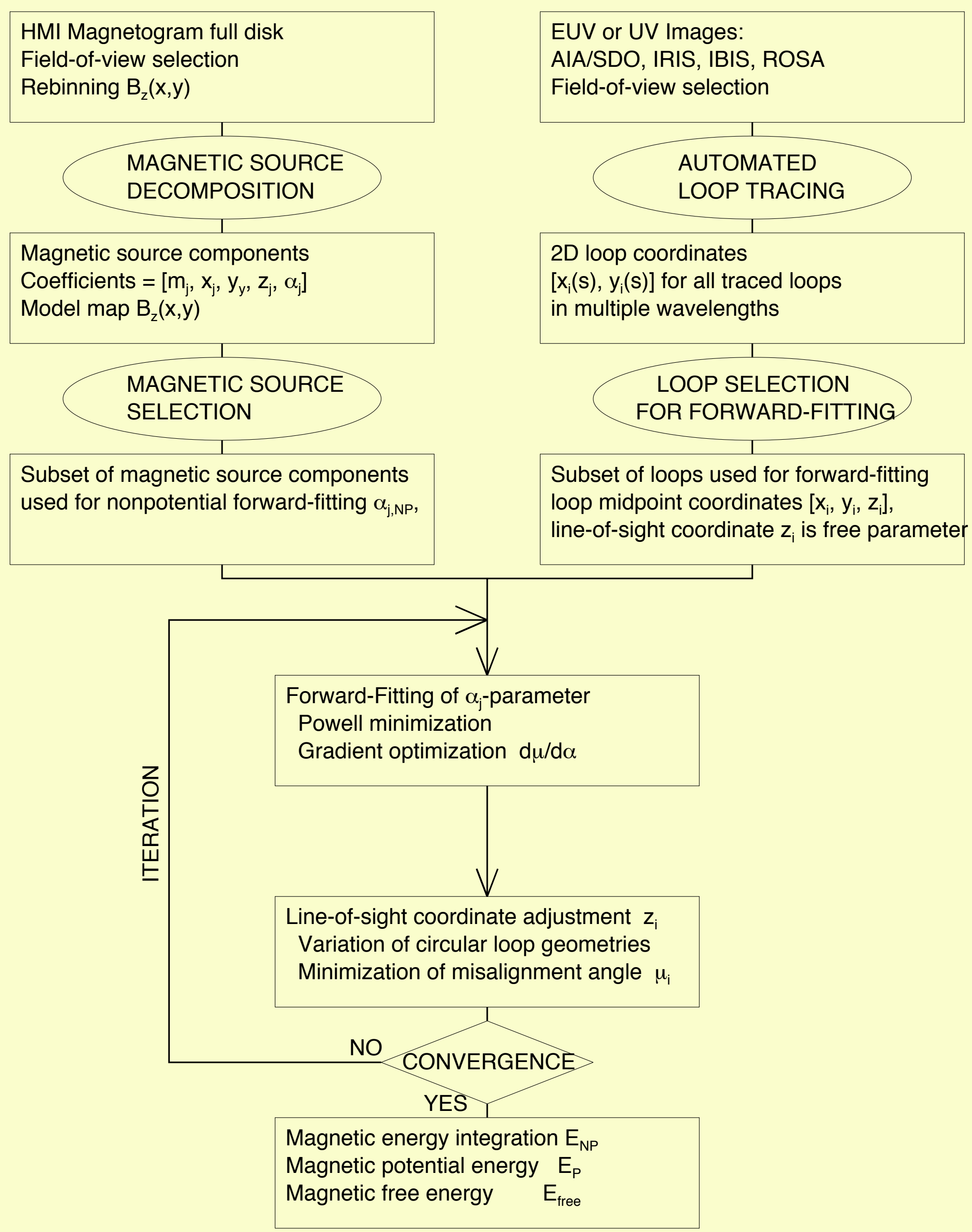

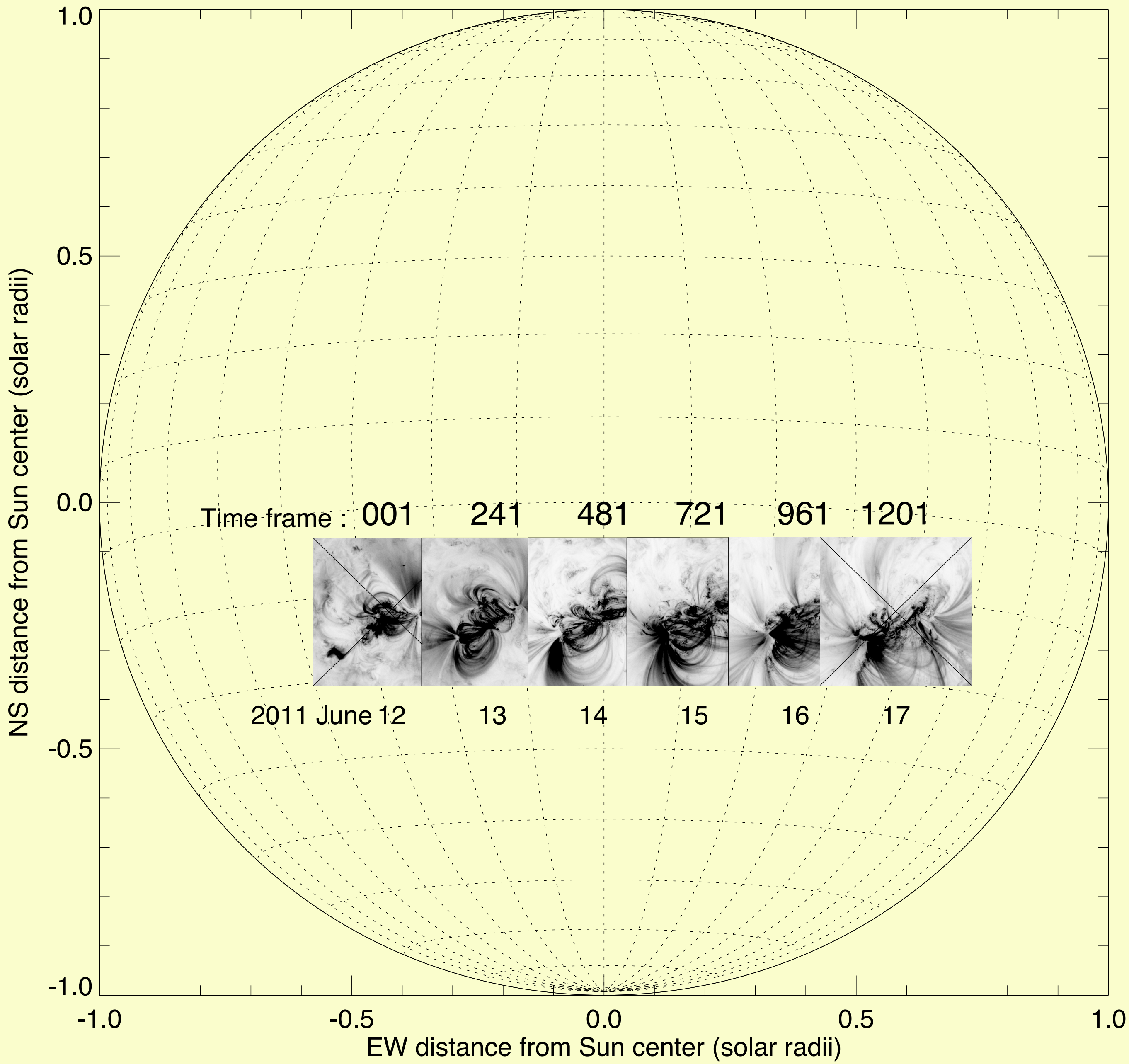
Time frame : 001 241 481 721 961 1201
2011 June 12 13 14 15 16 17
1.0
0.5
0.0
-0.5
-1.0
NS distance from Sun center (solar radii)
-1.0 -0.5 0.0 0.5 1.0
EW distance from Sun center (solar radii)

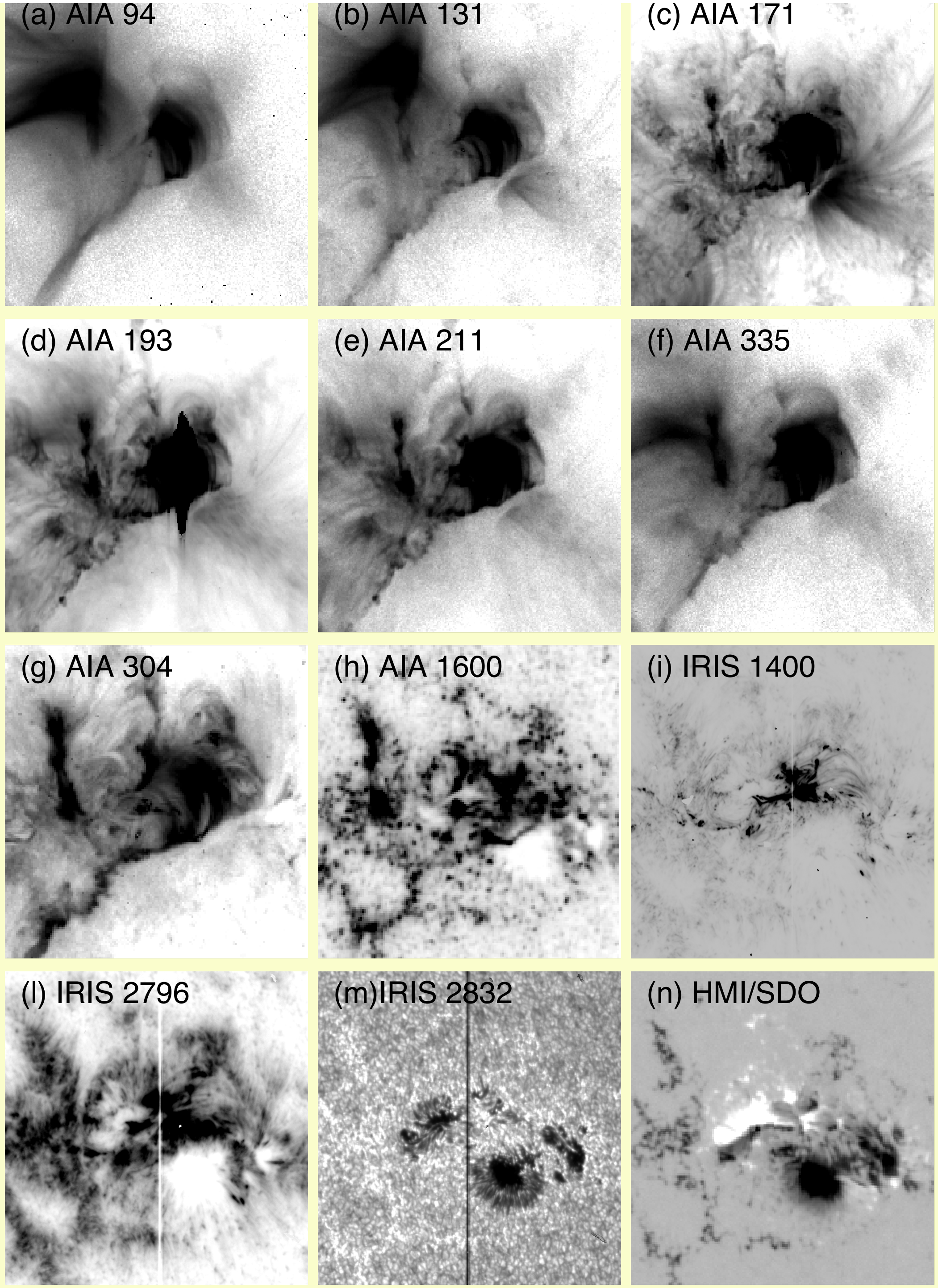
(a) AIA 94
(b) AIA 131
(c) AIA 171
(d) AIA 193
(e) AIA 211
(f) AIA 335
(g) AIA 304
(h) AIA 1600
(i) IRIS 1400
(l) IRIS 2796
(m)IRIS 2832
(n) HMI/SDO

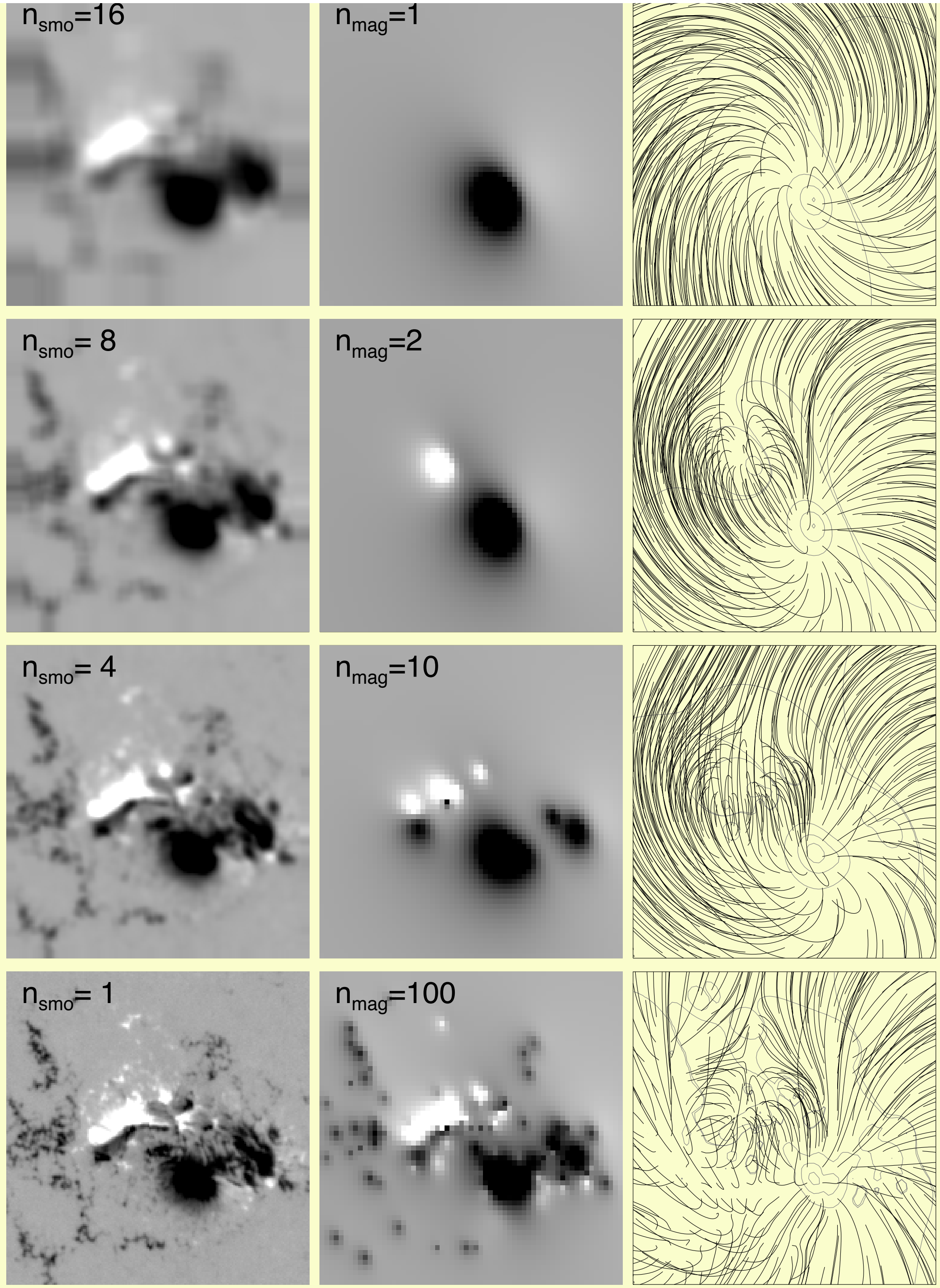

n_{smo}=16
n_{mag}=1
n_{smo}= 8
n_{mag}=2
n_{smo}= 4
n_{mag}=10
n_{smo}= 1
n_{mag}=100

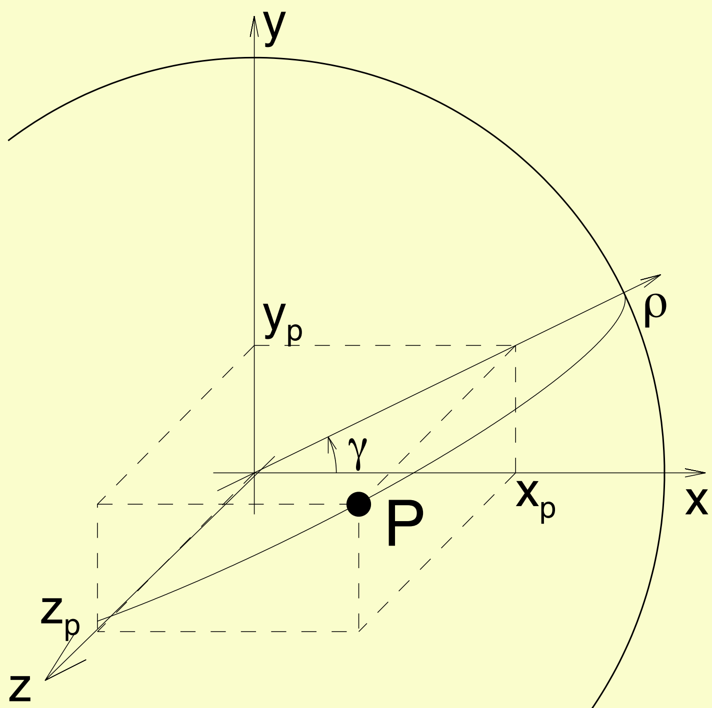
y
y_p
ρ
γ
x_p
x
P
z_p
z

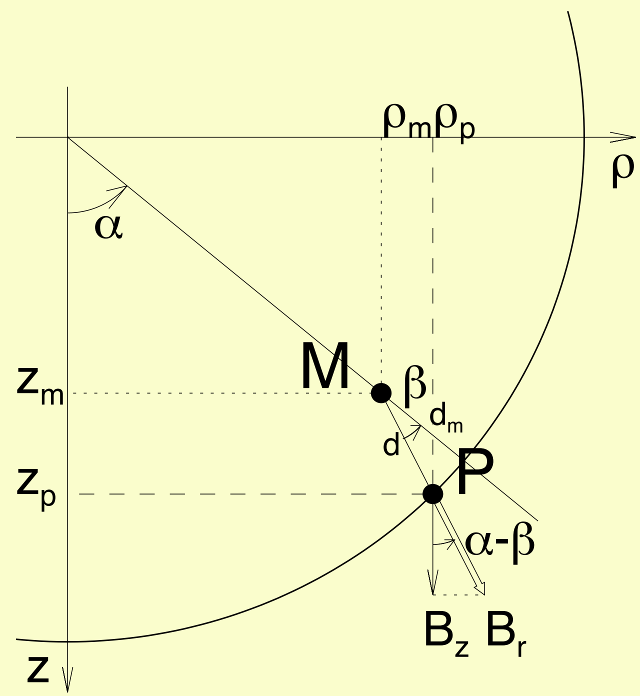
$\rho_m \rho_p$
ρ
α
z_m
M
β
d_m
d
z_p
P
α-β
B_z B_r
z

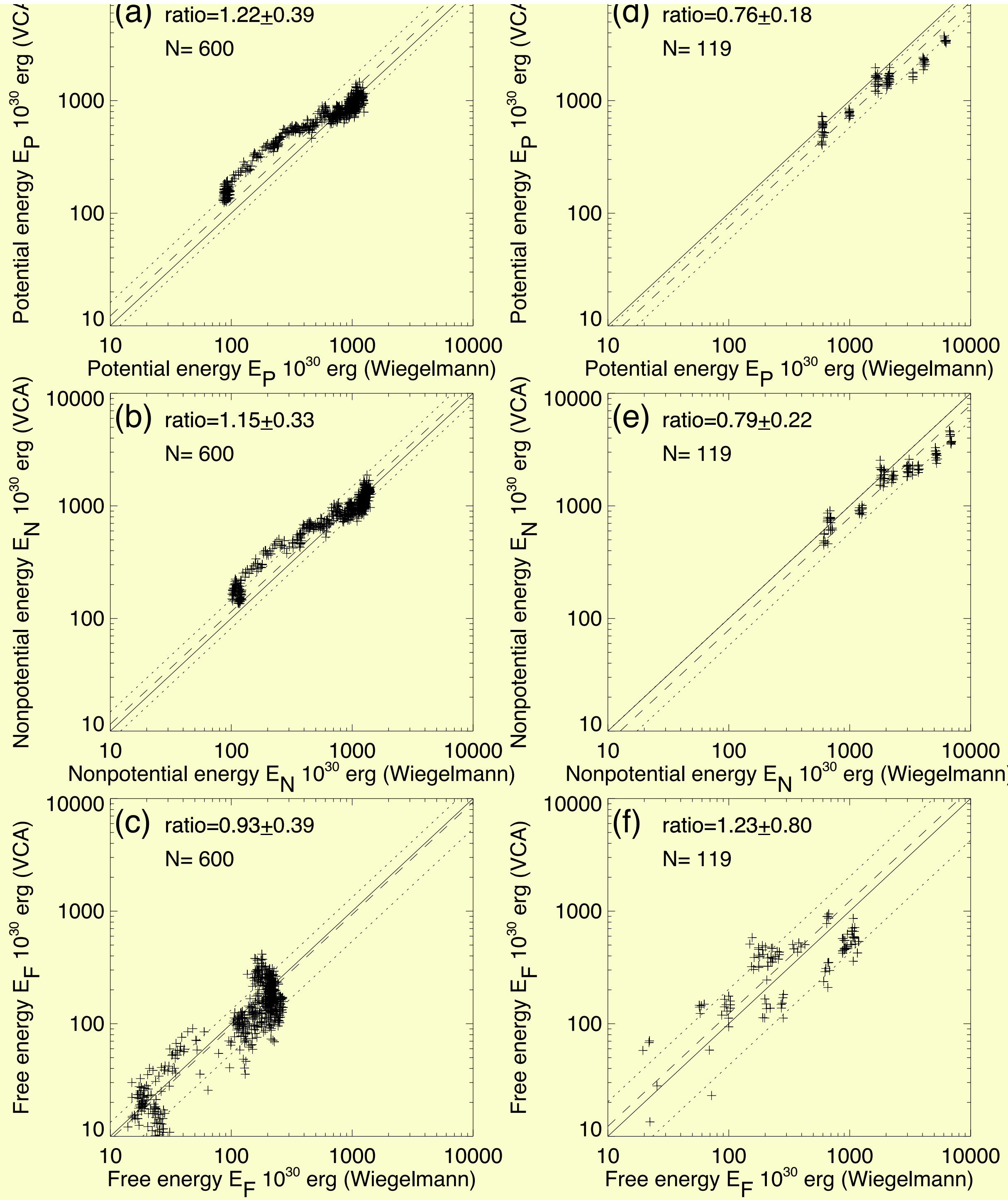
(a) ratio=1.22±0.39
N= 600
Potential energy E_P 10^{30} erg (VCA)
Potential energy E_P 10^{30} erg (Wiegelmann)
(b) ratio=1.15±0.33
N= 600
Nonpotential energy E_N 10^{30} erg (VCA)
Nonpotential energy E_N 10^{30} erg (Wiegelmann)
(c) ratio=0.93±0.39
N= 600
Free energy E_F 10^{30} erg (VCA)
Free energy E_F 10^{30} erg (Wiegelmann)
(d) ratio=0.76±0.18
N= 119
(e) ratio=0.79±0.22
N= 119
(f) ratio=1.23±0.80
N= 119
10
100
1000
10000

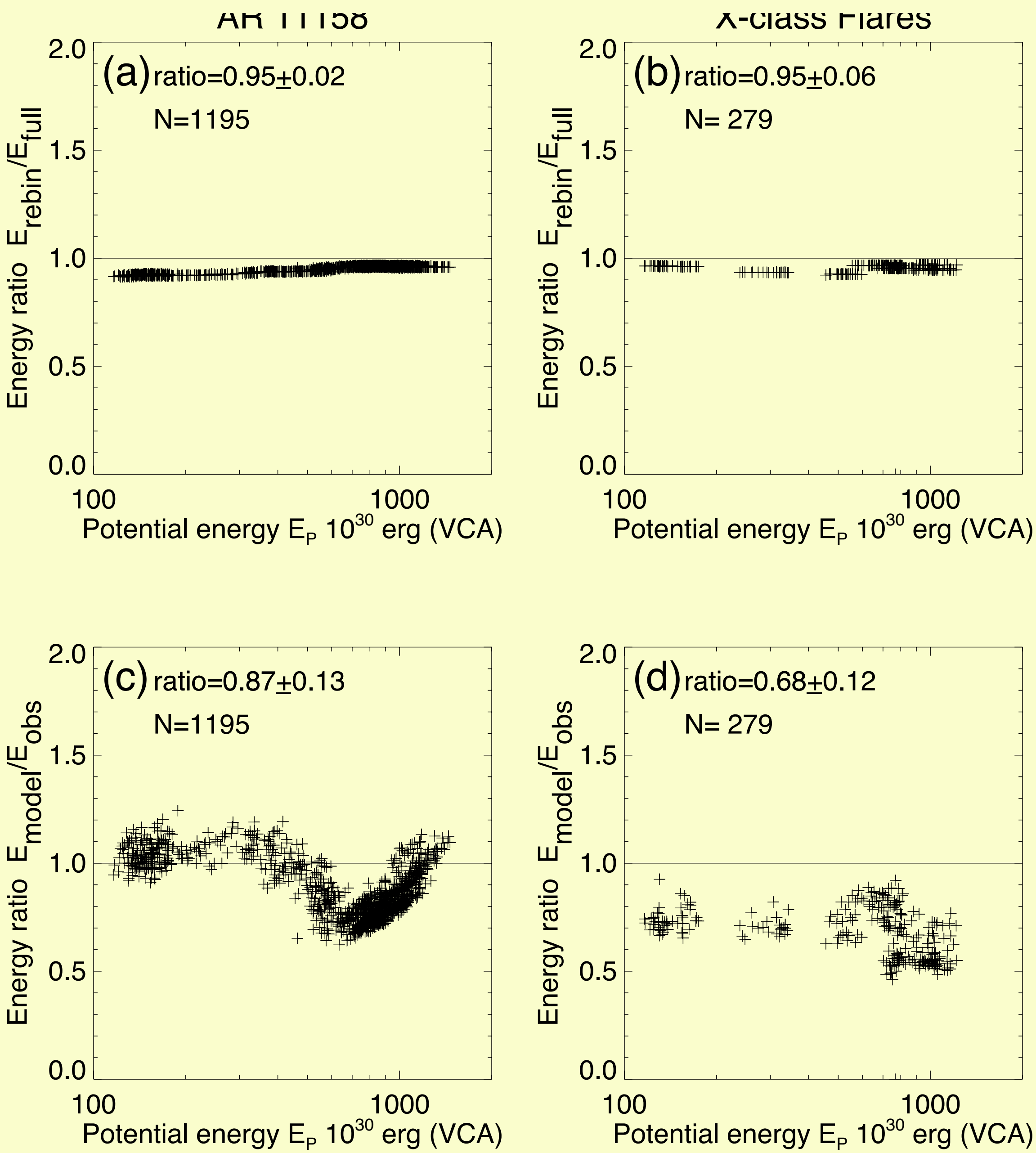
AR 11158
X-class Flares
(a) ratio=0.95±0.02
N=1195
(b) ratio=0.95±0.06
N= 279
(c) ratio=0.87±0.13
N=1195
(d) ratio=0.68±0.12
N= 279
Energy ratio E_rebin/E_full
Energy ratio E_model/E_obs
Potential energy E_P 10^30 erg (VCA)
2.0
1.5
1.0
0.5
0.0
100
1000

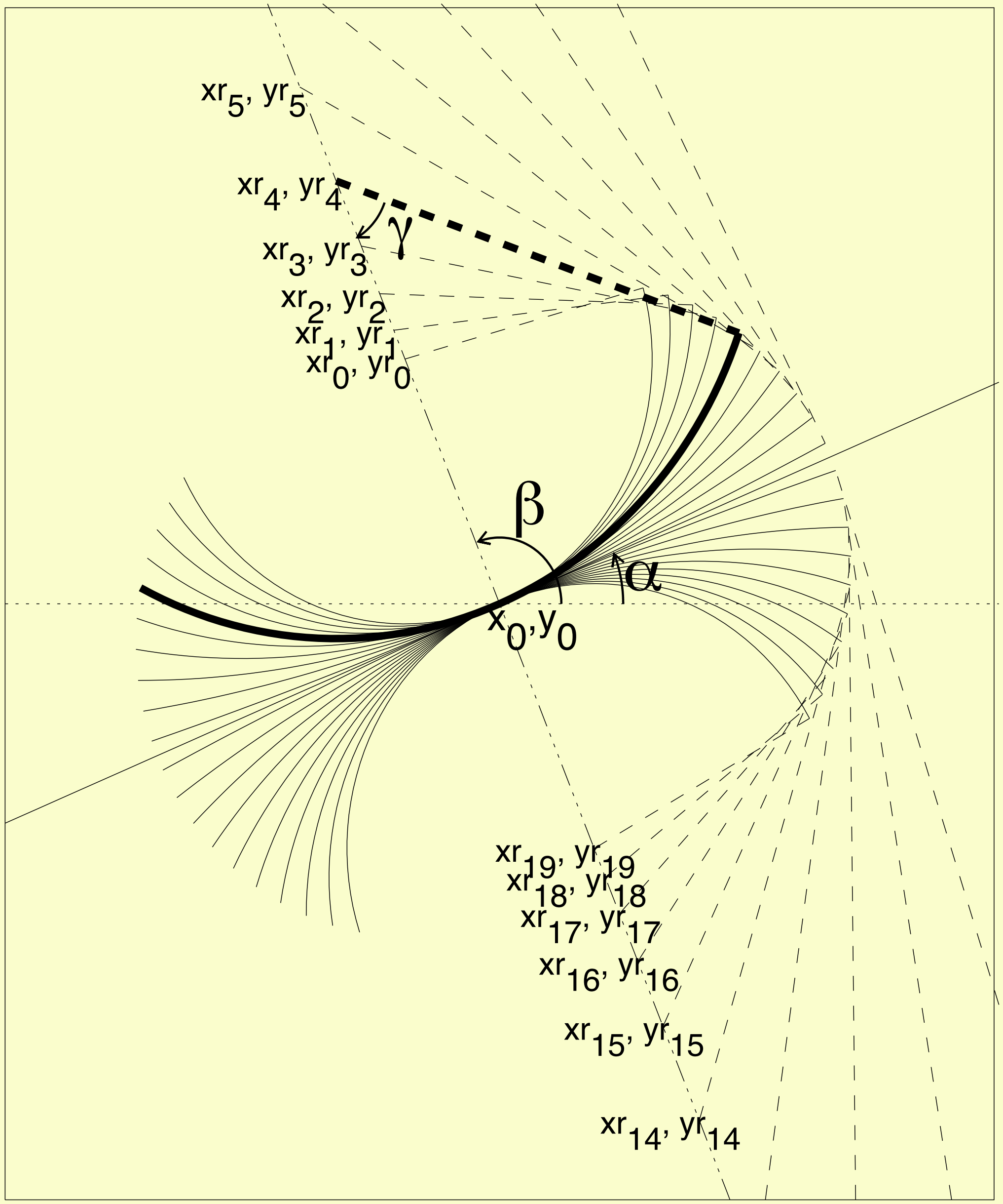
xr5, yr5
xr4, yr4
γ
xr3, yr3
xr2, yr2
xr1, yr1
xr0, yr0
β
α
x0,y0
xr19, yr19
xr18, yr18
xr17, yr17
xr16, yr16
xr15, yr15
xr14, yr14

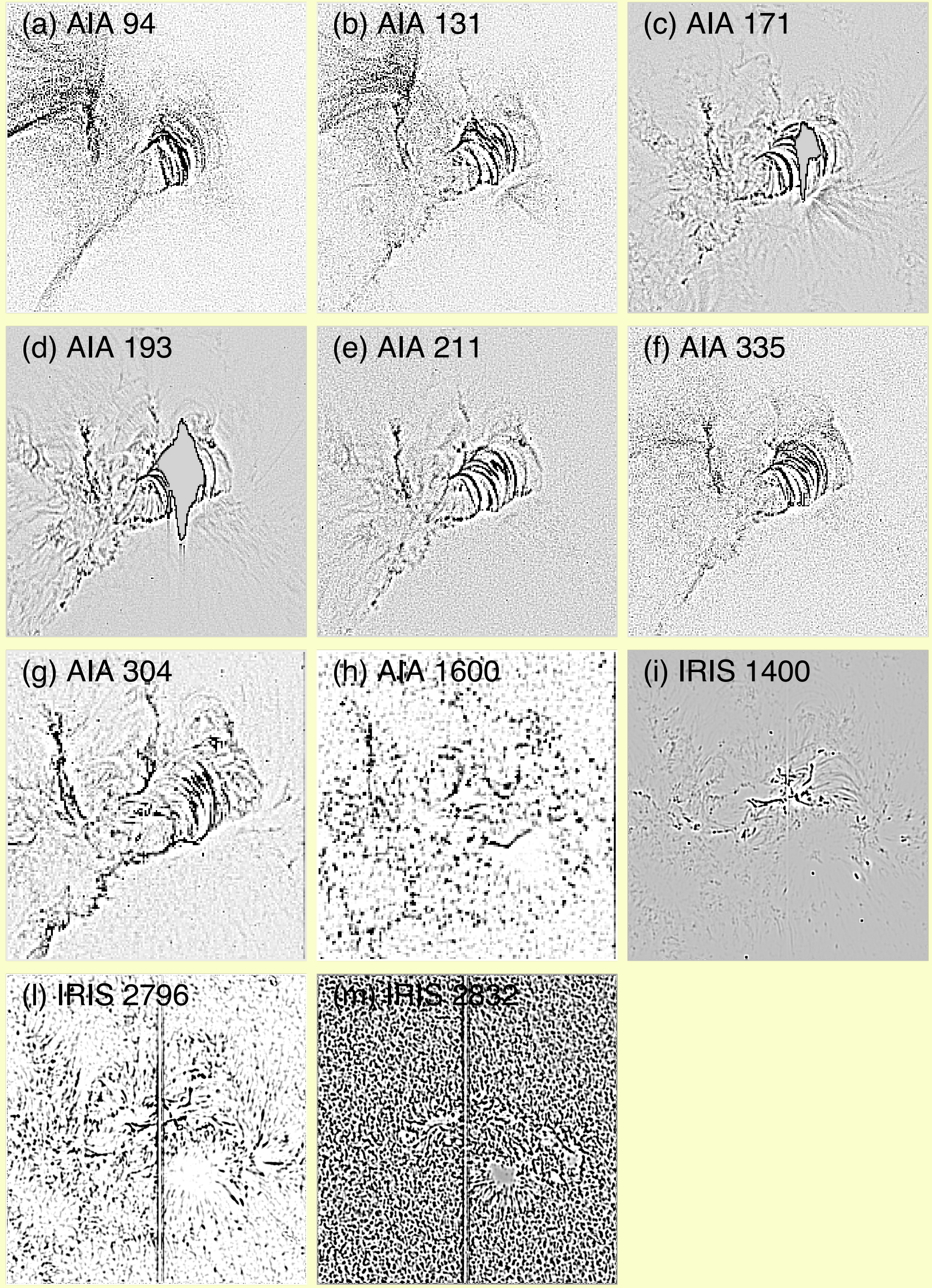
(a) AIA 94
(b) AIA 131
(c) AIA 171
(d) AIA 193
(e) AIA 211
(f) AIA 335
(g) AIA 304
(h) AIA 1600
(i) IRIS 1400
(l) IRIS 2796
(m) IRIS 2832

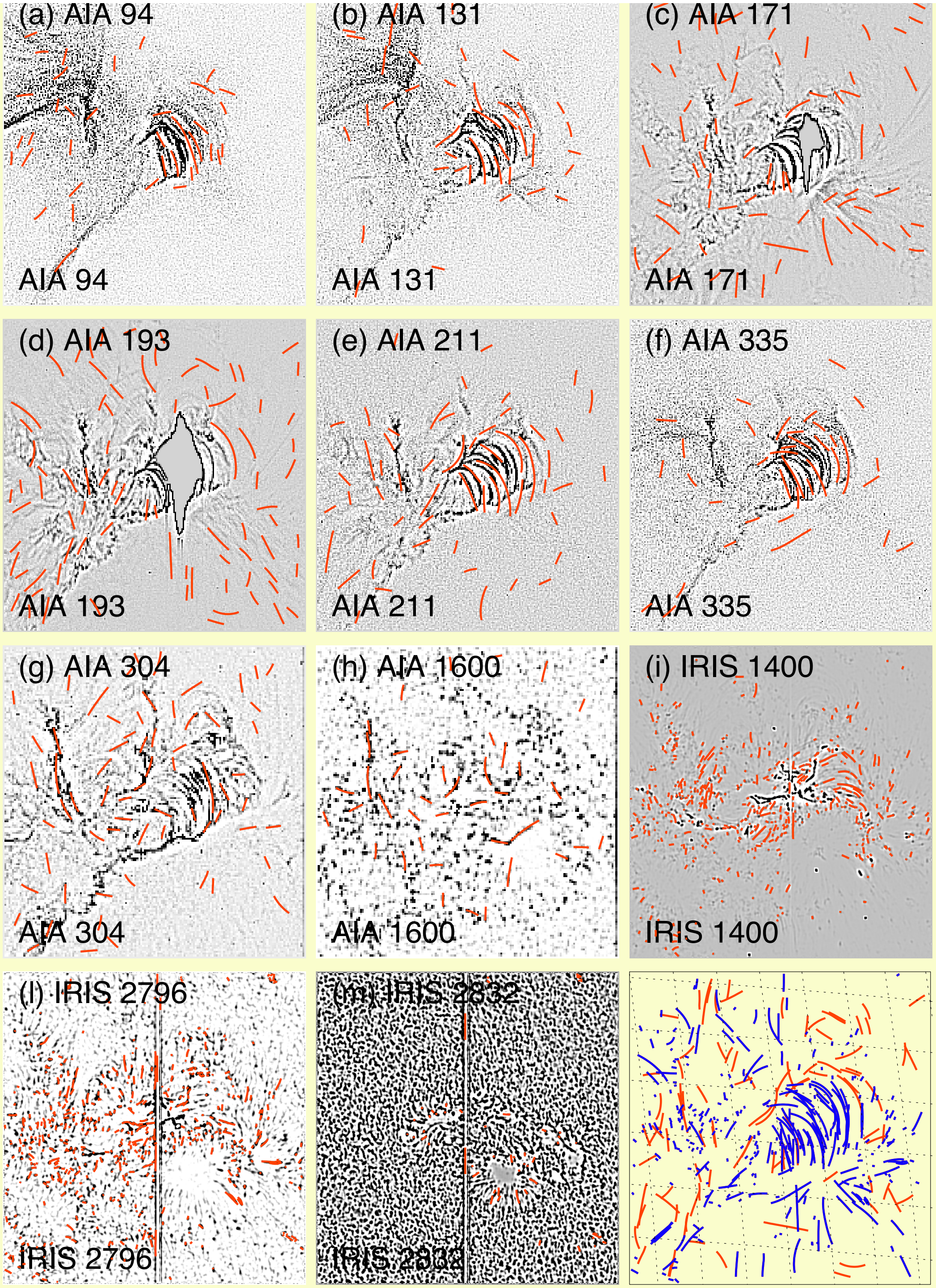
(a) AIA 94
AIA 94
(b) AIA 131
AIA 131
(c) AIA 171
AIA 171
(d) AIA 193
AIA 193
(e) AIA 211
AIA 211
(f) AIA 335
AIA 335
(g) AIA 304
AIA 304
(h) AIA 1600
AIA 1600
(i) IRIS 1400
IRIS 1400
(l) IRIS 2796
IRIS 2796
(m) IRIS 2832
IRIS 2832

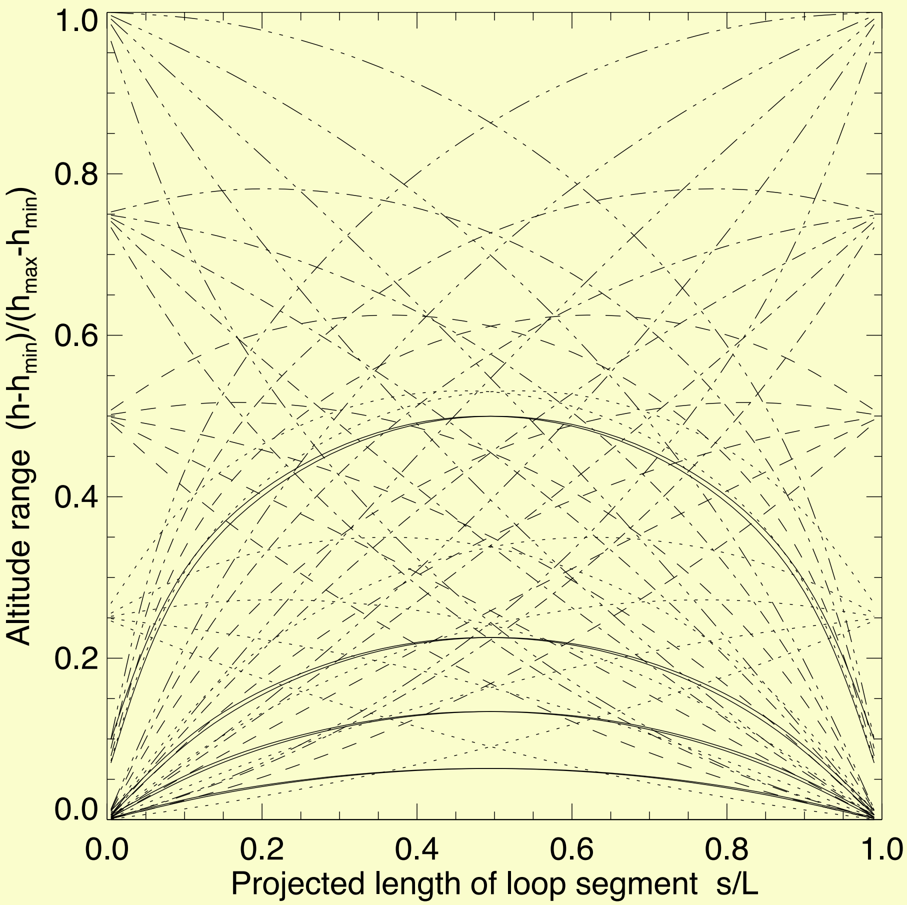

1.0
0.8
0.6
0.4
0.2
0.0
Altitude range (h-h_min)/(h_max-h_min)
0.0
0.2
0.4
0.6
0.8
1.0
Projected length of loop segment s/L

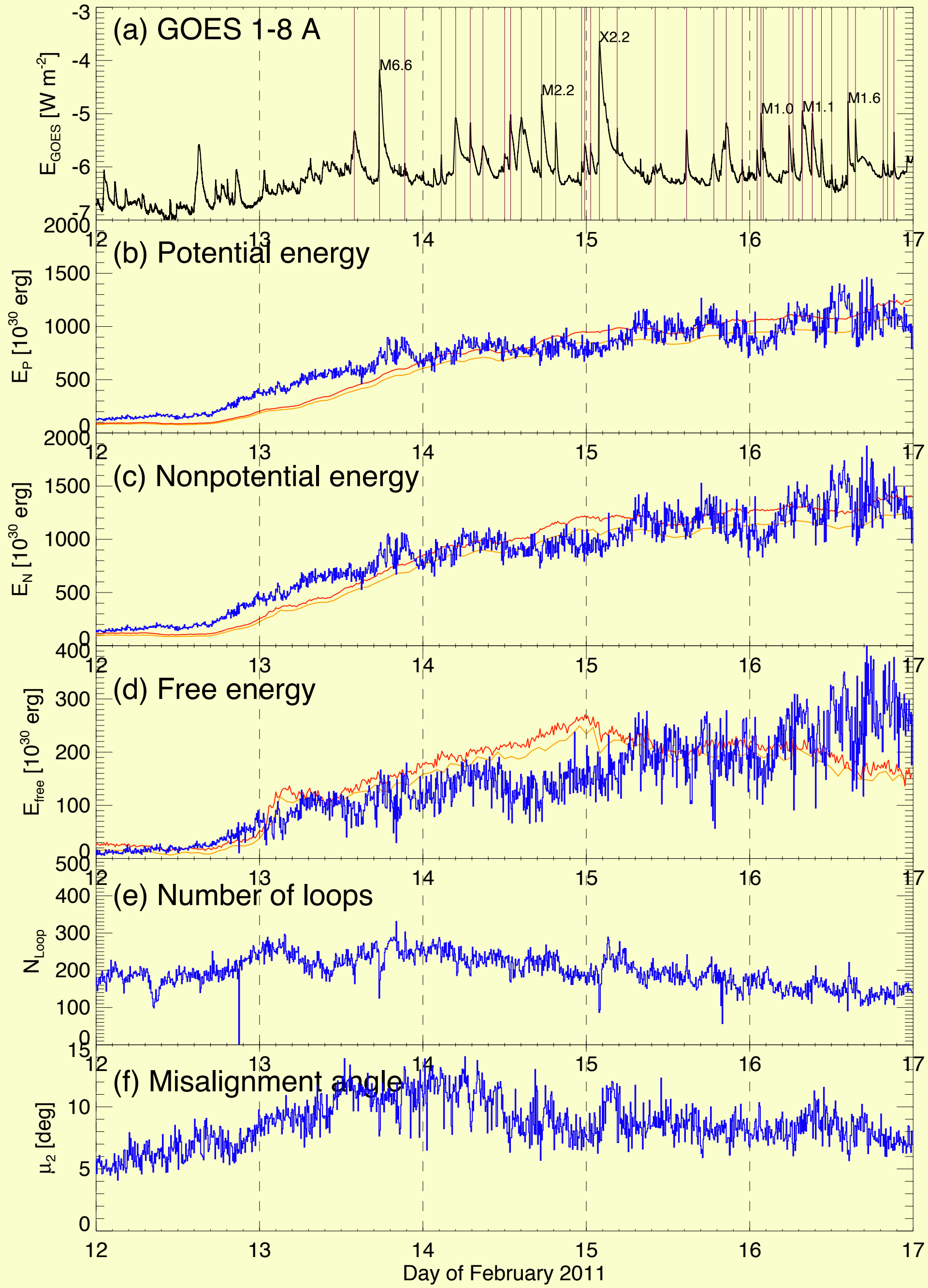

(a) GOES 1-8 A
M6.6
M2.2
X2.2
M1.0
M1.1
M1.6
E_GOES [W m^-2]
(b) Potential energy
E_P [10^30 erg]
(c) Nonpotential energy
E_N [10^30 erg]
(d) Free energy
E_free [10^30 erg]
(e) Number of loops
N_Loop
(f) Misalignment angle
μ_2 [deg]
Day of February 2011

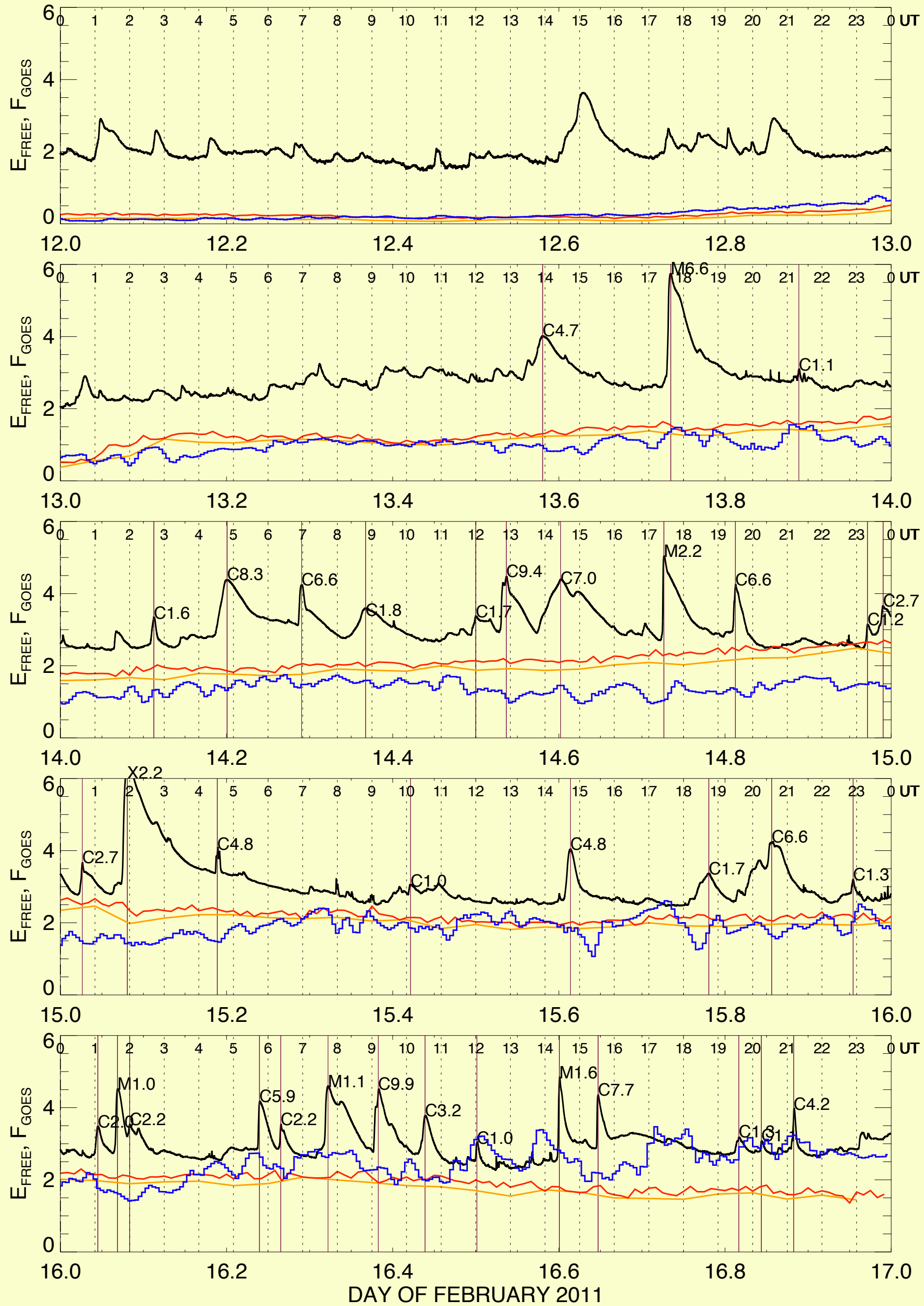

E_{FREE}, F_{GOES}
UT
12.0 12.2 12.4 12.6 12.8 13.0
C4.7 M6.6 C1.1
13.0 13.2 13.4 13.6 13.8 14.0
C1.6 C8.3 C6.6 C1.8 C1.7 C9.4 C7.0 M2.2 C6.6 C1.2 C2.7
14.0 14.2 14.4 14.6 14.8 15.0
X2.2 C2.7 C4.8 C1.0 C4.8 C1.7 C6.6 C1.3
15.0 15.2 15.4 15.6 15.8 16.0
M1.0 C2.0 C2.2 C5.9 C2.2 M1.1 C9.9 C3.2 C1.0 M1.6 C7.7 C1.3 C4.2
16.0 16.2 16.4 16.6 16.8 17.0
DAY OF FEBRUARY 2011

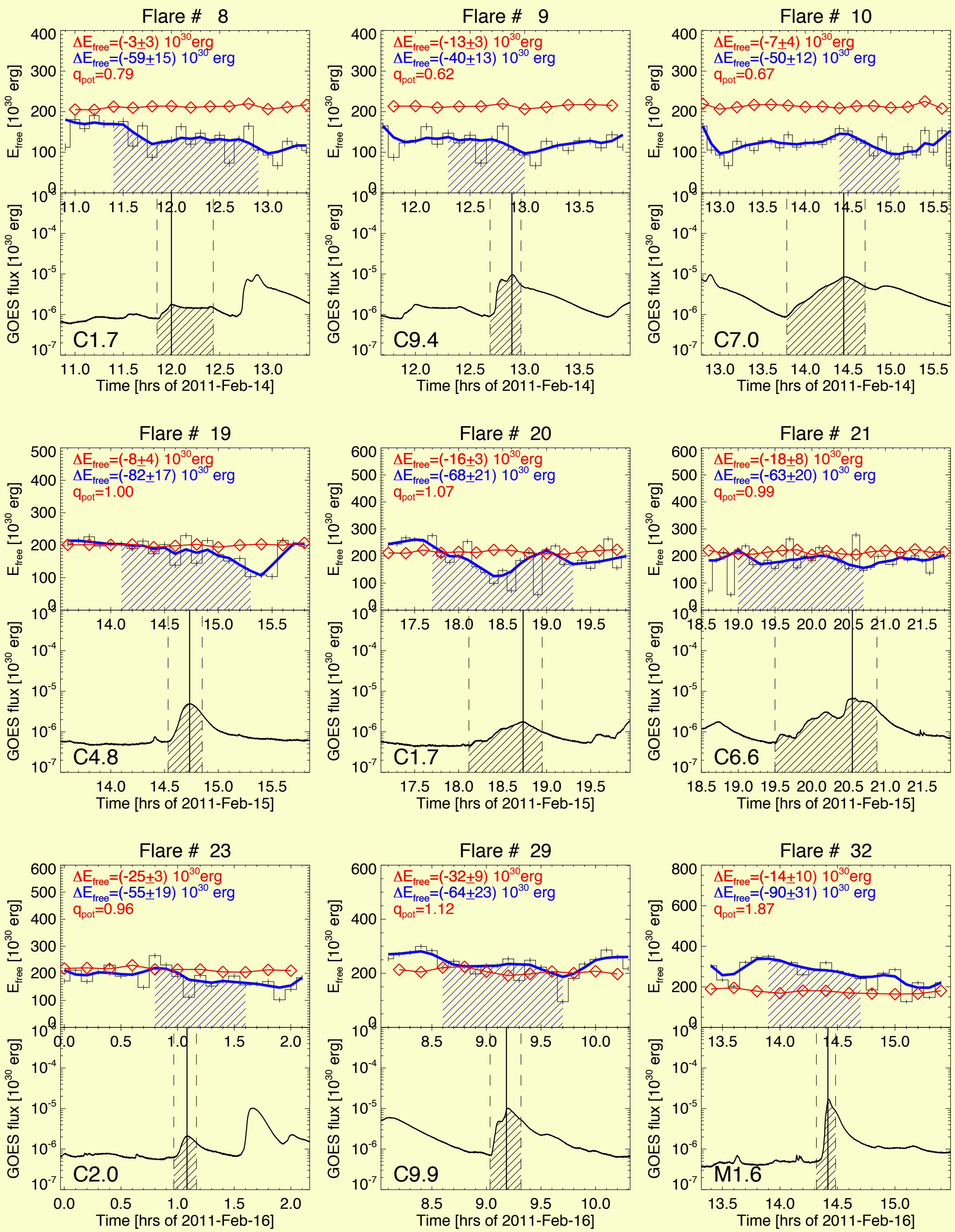
Flare # 8
ΔE_free=(-3±3) 10^30 erg
ΔE_free=(-59±15) 10^30 erg
q_pot=0.79
C1.7
Time [hrs of 2011-Feb-14]
Flare # 9
ΔE_free=(-13±3) 10^30 erg
ΔE_free=(-40±13) 10^30 erg
q_pot=0.62
C9.4
Time [hrs of 2011-Feb-14]
Flare # 10
ΔE_free=(-7±4) 10^30 erg
ΔE_free=(-50±12) 10^30 erg
q_pot=0.67
C7.0
Time [hrs of 2011-Feb-14]
Flare # 19
ΔE_free=(-8±4) 10^30 erg
ΔE_free=(-82±17) 10^30 erg
q_pot=1.00
C4.8
Time [hrs of 2011-Feb-15]
Flare # 20
ΔE_free=(-16±3) 10^30 erg
ΔE_free=(-68±21) 10^30 erg
q_pot=1.07
C1.7
Time [hrs of 2011-Feb-15]
Flare # 21
ΔE_free=(-18±8) 10^30 erg
ΔE_free=(-63±20) 10^30 erg
q_pot=0.99
C6.6
Time [hrs of 2011-Feb-15]
Flare # 23
ΔE_free=(-25±3) 10^30 erg
ΔE_free=(-55±19) 10^30 erg
q_pot=0.96
C2.0
Time [hrs of 2011-Feb-16]
Flare # 29
ΔE_free=(-32±9) 10^30 erg
ΔE_free=(-64±23) 10^30 erg
q_pot=1.12
C9.9
Time [hrs of 2011-Feb-16]
Flare # 32
ΔE_free=(-14±10) 10^30 erg
ΔE_free=(-90±31) 10^30 erg
q_pot=1.87
M1.6
Time [hrs of 2011-Feb-16]
E_free [10^30 erg]
GOES flux [10^30 erg]

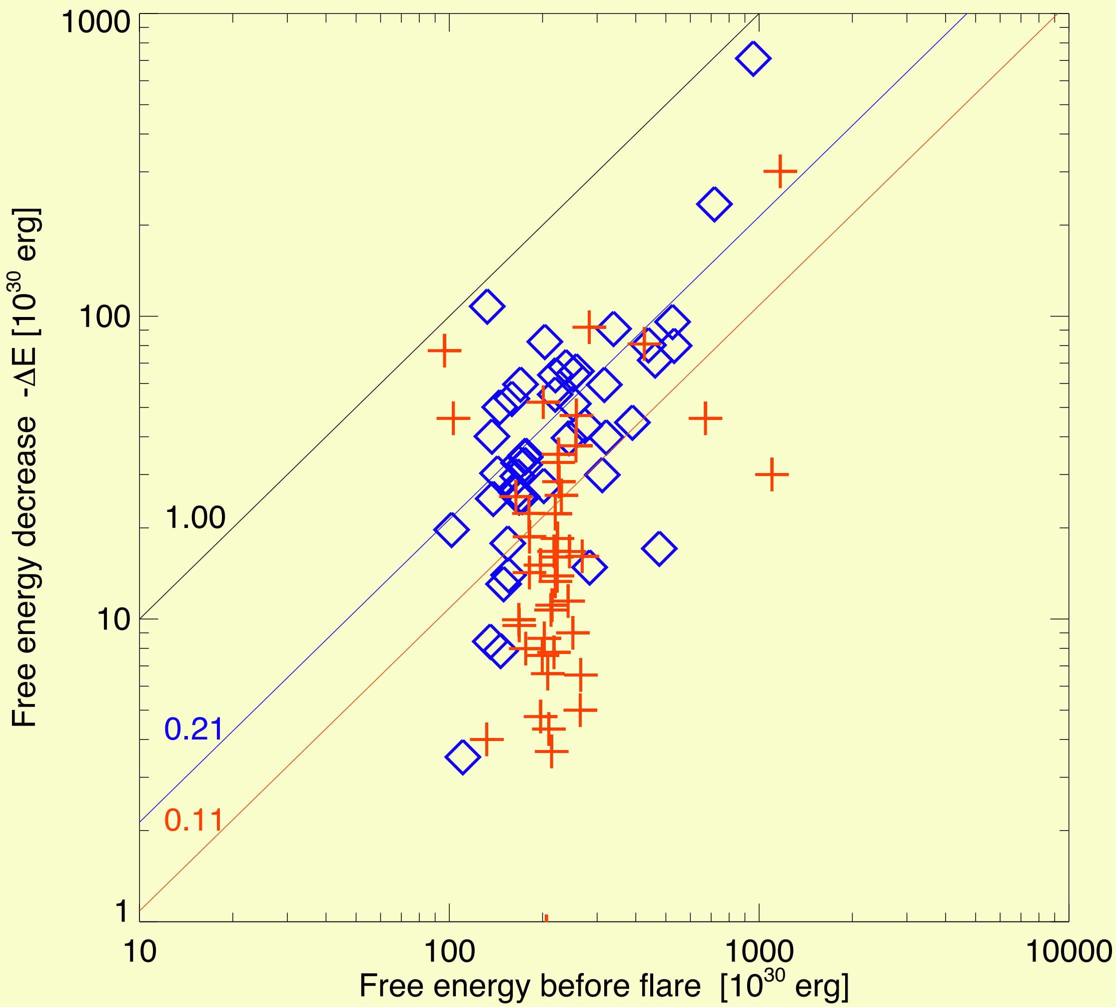

1000
100
10
1
10
100
1000
10000
Free energy decrease -ΔE [10^30 erg]
Free energy before flare [10^30 erg]
1.00
0.21
0.11

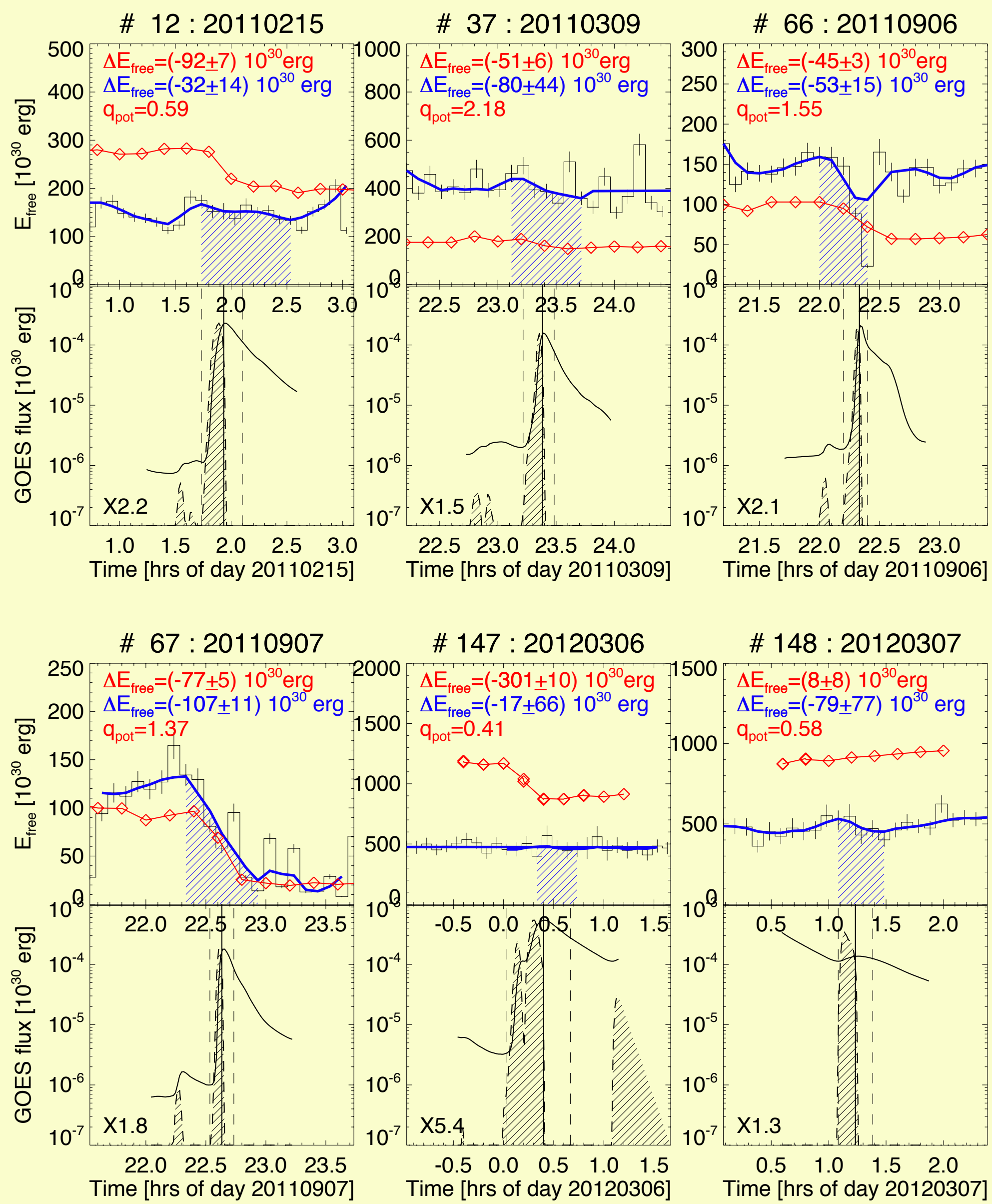

12 : 20110215
ΔEfree=(-92±7) 10^30erg
ΔEfree=(-32±14) 10^30 erg
qpot=0.59
X2.2
Time [hrs of day 20110215]
37 : 20110309
ΔEfree=(-51±6) 10^30erg
ΔEfree=(-80±44) 10^30 erg
qpot=2.18
X1.5
Time [hrs of day 20110309]
66 : 20110906
ΔEfree=(-45±3) 10^30erg
ΔEfree=(-53±15) 10^30 erg
qpot=1.55
X2.1
Time [hrs of day 20110906]
67 : 20110907
ΔEfree=(-77±5) 10^30erg
ΔEfree=(-107±11) 10^30 erg
qpot=1.37
X1.8
Time [hrs of day 20110907]
147 : 20120306
ΔEfree=(-301±10) 10^30erg
ΔEfree=(-17±66) 10^30 erg
qpot=0.41
X5.4
Time [hrs of day 20120306]
148 : 20120307
ΔEfree=(8±8) 10^30erg
ΔEfree=(-79±77) 10^30 erg
qpot=0.58
X1.3
Time [hrs of day 20120307]
Efree [10^30 erg]
GOES flux [10^30 erg]

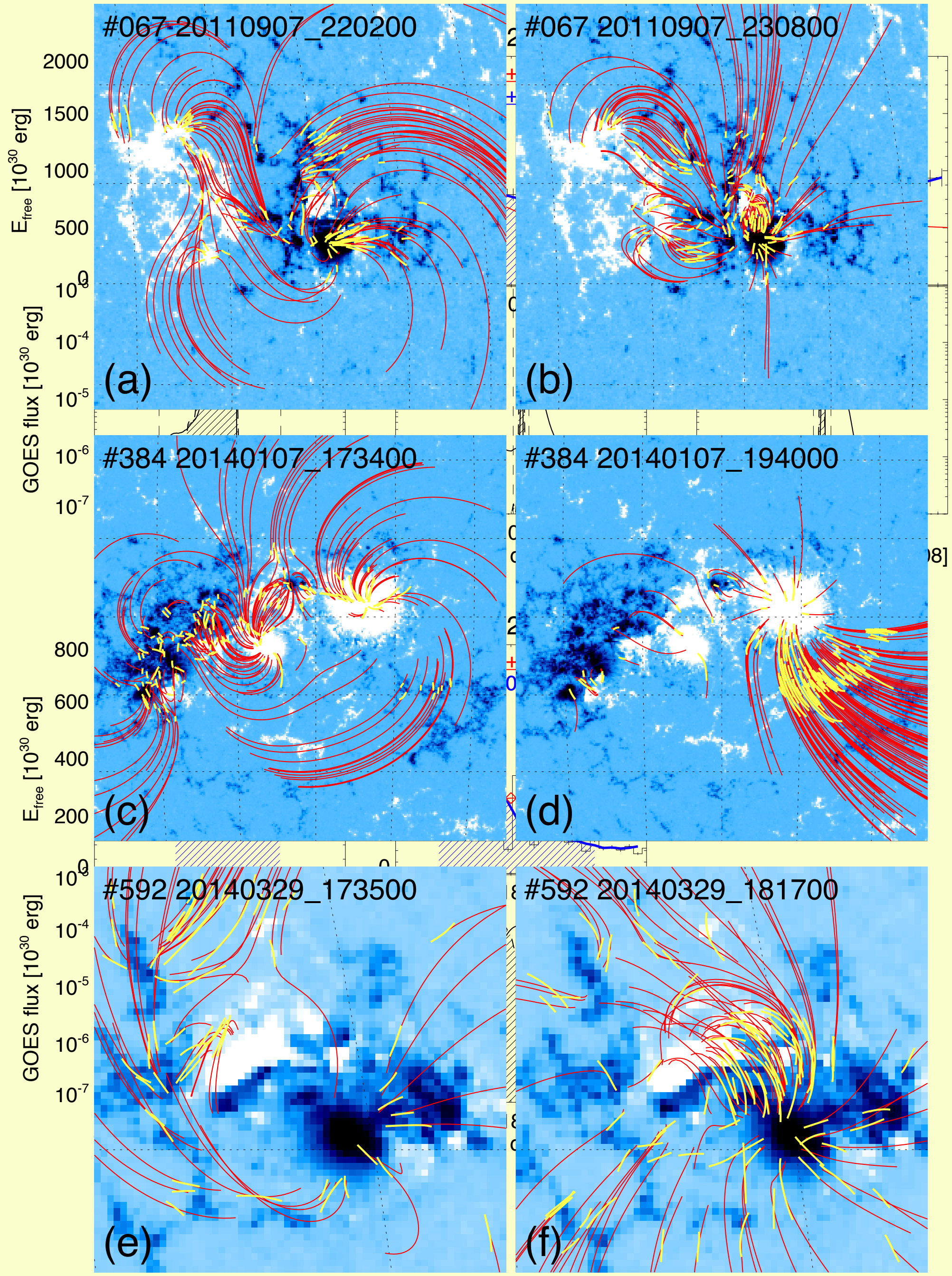
#067 20110907_220200
#067 20110907_230800
(a)
(b)
#384 20140107_173400
#384 20140107_194000
(c)
(d)
#592 20140329_173500
#592 20140329_181700
(e)
(f)

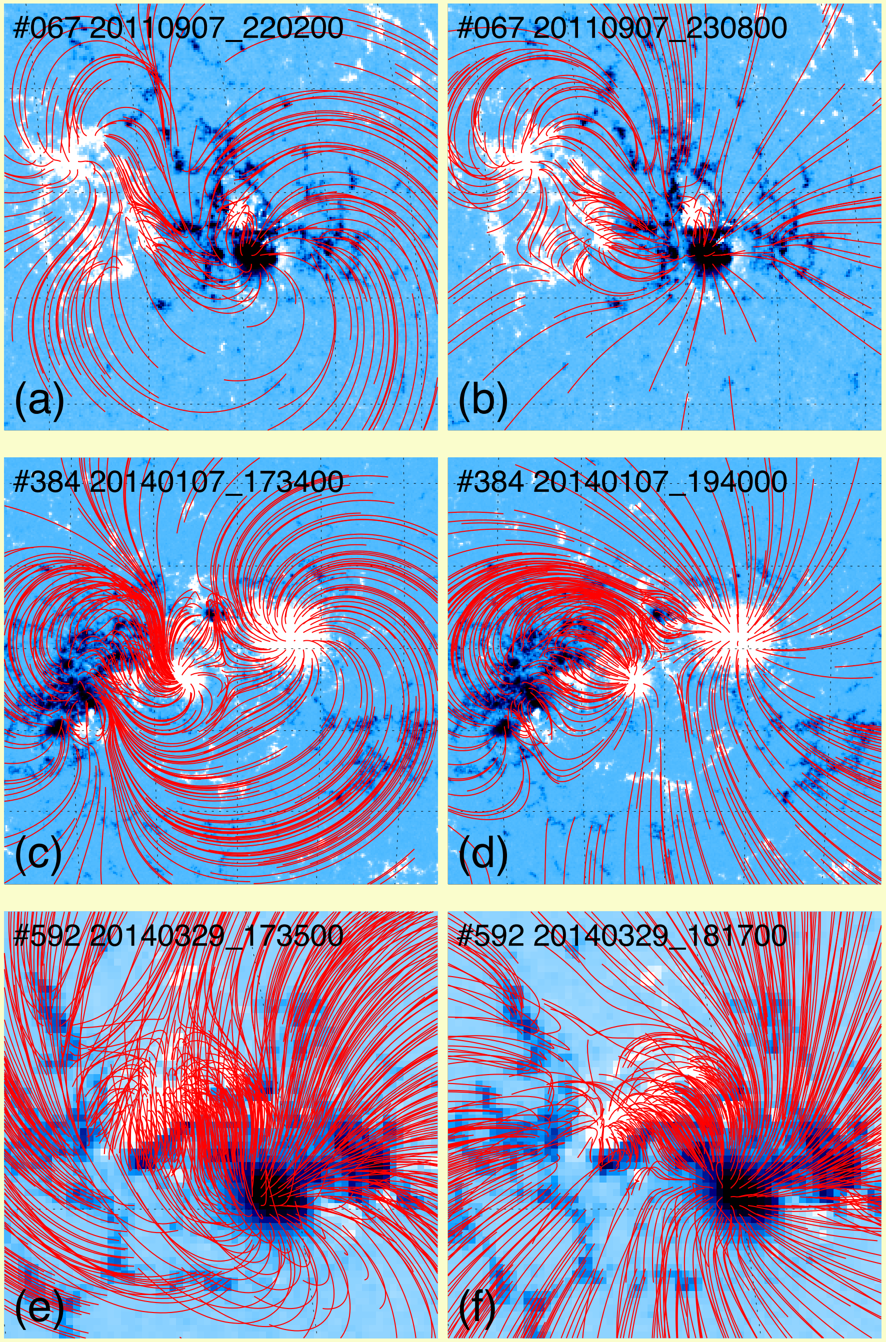
#067 20110907_220200
(a)
#067 20110907_230800
(b)
#384 20140107_173400
(c)
#384 20140107_194000
(d)
#592 20140329_173500
(e)
#592 20140329_181700
(f)

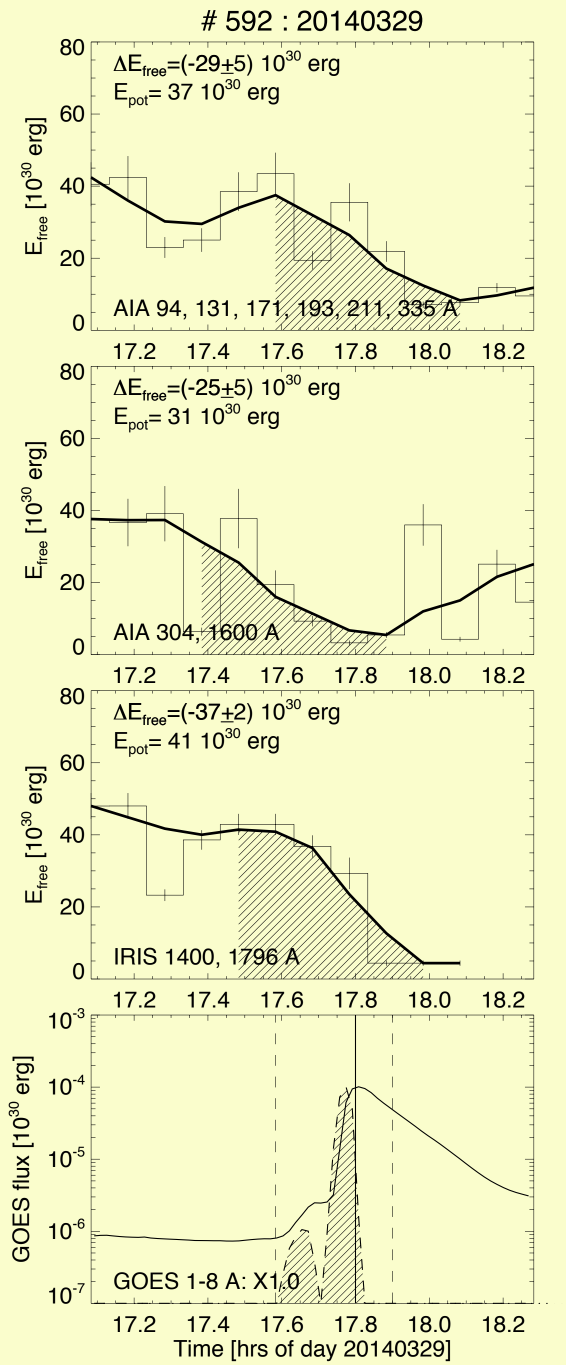

592 : 20140329
ΔE_free=(-29±5) 10^30 erg
E_pot= 37 10^30 erg
AIA 94, 131, 171, 193, 211, 335 A
ΔE_free=(-25±5) 10^30 erg
E_pot= 31 10^30 erg
AIA 304, 1600 A
ΔE_free=(-37±2) 10^30 erg
E_pot= 41 10^30 erg
IRIS 1400, 1796 A
E_free [10^30 erg]
GOES 1-8 A: X1.0
GOES flux [10^30 erg]
Time [hrs of day 20140329]

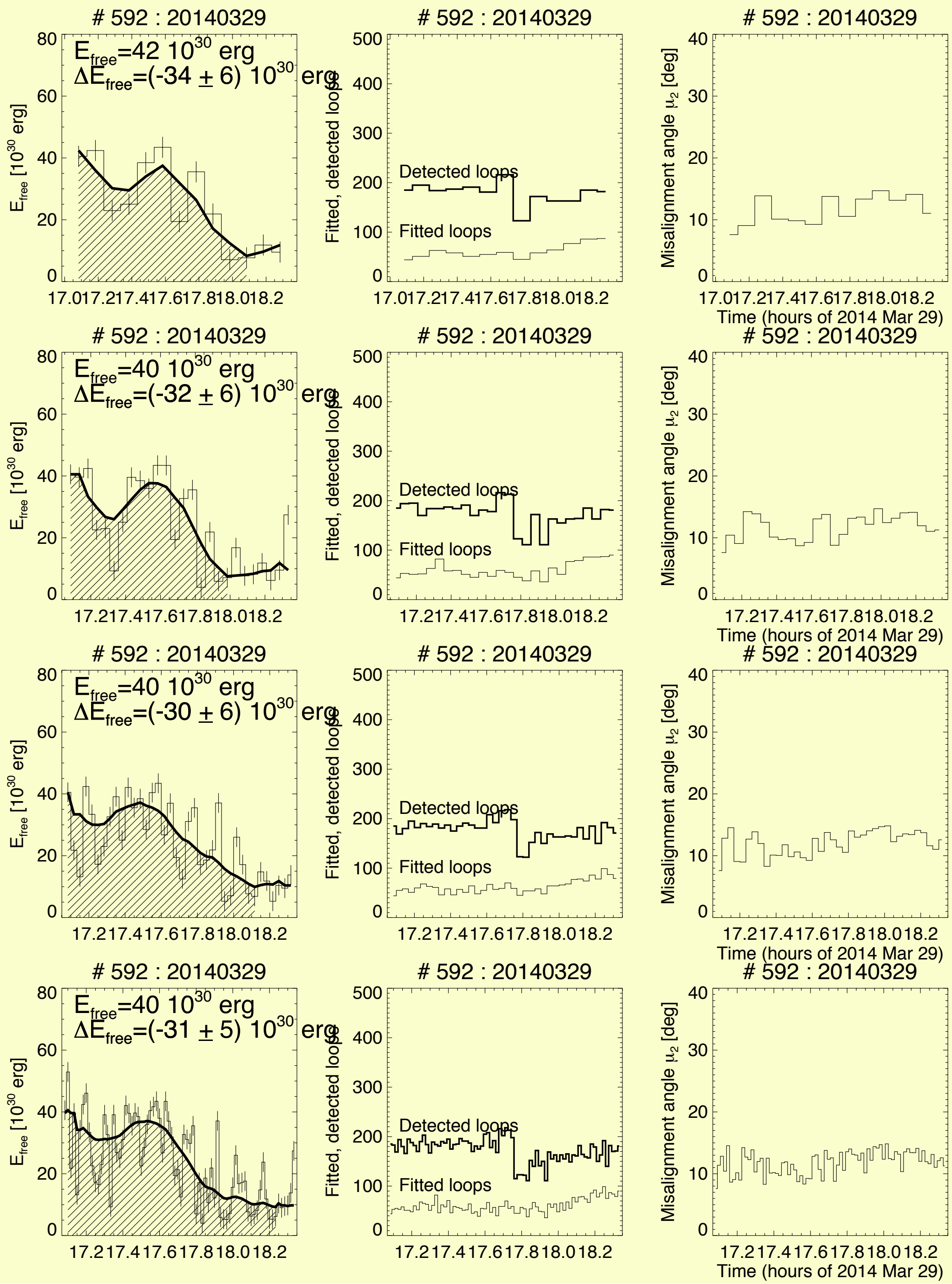

592 : 20140329
E_{free}=42 10^{30} erg
ΔE_{free}=(-34 ± 6) 10^{30} erg
E_{free} [10^{30} erg]
17.017.217.417.617.818.018.2
592 : 20140329
Detected loops
Fitted loops
Fitted, detected loops
17.017.217.417.617.818.018.2
592 : 20140329
Misalignment angle μ_2 [deg]
17.017.217.417.617.818.018.2
Time (hours of 2014 Mar 29)
592 : 20140329
E_{free}=40 10^{30} erg
ΔE_{free}=(-32 ± 6) 10^{30} erg
E_{free} [10^{30} erg]
17.217.417.617.818.018.2
592 : 20140329
Detected loops
Fitted loops
Fitted, detected loops
17.217.417.617.818.018.2
592 : 20140329
Misalignment angle μ_2 [deg]
17.217.417.617.818.018.2
Time (hours of 2014 Mar 29)
592 : 20140329
E_{free}=40 10^{30} erg
ΔE_{free}=(-30 ± 6) 10^{30} erg
E_{free} [10^{30} erg]
17.217.417.617.818.018.2
592 : 20140329
Detected loops
Fitted loops
Fitted, detected loops
17.217.417.617.818.018.2
592 : 20140329
Misalignment angle μ_2 [deg]
17.217.417.617.818.018.2
Time (hours of 2014 Mar 29)
592 : 20140329
E_{free}=40 10^{30} erg
ΔE_{free}=(-31 ± 5) 10^{30} erg
E_{free} [10^{30} erg]
17.217.417.617.818.018.2
592 : 20140329
Detected loops
Fitted loops
Fitted, detected loops
17.217.417.617.818.018.2
592 : 20140329
Misalignment angle μ_2 [deg]
17.217.417.617.818.018.2
Time (hours of 2014 Mar 29)

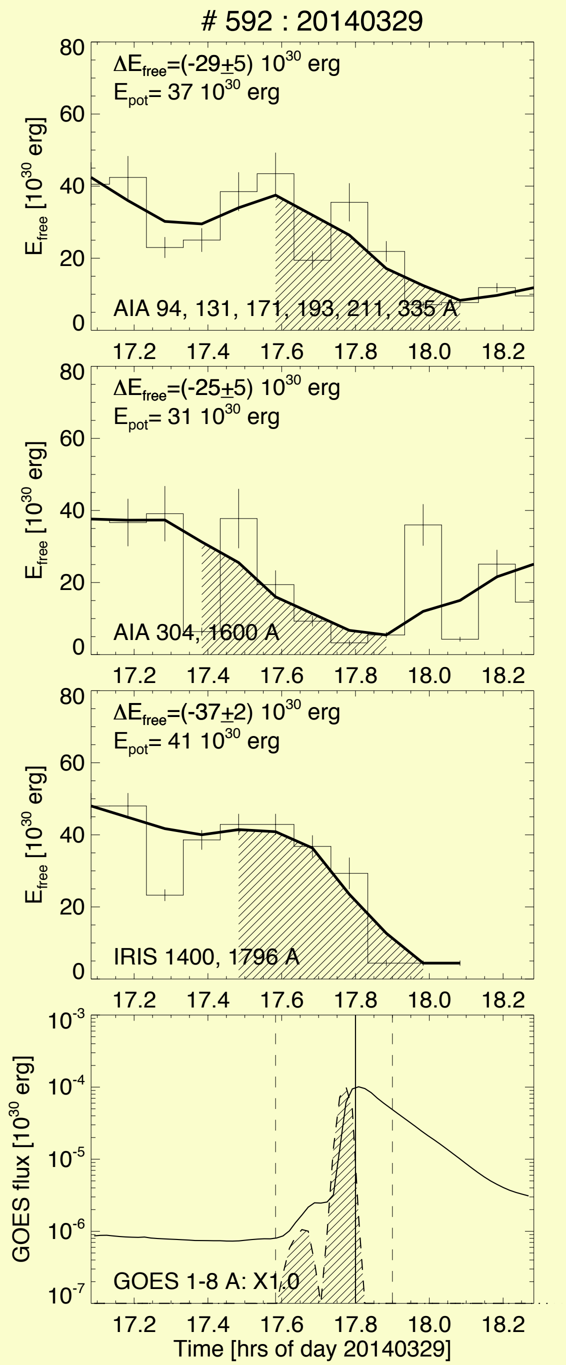

592 : 20140329
ΔE_free=(-29±5) 10^30 erg
E_pot= 37 10^30 erg
AIA 94, 131, 171, 193, 211, 335 A
ΔE_free=(-25±5) 10^30 erg
E_pot= 31 10^30 erg
AIA 304, 1600 A
ΔE_free=(-37±2) 10^30 erg
E_pot= 41 10^30 erg
IRIS 1400, 1796 A
GOES 1-8 A: X1.0
E_free [10^30 erg]
GOES flux [10^30 erg]
Time [hrs of day 20140329]

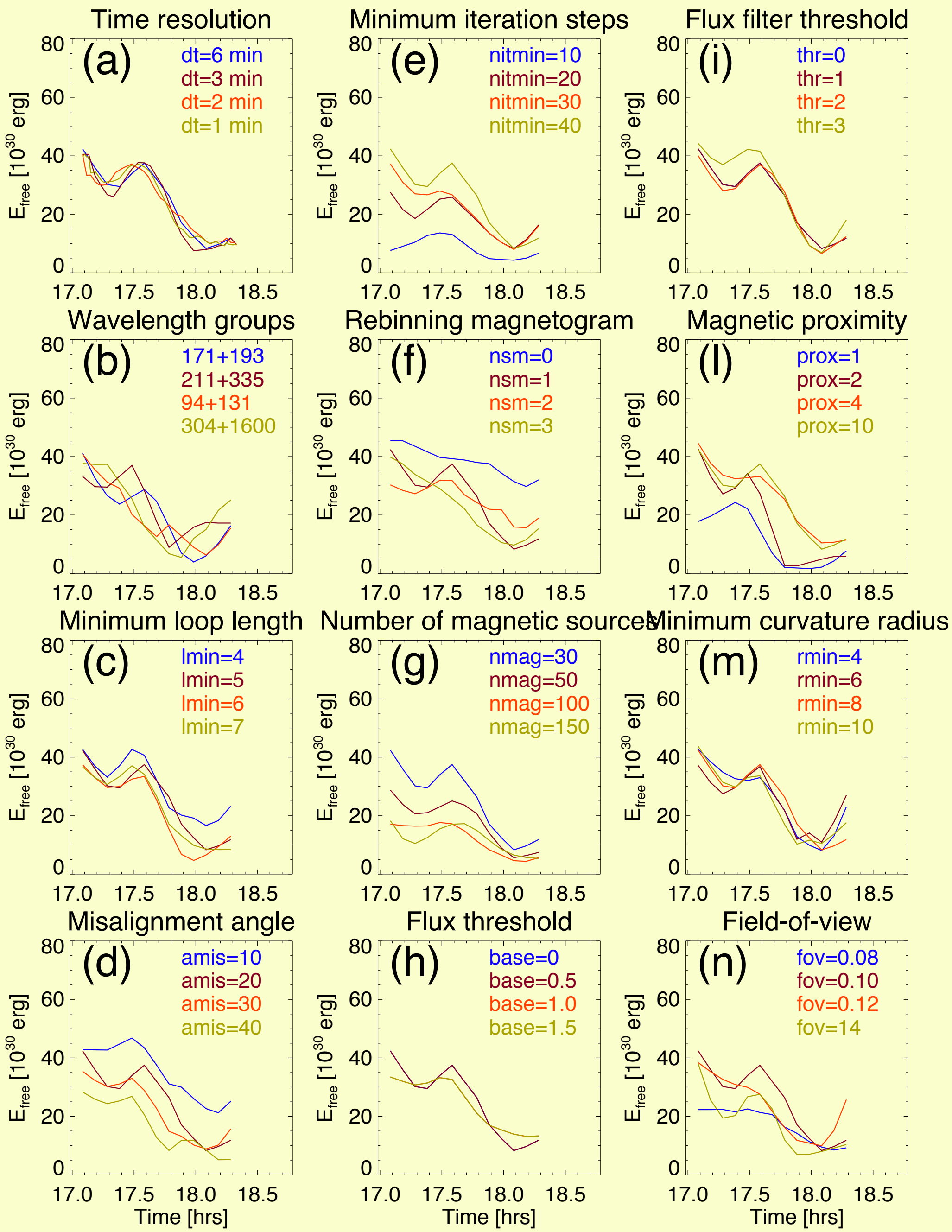

Time resolution
(a)
dt=6 min
dt=3 min
dt=2 min
dt=1 min
Minimum iteration steps
(e)
nitmin=10
nitmin=20
nitmin=30
nitmin=40
Flux filter threshold
(i)
thr=0
thr=1
thr=2
thr=3
Wavelength groups
(b)
171+193
211+335
94+131
304+1600
Rebinning magnetogram
(f)
nsm=0
nsm=1
nsm=2
nsm=3
Magnetic proximity
(l)
prox=1
prox=2
prox=4
prox=10
Minimum loop length
(c)
lmin=4
lmin=5
lmin=6
lmin=7
Number of magnetic sources
(g)
nmag=30
nmag=50
nmag=100
nmag=150
Minimum curvature radius
(m)
rmin=4
rmin=6
rmin=8
rmin=10
Misalignment angle
(d)
amis=10
amis=20
amis=30
amis=40
Flux threshold
(h)
base=0
base=0.5
base=1.0
base=1.5
Field-of-view
(n)
fov=0.08
fov=0.10
fov=0.12
fov=14
E_free [10^30 erg]
Time [hrs]
0 20 40 60 80
17.0 17.5 18.0 18.5